Strategies for Reservoir Characterization and Identification of Incremental Recovery Opportunities in Mature Reservoirs in Frio Fluvial-Deltaic Sandstones, South Texas: An Example from Rincon Field, Starr County

Topical Report

by

Lee E. McRae
Mark H. Holtz
Tucker Hentz
Chun-Yen Chang
Paul R. Knox

September 1995

Work performed under Contract No. DE-FC22-93BC14959

Prepared for
U.S. Department of Energy
Assistant Secretary for Fossil Energy

Edith Allison, Project Manager
Bartlesville Project Office
P.O. Box 1398
Bartlesville, Oklahoma 74005

Prepared by
Bureau of Economic Geology
Noel Tyler, Director
The University of Texas at Austin
Austin, Texas 78713-8924

QAe5634

CONTENTS

Figures

Tables

ABSTRACT

Fluvial-deltaic sandstone reservoirs in the United States are being abandoned at high rates, yet they still contain more than 34 billion barrels of unrecovered oil. The mature Oligocene-age fluvial-deltaic reservoirs of the Frio Formation along the Vicksburg Fault Zone in South Texas are typical of this class in that, after more than three decades of production, they still contain 61 percent of the original mobile oil in place, or 1.6 billion barrels. This resource represents a tremendous target for advanced reservoir characterization studies that integrate geological and engineering analysis to locate untapped and incompletely drained reservoir compartments isolated by stratigraphic heterogeneities.

The D and E reservoir intervals of Rincon field, Starr County, South Texas, were selected for detailed study to demonstrate the ability of advanced characterization techniques to identify reservoir compartmentalization and locate specific infield reserve-growth opportunities. Reservoir architecture, determined through high-frequency genetic stratigraphy and facies analysis, was integrated with production history and facies-based petrophysical analysis of individual flow units to identify recompletion and geologically targeted infill drilling opportunities.

Each of the two reservoir intervals selected approximates a fourth-order genetic unit and contains four to six higher frequency genetic units that act as individual flow units. Flow units progress from aggradational fluvial (upper delta plain) settings at the base of the E interval through retrogradational, then progradational channel and delta front bar settings at the top of the E and base of the D intervals. Uppermost D units represent a return to aggradational fluvial reservoirs. Greatest heterogeneities and lowest recovery efficiencies exist in the strongly retrogradational and weakly progradational units. Estimates of original oil in place versus cumulative production in D and E reservoirs suggest that potential reserve growth exceeds 4.5 million barrels. Comparison of reservoir architecture and the distribution of completions in each flow unit indicates a large number of reserve-growth opportunities. Potential reserves can be assigned to each opportunity by constructing an $S_o \phi h$ map of remaining mobile oil, which is

the difference between original oil in place and the volumes drained by past completions. The methodology demonstrated in this study has direct application to other reservoirs in Rincon field, other fields in the Frio Fluvial-Deltaic Play of South Texas, and mature reservoirs across the U.S. formed in analogous depositional settings.

INTRODUCTION

Fluvial-deltaic sandstone reservoirs represent significant opportunities for re-development in mature fields throughout the world. These reservoirs presently account for more than 34 billion barrels (Bbbl) of unrecovered oil resources in the United States and, as a class, represent the highest percentage of remaining mobile oil resources in clastic reservoirs throughout the state of Texas. The stratigraphic complexity inherent in these deposits causes low recovery efficiencies in large part because of the isolation of significant volumes of mobile oil in undeveloped reservoir compartments. These unproduced zones can be identified by integrated geological and engineering reservoir characterization and targeted for near-term incremental recovery by recompletions and infill drilling.

Frio fluvial-deltaic reservoirs are being abandoned at high rates in fields throughout South Texas, but recent resource calculations estimate that more than 1.6 BSTB of unrecovered mobile oil still resides in reservoirs within a play that has already produced nearly 1 Bbbl of oil (Holtz and McRae, 1995b). Because of the stratigraphic complexity inherent in fluvial-deltaic sandstone reservoirs, significant volumes of mobile oil are commonly isolated in undeveloped reservoir compartments. This large oil resource will remain unproduced unless advanced multidisciplinary reservoir characterization techniques can be applied to identify untapped and incompletely drained compartments that have been overlooked by previous development efforts.

Frio reservoirs in Rincon field located in the South Texas Gulf Coast were studied to better characterize interwell stratigraphic heterogeneity in fluvial-deltaic depositional systems and determine controls on locations and volumes of unrecovered oil. Well log correlations carried out within a high-frequency stratigraphic framework, reservoir mapping, core analyses, and evaluation of production data were used to characterize variability of reservoirs within the field. Differences in sandstone depositional styles and production behavior were assessed to identify zones with significant stratigraphic heterogeneity and a high potential for containing unproduced oil. Integrated geologic and engineering reservoir characterization was completed on two selected reservoir zones within Rincon field that have experienced different production histories and exhibit different reservoir architectural styles. Development of reservoir flow-unit architecture, described by log facies supplemented with petrophysical core studies and integrated with production data, forms the basis for recognizing primary controls on hydrocarbon production that, in turn, directly aid in identifying potential locations of unproduced recoverable oil. The methodology demonstrated here has direct application to other reservoirs in these fields, other fields in the Frio Fluvial-Deltaic Sandstone Play in South Texas, as well as fields outside the play formed in analogous depositional settings.

RESERVOIR CHARACTERIZATION OF FLUVIAL-DELTAIC SANDSTONES: A METHODOLOGY FOR IDENTIFYING HETEROGENEITY AND DELINEATING RESERVE GROWTH OPPORTUNITIES

Stratigraphic compartmentalization is inherent in fluvial-deltaic depositional systems and is responsible for the incomplete and inefficient recovery of available oil and gas resources. Identification and production of incremental mobile oil resources depend on identifying which parts of the reservoir have not been effectively contacted or swept because of heterogeneity and the resultant reservoir compartmentalization. Successful advanced recovery approaches in fluvial-deltaic reservoirs depend on reservoir characterization strategies that integrate geological facies models with engineering assessments of reservoir behavior and production histories.

The general workflow for the characterization process used in this study is shown in Fig. 1. All available data, including well logs, cores, fluid characteristics, and other well information, were used in this multidisciplinary approach. Interpretations of general field and reservoir stratigraphy, detailed stratigraphic and structural reservoir architecture, and microscopic rock properties were integrated with evaluations of facies-based reservoir petrophysics and past production history. The following sections give a brief overview of each of these processes and provide a framework in which the characterization of example reservoirs will be presented in this report.

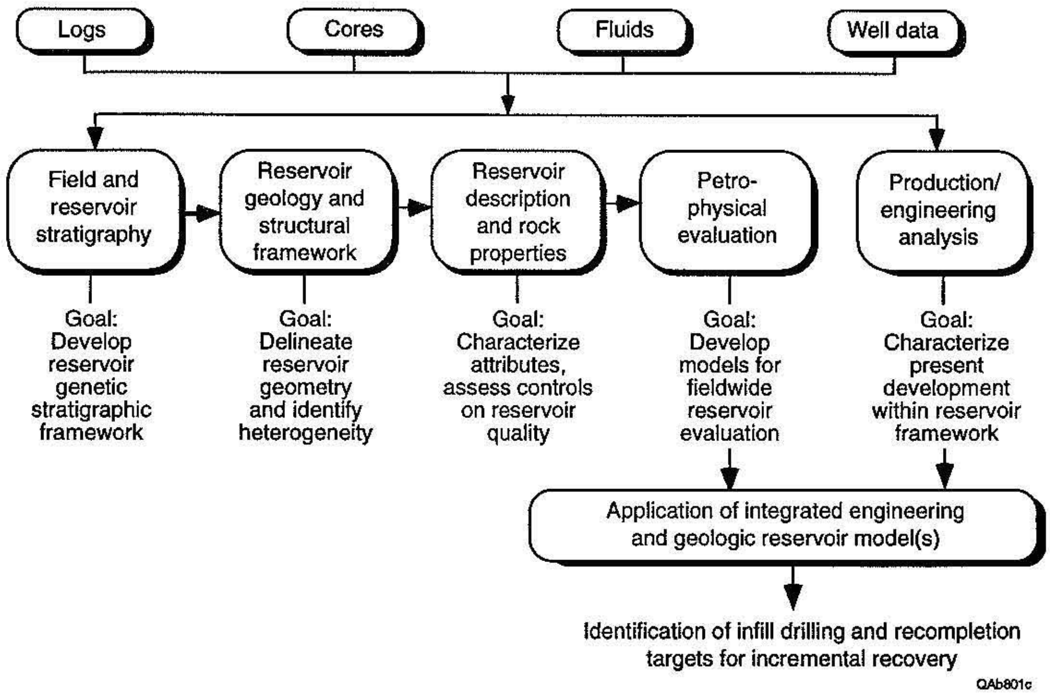

Figure 1. Workflow diagram for multidisciplinary advanced reservoir characterization studies.

Field and Reservoir Stratigraphy: Establishing a Framework

The architecture of sandstones in clastic reservoirs has a direct impact on hydrocarbon recovery. Reservoir architecture is a function of depositional setting and position within a large-scale (3rd order) depositional cycle or genetic sequence (Knox and McRae, 1995). As a consequence, establishing the position of reservoirs within a specific depositional system, structural trend, and genetic sequence provides much general information regarding their recovery efficiency, heterogeneity style, and the potential for compartmentalization (McRae and others, 1994). This fundamental concept is the foundation of the Department of Energy reservoir class system (DOE, 1991).

Much knowledge about the general depositional, stratigraphic, and structural framework can be determined from previous regional studies. For example, the position of Frio fluvial-deltaic sandstone reservoirs within a depositional system has been established by Galloway and others (1982) and the primary structural framework of the Frio producing trends has been documented in Galloway and others (1983). The overall genetic stratigraphic framework for the Frio Formation has also been identified in previous literature (Galloway, 1986). A review of fields within the Frio Fluvial-Deltaic Sandstone (Vicksburg Fault Zone) Play resulted in the identification of Rincon field, Starr Company, as a field containing an excellent data set and significant reserve-growth potential (McRae and others, 1994).

Fieldwide correlation of well logs was used to identify major rock units bounded by stratigraphically significant markers such as flooding surfaces, thereby establishing a stratigraphic framework for the reservoir interval. That framework was then correlated to published genetic stratigraphic framework for the Frio to determine the sequence stratigraphic implications of identified stratigraphic markers. The resulting field-scale genetic stratigraphic framework aided in detailed well log correlations because it established a basis for higher frequency stratigraphic correlation and for predicting depositional facies from lithology and, consequently, predicting reservoir architecture.

Reservoir Geology: Determining Reservoir Architecture

Internal features within reservoir sandstone units define the geometry of fluid pathways that control the efficiency of hydrocarbon migration to the well bore and therefore provide fundamental constraints on the ultimate volume of conventionally recoverable oil and gas that remain in the ground when the reservoir is abandoned (Tyler and others, 1992). High-frequency stratigraphic analysis can identify these intervals in well logs and predict their occurrence between well locations. Understanding the details of reservoir architecture and its inherent control on fluid migration is critical to efficiently targeting the remaining recoverable oil resource in maturely developed reservoirs.

The internal geometry of sandstone bodies and the degree of interconnectedness, communication, or compartmentalization between individual reservoir sandstone bodies are products of the nonuniformity, or heterogeneity, of a rock reservoir (Alpay, 1972). Reservoir structure can be exceedingly complex, containing heterogeneities from scales of kilometers down to scales of less than 1 millimeter (Lasseter and others, 1986). The scale of heterogeneity that is most critical in controlling fluid flow pathways and that is the key to accessing unrecovered mobile oil remaining in the reservoir is the intermediate, interwell, or macroscopic scale of heterogeneity. This level of heterogeneity most closely corresponds to the reservoir flow unit. Macroscale features include variations in depositional and diagenetic facies that serve to compartmentalize a reservoir. Physical bounding elements that define the permeability structure of a reservoir and divide it into separate flow units include both bedding surfaces as well as nonpermeable rock types that act as intrareservoir seals between individual reservoir compartments (Fig. 2).

Lateral and vertical reservoir heterogeneity is controlled by the depositional processes responsible for creating the reservoir, and this heterogeneity in turn is responsible for developing the reservoir architecture that provides the fundamental control on hydrocarbon recovery efficiency in a given reservoir unit (Tyler and Finley, 1991). Developing a detailed understanding of the processes, styles, and scales of heterogeneity that characterize a particular reservoir type can become a powerful predictive tool for identifying and delineating additional unrecovered oil and gas resources. Untapped and incompletely drained reservoir compartments are the primary targets that can be identified through detailed depositional facies analysis and the identification of interwell scale heterogeneities that divide reservoir facies into separate flow units.

Reservoir Description: Microscopic Rock Properties

Whereas reservoir architecture controls the macroscopic scwale of heterogeneity and fluid flow, rock texture, mineralogy, and pore structure determine the microscopic heterogeneity and fluid flow as well as the physical response of the reservoir to investigative tools such as geophysical well logs. Heterogeneity at this microscale causes variations in capillarity that control the nature of oil saturation and the retention of residual oil in the vicinity of the well bore (McRae and others, 1994). This heterogeneity is largely a function of diagenetic processes, which may vary in nature and extent between facies.

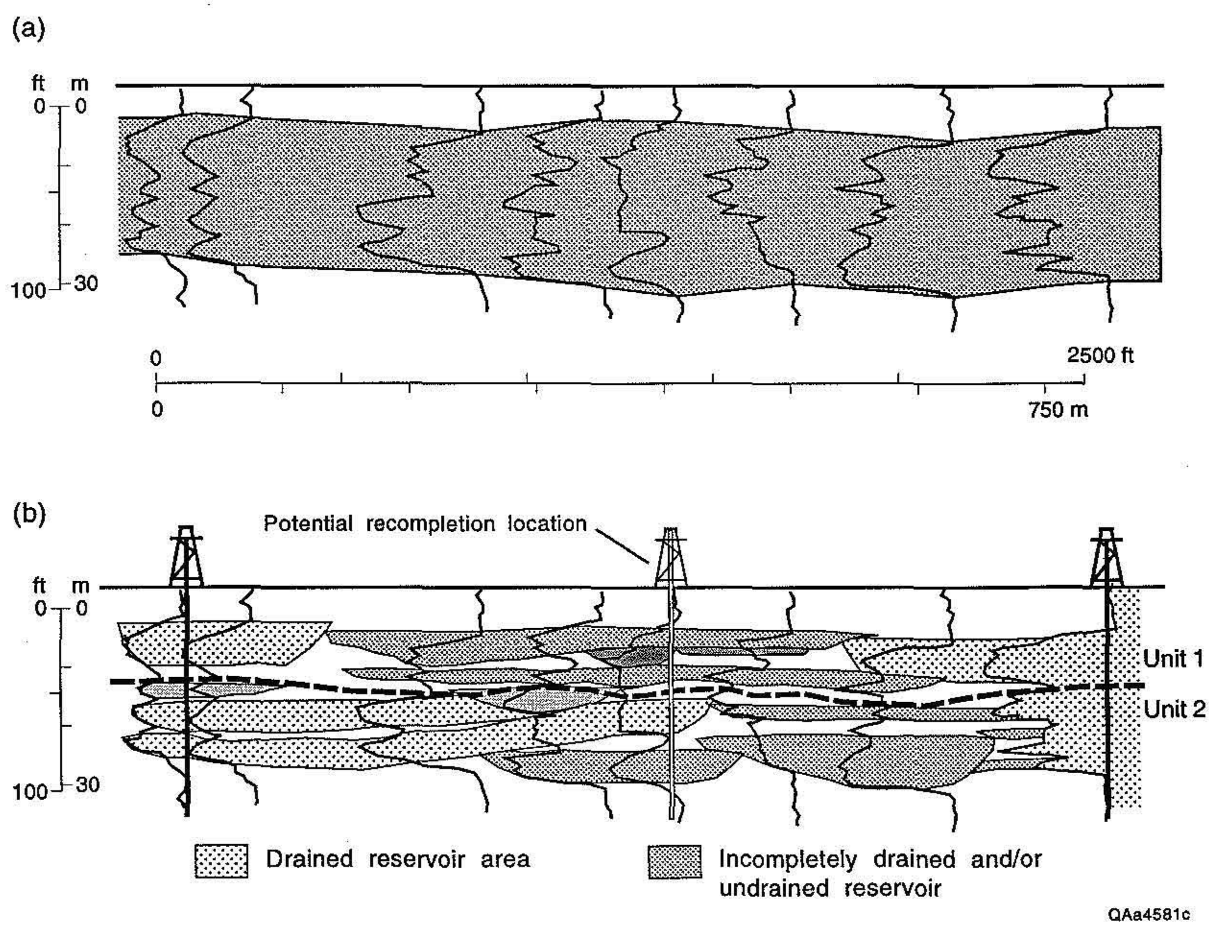

Figure 2. Schematic geological cross section contrasting the generalized interpretation of a sandstone reservoir as a simple, laterally continuous (homogeneous) producing zone (a) with a more detailed interpretation of the same sandstone unit as a complex heterogeneous zone consisting of multiple reservoir compartments (b). In the traditional example of the simple reservoir unit (a), good reservoir continuity suggests that the reservoir can be completely drained at the current well spacing. The complex architecture illustrated in (b) indicates the presence of facies boundaries within the sandstone that create multiple compartments, some of which are only partially drained or are completely untapped at the present well spacing. Modified from Jackson and Ambrose (1989).

Microscopic heterogeneity can be identified through thin section and scanning electron microscopy (SEM). Grain size, mineralogy, clay content, and the geometries of pores and pore throats can be observed. Generalities regarding the communication within the pore system can be deduced and potential undesirable interactions with production fluids can be predicted (Almon and Davies, 1981).

Petrophysical Evaluation

The goal of petrophysical analysis is accurate determination of original and subsequent fluid saturations within the reservoir rock, as well as quantification of fluid flow capacity of the reservoir. Specifically, this requires determination of reservoir porosity, permeability, porosity–permeability relationships, total oil saturation, residual oil saturation, and irreducible water saturation. Routinely, average values of these quantities are determined for an entire reservoir and applied uniformly to calculate such critical values as total reservoir volume. Such an approach can be grossly misleading in heterogeneous reservoirs. Instead, average values must be determined for each specific facies encountered, and the volumetric importance of each facies must be established. Neglecting such details can result in significant errors in the evaluation of original oil in place, leading to inaccurate conclusions regarding remaining reserves.

Petrophysical analysis is routinely accomplished through quantitative analysis of core material, including special core analysis, and modern geophysical logs. However, in mature fields, especially those discovered and developed several decades ago such as fields within the Frio Fluvial-Deltaic Play, modern well log suites are rare and very little reliable special core analysis data is available. Complicating matters, nearly all of the core material originally obtained from these fields has since been destroyed.

Such is the case with Rincon field. The few available modern well logs were complimented with special core analysis data from two relatively recent cores, including capillary pressure, formation resistivity factor (FRF), and core flood measurements to establish a reference data set. In older well log suites where porosity logs were not available, an algorithm was developed to determine porosity from spontaneous potential (SP) and resistivity logs. These values were then compared with the reference porosity values obtained from modern wells to assure accuracy.

Calculated porosity values were then combined with cementation exponents (constrained by FRF measurements) and measured resistivity to determine total oil saturations. Residual oil saturations and irreducible water saturations, determined from special core analysis, were then subtracted from total saturations to deduce mobile oil saturations.

Porosity values from old logs were also used to determine permeability in wells where no routine core analysis data was available. This was accomplished by establishing a facies-by-facies porosity–permeability relationship using modern well logs and abundant routine core analysis. The porosities derived from old logs were then transformed through this relationship into permeabilities, which were used to apportion commingled production data to individual flow units.

Production History Analysis

Establishing the production history of a reservoir is critical to identifying the residency of the remaining resource. Cumulative production on a flow-unit by flow-unit basis must be tabulated in order to calculate remaining reserves for each flow unit using values of original oil in place. The cumulative production from each flow unit in each well must also be plotted as drainage radii in map view to identify areas of drained and undrained reservoir. Produced volumes are then compared to the size of the compartment contacted by the pertinent completion to determine possible incompletely drained compartments (if produced volumes are less than compartment volumes) or as a check of interpreted compartment boundaries (if produced volumes are larger than compartment volumes).

In addition, a year-by-year mapping of water cut can be used to document water encroachment, which likewise would serve as a check of interpreted compartment boundaries. The fluid and pressure history of individual completions can provide information regarding communication between compartments across sealing boundaries or baffles (Lord and Collins, 1992). For example, if pressures or volumes increase in a well following a shut-in period, this may indicate that the compartment contacted by that well bore has been partially replenished by an adjoining compartment across a leaky compartment boundary.

In many mature fields, operators may have completed several zones or flow units simultaneously to increase production rates. In this case, no definitive record of production from a compartment or flow unit may exist, and it must therefore be estimated if an analysis of the residency of remaining reserves is to be done. Many instances of commingling exist within the study area at Rincon field. Permeability values determined from log-derived porosity values and porosity–permeability relationships were used to calculate permeability-ft (Kh) values that can serve as estimates of flow capacity. Where production has been commingled, the relative flow capacities of individual zones contributing to production were used to allocate a percentage of the total well production to each zone. Though somewhat inexact, this step was required if an effective integration of geologic and engineering parameters was to proceed.

Integration: Identifying the Residency of Remaining Reserves

The distribution of remaining reserves is a function of the architecture of reservoir facies, the volume of total original oil in place, and the volume of oil produced. Documenting this residency requires an integration of all characterization efforts. The results of petrophysical analyses must be integrated with the identified reservoir architecture to document the residency of original oil in place. The production history is then introduced to determine which reservoir compartments have been thoroughly drained, which are partially drained, and which compartments are untapped. The production history also must be compared carefully with compartment distribution, as mentioned previously, to evaluate the accuracy of geologic interpretations and identify any partially leaky compartment boundaries.

A preliminary assessment of reserve growth opportunities in each flow unit has been performed by calculating an estimate of original oil in place for the unit, subtracting residual oil volumes calculated using a playwide average residual oil saturation value, and qualitatively comparing this with maps of unit completions. Estimates of recovery efficiency can be calculated by comparing estimates of original oil in place and cumulative production, whereas estimates of effective drainage radii for each completion can be calculated by dividing the ratio of production to original mobile oil in place (multiplied by the total reservoir area) by the number of completions.

Before project completion, a more detailed assessment of the residency of remaining reserves will be established. This will be done by constructing maps of original mobile oil in place and subtracting mapped values of reservoir area drained. This generation of maps will take advantage of detailed petrophysical analyses in which porosity, saturation, and permeability values are calculated for each specific facies. The result of the subtraction of the two maps will be a map of remaining mobile oil volume, which can then be used to delineate final reserve growth opportunities.

Designing an Optimized Recovery Program

The result of the integration process is a map for each flow unit of remaining mobile oil, as well as information regarding effective drainage radii for each flow unit. This information can be combined to determine areas of remaining mobile oil that can be drained by existing well bores (recompletion opportunities) and those areas that must be reached with new well bores through geologically targeted infill drilling. Maps of these reserve growth opportunities should then be overlain to identify areas containing multiple vertically stacked infill potential. Alternately, laterally adjacent infill potential within a single flow unit can be targeted with a horizontal well bore. The key to optimizing the economic viability of infill wells is to establish infill opportunities in as many flow units as possible such that a straight or directional well bore intercepts a large total volume of reserves.

IDENTIFICATION OF INCREMENTAL RECOVERY OPPORTUNITIES IN RINCON FIELD: THE D AND E RESERVOIR INTERVALS

Rincon Field and Reservoir Setting

Structural and Stratigraphic Setting of the Frio Fluvial-Deltaic Sandstone Play

The entire Frio Formation in Texas has been divided into 10 plays based on regional variations in structure and depositional setting (Kosters and others, 1989). Fields in the play known as the Frio Fluvial-Deltaic Sandstone Play produce oil and gas from the eastern, downthrown side of the Vicksburg Fault Zone, a major down-to-the-coast listric normal growth fault system that parallels the Gulf coastline for 100 mi (Fig. 3). Faulting not only offsets the Vicksburg Formation but also affects the lower portions of the overlying Frio Formation. Oil-bearing traps consist predominantly of shallow rollover anticlines that formed during later stages of fault movement along the fault zone (Stanley, 1970; Tyler and Ewing, 1986). Deeper structures within Vicksburg strata are characterized by synthetic and antithetic faults with large displacements commonly in excess of hundreds of feet. Oil and gas reservoirs in this play occur within a 2,000-ft stratigraphic interval in fluvial-deltaic sandstones primarily of the Oligocene Frio Formation.

The Frio Formation is part of a sedimentary wedge that records a major depositional offlap episode of the northwestern shelf of the Gulf of Mexico Basin (Fig. 4). Frio sediments in South Texas represent the entry of a major extrabasinal river into the Gulf Coast Basin along the axis of the Rio Grande Embayment in Oligocene time. This ancient fluvial-deltaic complex has been divided into the Gueydan fluvial and Norias delta systems (Galloway and others, 1982). Fields within the Frio Fluvial-Deltaic Sandstone Play occupy a transitional area between these two depositional systems (Fig. 5). In general, lower Frio sandstones represent deltaic facies of the ancestral Norias delta system, and middle and upper Frio sandstones predominantly reflect deposition in fluvial channels of the Gueydan fluvial system (Galloway and others, 1982).

Important oil reservoirs in this sequence occur within progradational, fluvial-dominated deltaic depositional facies within the upper Vicksburg and lower Frio intervals and in aggradational fluvial facies in the middle Frio section.

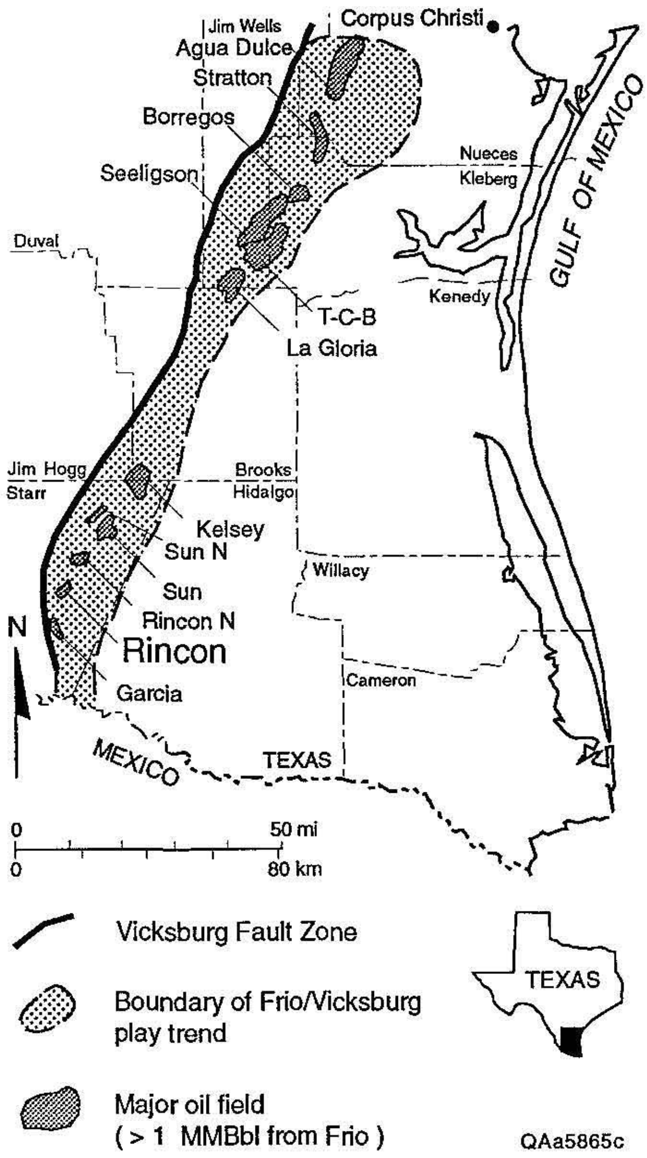

Figure 3. Map of South Texas showing location of fields within the Frio Fluvial-Deltaic Sandstone Play along the Vicksburg Fault Zone. Fields shown include those which have produced more than 1 MMbbl. (Modified from Galloway and others, 1983, and Kosters and others, 1989.)

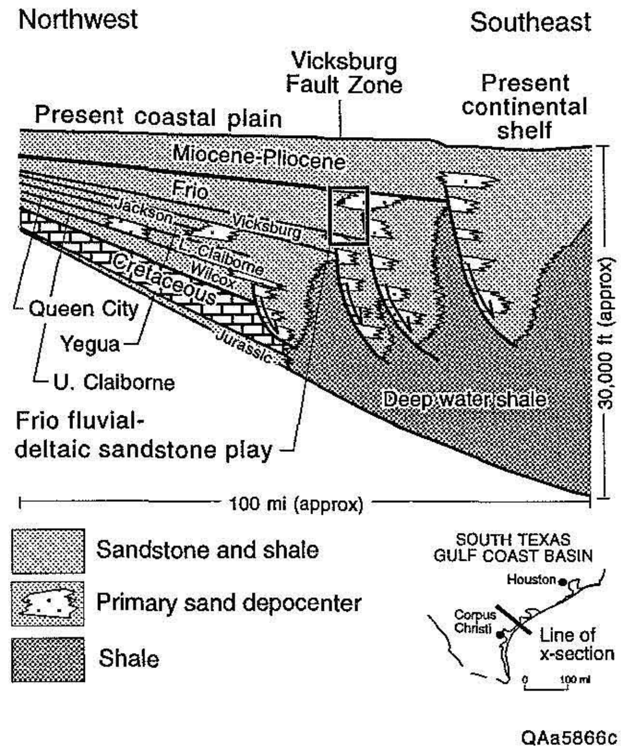

Figure 4. Schematic cross section of the South Texas Gulf Coast Basin. Modified from Bebout and others, 1982.

Selection of Rincon Field for Detailed Study

In an earlier study, engineering and geologic data were compiled and screened from reservoirs distributed among fields along the entire play in South Texas that have produced more than 1 MMSTB and have wells currently producing oil from Frio zones (Holtz and others, 1994). Data including the number and sizes of individual Frio reservoirs, cumulative past production, and the present status of Frio production were summarized and compared between fields. Preliminary estimates of volumes of original oil in place and cumulative production, completion densities for individual fields, and current reservoir recovery efficiencies formed the basis for identifying representative reservoirs that have a large remaining oil resource, are in danger of premature abandonment, and have geological and production data in sufficient quantity and of suitable quality to facilitate detailed reservoir characterization studies. Frio reservoirs in Rincon field satisfied these criteria and were selected for detailed study (Table 1).

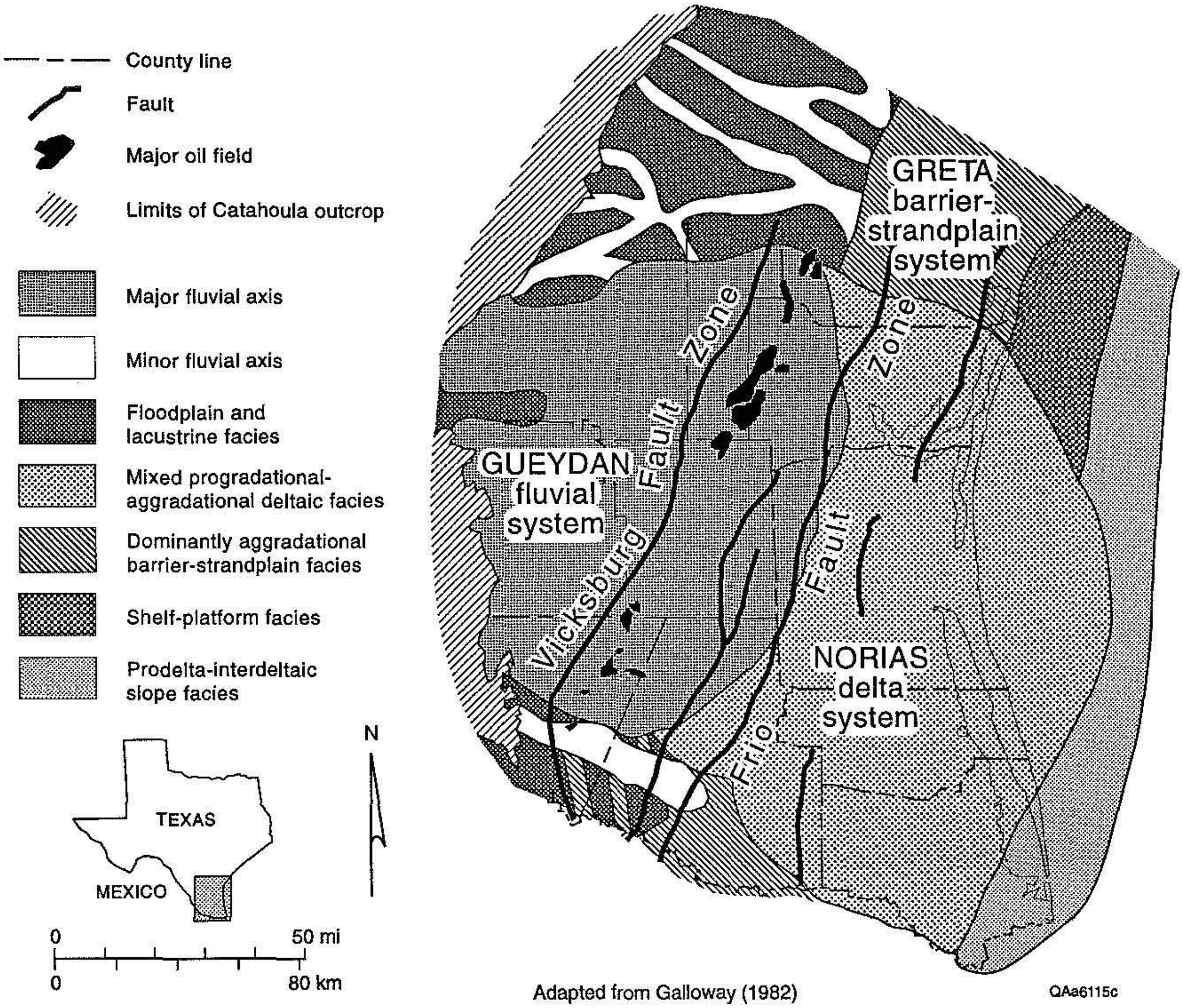

Figure 5. General distribution of the Norias delta and Gueydan fluvial depositional systems responsible for deposition of the Frio stratigraphic unit. The Frio sediments in the vicinity of the Vicksburg Fault Zone were primarily deposited in moderate to high sinuosity mixed-load stream environments of the Gueydan Fluvial system. (Map distribution from Galloway and others, 1982).

The primary objectives of initial reservoir studies in Rincon field (Table 2) were to (1) identify general styles of interwell stratigraphic heterogeneity, (2) evaluate past production behavior, (3) complete a preliminary assessment of additional resource potential of individual reservoir units, and (4) select individual reservoir zones with significant potential for incremental recovery for further analysis to delineate specific locations and volumes of unrecovered mobile

Table 1. Key criteria for reservoir selection.

KEY CRITERIA	*BENEFITS*
1. Reserve growth potential of unrecovered resources and declining well counts	• Targets large volumes of mobile oil resources in greatest danger of remaining undeveloped
2. Large producing area, limited well completion density	• Increased opportunity for infill potential
3. Amount, quality, and type of field data	• Provides resources to perform detailed reservoir characterization studies, identify untapped and incompletely drained compartments, and quantify additional recoverable resources
4. Stratigraphically complex and structurally simple field area	• Greater reservoir heterogeneity, more likely to contain unproduced compartments
5. Current drilling activity within reservoir	• Indication of operator cooperation and commitment to further drilling • Presents opportunities for study results to provide near-term impact on development

Table 2. Field-scale reservoir characterization strategies.

Field-scale reservoir characterization

Goals:

- Characterize reservoir variability and degree of heterogeneity.
- Identify zones with significant reservoir heterogeneity and a high potential for containing unproduced oil.

Methodology:

- Stratigraphic log correlations, reservoir mapping, analyses of petrophysical and production data.
- Assess differences in sandstone depositional styles and production behavior to evaluate potential for compartmentalization of significant volumes of unrecovered oil.

oil. A thorough evaluation of available engineering and geological data from Frio reservoirs in the Rincon field study area was completed. Engineering data were used to determine completion density, assess past production behavior, including a reservoir's response to waterflooding, and estimate overall recovery efficiency. Preliminary geologic characterization efforts in Rincon field consisted of refining the stratigraphic framework of the productive reservoir section and assessing the stratigraphic distribution of remaining oil potential within the field study area (McRae and Holtz, 1994). Reservoir mapping and stratigraphic log correlations were used to describe general depositional styles within the productive 1,000-ft-thick stratigraphic interval and to assess the potential for compartmentalization of significant volumes of unrecovered oil. Evaluation of production histories for important Frio oil reservoirs was integrated with preliminary studies of facies architecture to identify zones with high potential for containing compartments with unproduced oil, and reservoir zones were prioritized for incremental reserve growth opportunities. Petrophysical data were summarized for reservoirs within the field to establish mean values and ranges for each of the engineering attributes that influence the calculation of oil volume (Fig. 6). Reservoir data were further evaluated to identify relationships between stratigraphic position and porosity–permeability characteristics of selected reservoir sandstones and their ability to produce hydrocarbons. Data from the two most prolific reservoirs in the field, the Frio D and E sandstones, were selected to be the focus of detailed characterization and delineation efforts.

Location and Geologic Setting of Rincon Field

Rincon field is located in eastern Starr County, Texas, approximately 120 mi southwest of Corpus Christi and approximately 20 mi north of the United States–Mexico border (Fig. 3). The entire Rincon field area covers over 20,000 acres and contains more than 640 wells. The area of investigation covers approximately 5,000 acres in the northern portion of the field, includes nearly 200 wells (Fig.7), and is limited to productive reservoir sandstones within the Frio section.

The general structure in the shallow Frio section at Rincon is characterized by a northeast-trending, downthrown asymmetric rollover anticline that plunges gently to the northeast and is bounded to the west by the Sam Fordyce–Vanderbilt Fault, a major growth fault associated with the large Vicksburg Fault Zone system (Fig. 8). Frio production associated with the shallow structure is both stratigraphically and structurally controlled. Hydrocarbons are trapped in zones within the rollover anticline downdip of the major growth fault and exist in multistoried and multilateral sandstone reservoirs that form complex stratigraphic traps draped over an anticlinal nose.

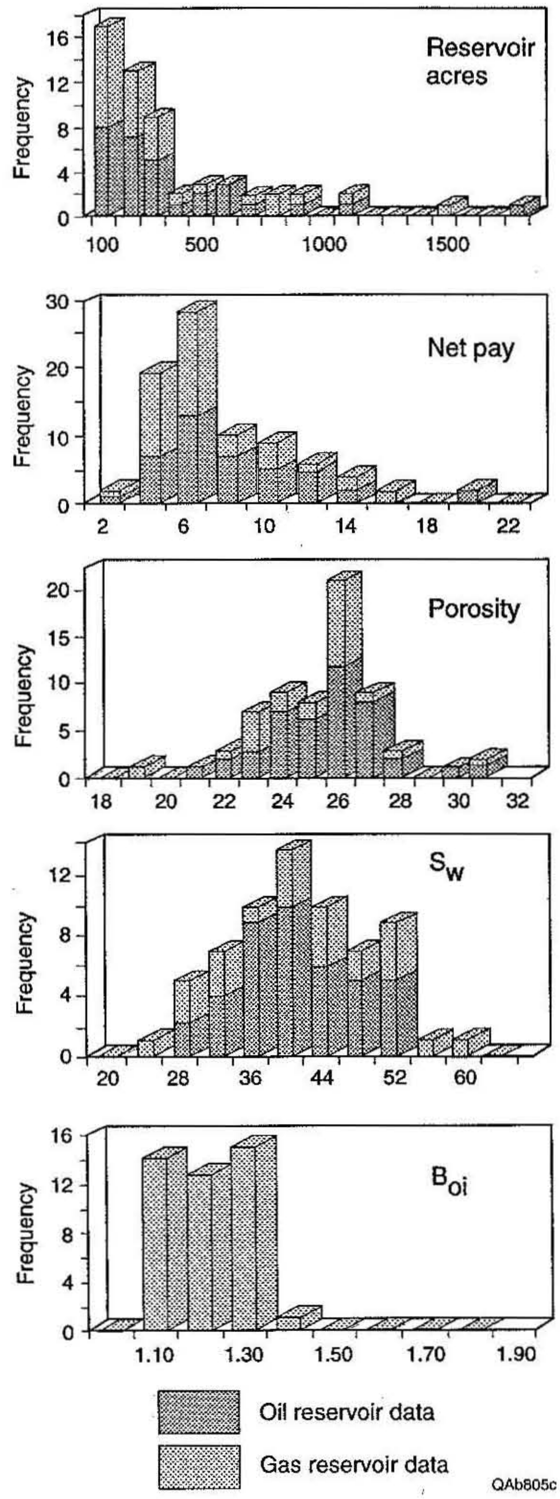

Figure 6. Histograms of engineering attributes for reservoirs within Rincon field. Solid bars represent values for oil reservoirs and hachured bars signify gas reservoir values.

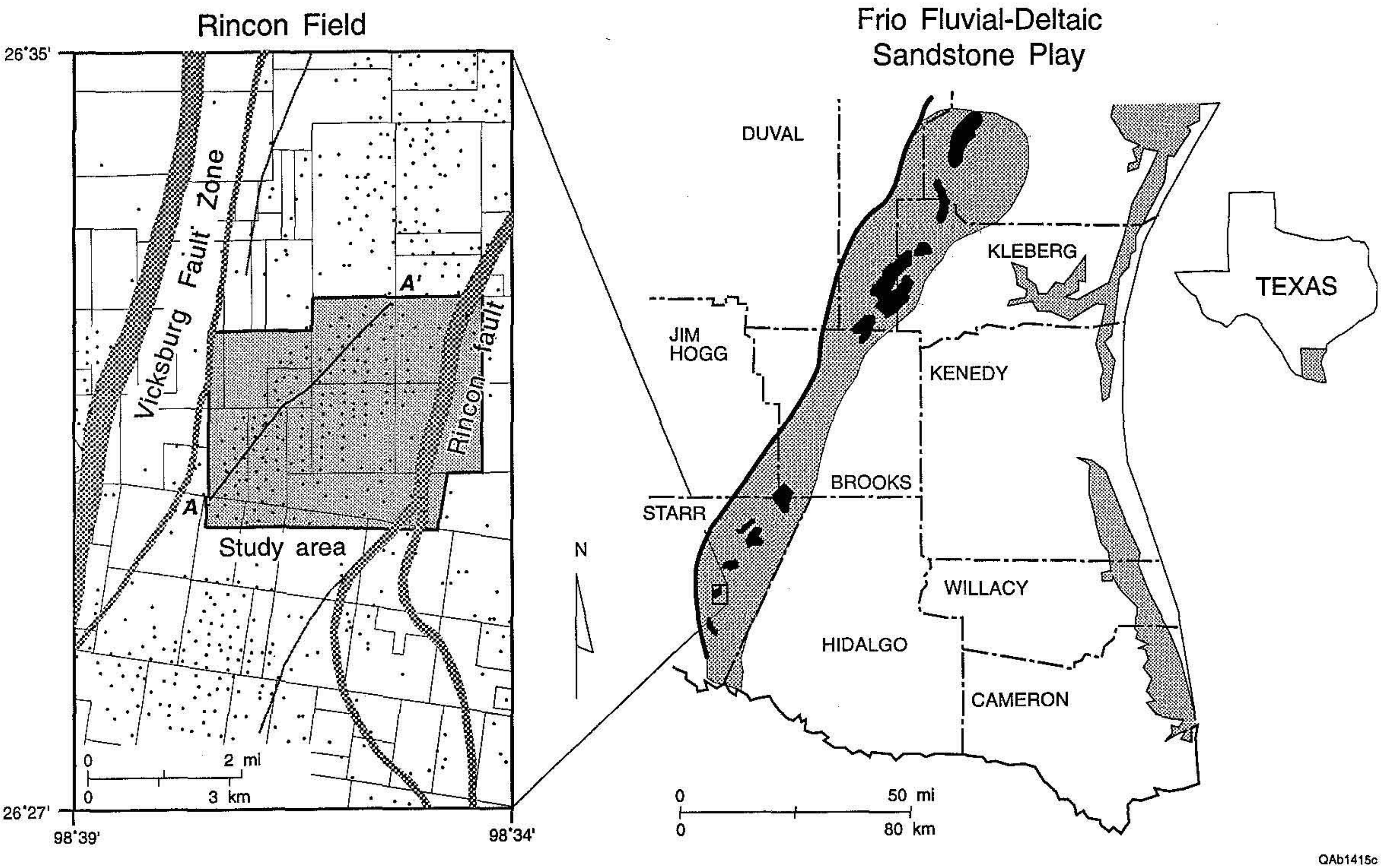

Figure 7. Location map of Rincon field within the Frio Fluvial-Deltaic Sandstone Play and area of field selected for detailed reservoir studies. Cross section A–A′ shown in Fig. 11.

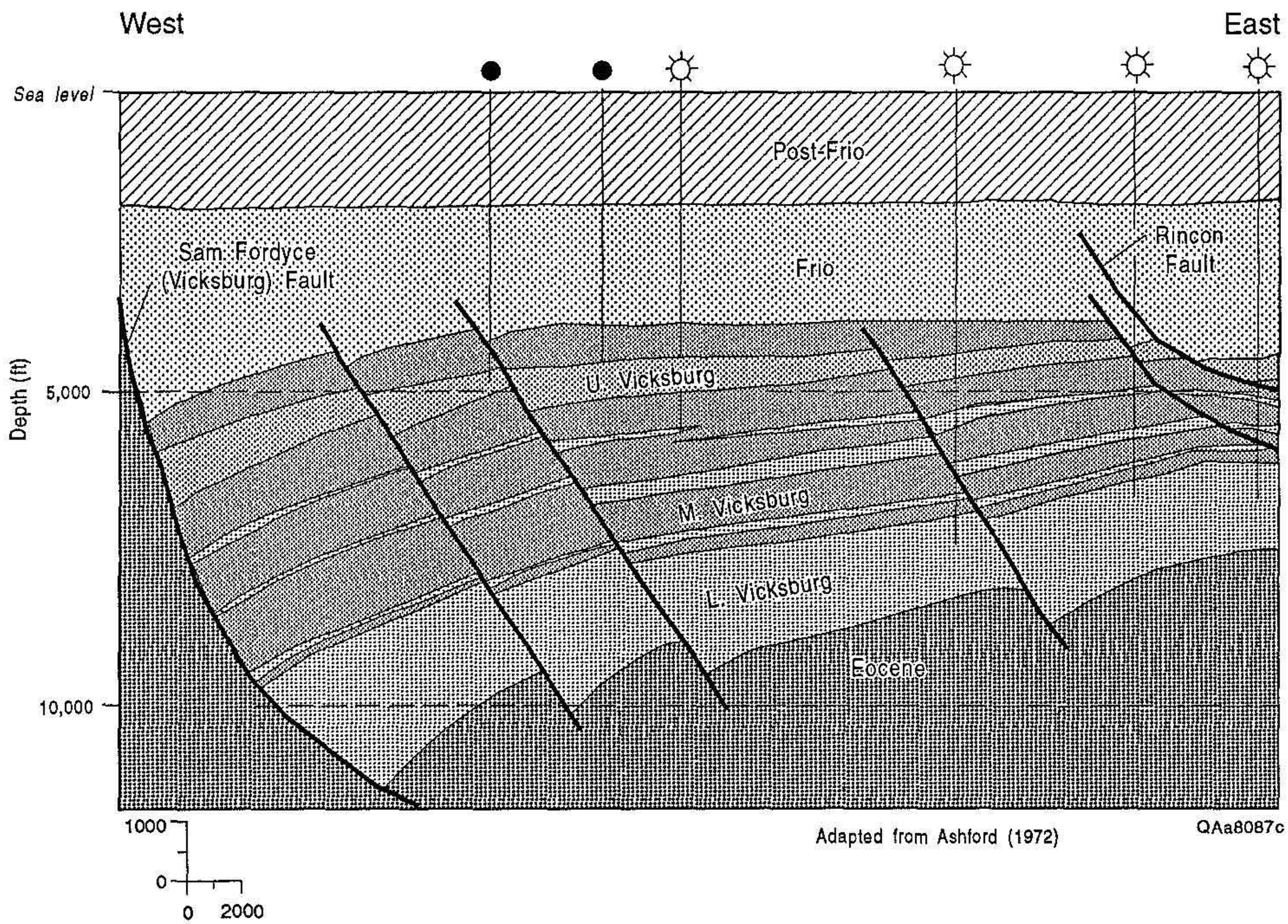

Figure 8. Generalized west-to-east cross section through Rincon field illustrating structural setting of a representative field in the Frio Fluvial-Deltaic Sandstone Play (adapted from Ashford, 1972).

More than 50 individual productive reservoirs within the stratigraphic interval from 3,000 to 5,000 ft have been identified and mapped across the Rincon field area, and they range in dimension from only a few acres to complex, interrelated reservoir systems that are present across the entire field. Individual reservoir units occur both as narrow channel-fill sandstones isolated vertically and laterally by very low permeability overbank facies and floodplain mudstones and as large channel complexes consisting of multiple thin sand units that combine into a single large communicating reservoir. The variability in sandstone geometries and the complex multilateral and multistacked nature of these reservoirs provide excellent potential for identifying additional hydrocarbons that have been isolated in untapped and incompletely drained reservoir compartments.

Rincon Field Production History

Frio and Vicksburg reservoirs in Rincon field have produced more than 65 million barrels (MMbbl) of oil under combined natural water drive and gas cap expansion since discovery of Rincon field 55 years ago in 1939. Frio production peaked in 1944, when production averaged approximately 7,300 bbl/d. Vicksburg production began in 1950, and, since that time, most field exploration efforts have focused on prolific deeper Vicksburg structures (Fig. 8) . Production from 38 separate Frio reservoirs has yielded over 45 MMbbl of oil (Table 3).

Three main Frio reservoirs, the D, E, and G sandstone units, account for 69 percent of all completions and 88 percent of the oil produced in the field area selected for study (McRae and others, 1994). Most of the Frio oil reservoirs had initial gas caps, and reservoirs have produced under a combined natural water drive and gas cap expansion. Gas injection took place during the early years of field production in order to maintain reservoir pressure and extend the flowing life of the wells. Waterfloods performed in each of these large reservoir zones met with varying degrees of success. Oil production from these major reservoirs has declined steadily since 1968 and has been accompanied by increasing abandonments of individual reservoir zones. As of

1990, there were only 27 oil wells remaining in the field that were producing or had shut-in status, and average daily rates had declined to 373 bbl of oil and 4,576 Mcf of gas.

Table 3. Production summary and reservoir statistics for Rincon field.

General field information		***Reservoir characteristics*** **ranges (mean)**	
Discovery year:	1939	Porosity (%)	16–30 (26)
Total acres:	20,520	Permeability (md)	41–1,649 (80)
Wells:	640+	Initial S_w (%)	28–67 (42)
Production characteristics		Net pay (ft)	5.0–20.4 (8.8)
Depth range of producing interval:	3,000–5,000 ft	Reservoir area (acres)	20–2,200 (400)
Number of reservoirs:	30		
Cumulative oil production:	65 MMBO (total) 45 MMBO (Frio only)	***Fluid characteristics***	
No. of reservoirs with >1 MMBO production:	14	Oil gravity	40°–48 °API (42°)
Active completions: (as of 1991)	25 oil, 30 gas	Formation volume factor	1.14–2.05 (1.26)
Current flow rates: (as of 1991)	373 bopd 4576 Mcf/d		

Development of a Reservoir Stratigraphic Framework

The development of a detailed regional stratigraphic and structural context for a reservoir is a critical step in evaluating its potential for secondary hydrocarbon recovery. Sequence-stratigraphic concepts provide a chronostratigraphic framework in reservoir studies that is useful in delineating the structure of reservoir flow units and also provide a means of transporting results of reservoir studies to other fields in analogous stratigraphic settings. Construction of a reservoir framework at the sequence and parasequence scales provides a means for the natural packaging of strata into genetic units that correlate well to petrophysically defined units at the interwell scale (Tyler and others, 1992). Definition of lithologic and diagenetic reservoir flow-unit architecture of fluvial-deltaic sandstones within the context of a well-defined sequence-stratigraphic framework can provide a model to predict the distribution and continuity of permeable zones in other reservoirs deposited in analogous depositional settings. Previous detailed work on the regional geology of the Frio depositional sequence in South Texas (Galloway, 1977, 1982, 1989; Galloway and others, 1982) and several recent reservoir characterization studies of Frio gas reservoirs (Jirik, 1990; Kerr, 1990; Kerr and Jirik, 1990; Kerr and others, 1992, Grigsby and Kerr, 1993) provide an excellent context in which to study individual facies components of oil-bearing reservoirs in the Fluvial-Deltaic Sandstone Play.

In the Rincon field section, a prominent low resistivity marker interpreted to be an important flooding surface separates the thicker, generally coarsening upward progradational units in the lower Frio third-order unit from thinner, dominantly aggradational channel deposition in the middle Frio section (Fig. 9a). The majority of Frio production at Rincon occurs within a 1,000-ft interval of interstratified sandstones and mudstones (Fig. 9b). Laterally persistent low-resistivity surfaces interpreted to represent floodplain or interdeltaic mudstones separate primary reservoir sandstone zones that are commonly 50 to 150 ft thick. These fourth-order reservoir zones are, in turn, composed of several individual, 5- to 30-ft-thick channel-fill units (Fig. 9c). The major cause for stratigraphic complexity and compartmentalization of hydrocarbons in these sandstones is their variability in geometry and the multilateral and multistacked nature of individual fifth-order reservoir units. Fourth-order reservoir units at Rincon field were evaluated to identify specific reservoir styles that are representative of those observed throughout the play. Understanding the specific stratigraphic context of the reservoirs selected for study will facilitate the transfer results of this study to other reservoirs, other fields, and other analogs beyond the Frio in South Texas.

The stratigraphic positions of important reservoir units in Rincon field within the context of the larger scale genetic stacking sequence were identified to assess the importance of reservoir stratigraphy on hydrocarbon production, recovery efficiency, heterogeneity style, and the potential for compartmentalization of additional oil resources. Twenty-four low-resistivity markers representing seven major (4th order) bounding surfaces and 17 secondary (5th order) surfaces in 184 wells were correlated in a series of stratigraphic cross sections across the field study area. Wireline core data representing more than 1,500 analyses from more than 100 wells in the Rincon field study area were assigned to individual upper Vicksburg, lower Frio, and middle Frio reservoir subunits and evaluated to assess heterogeneity within each of these major reservoir stacking intervals.

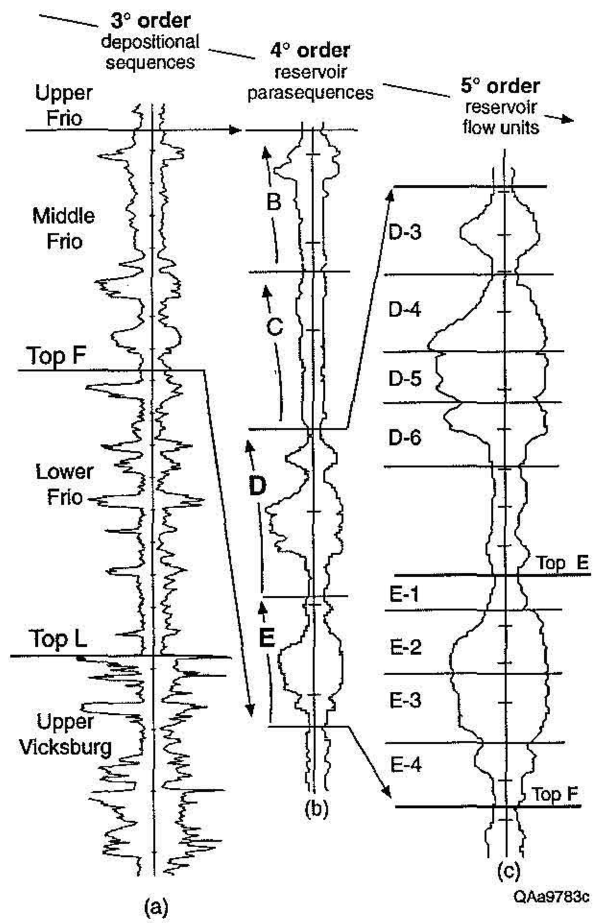

Figure 9. Type logs illustrating (a) the general depositional sequence for the productive Frio–upper Vicksburg reservoir interval, (b) the stratigraphic context of the middle Frio reservoir sequence in Rincon field, and (c) the reservoir nomenclature of individual producing units within the Frio D–E interval selected for detailed study.

Depositional Systems and Reservoir Attributes

A typical log from the productive reservoir interval in Rincon field is shown in Fig. 10. The F shale marker represents the division between lower and middle Frio reservoirs, as it is located where a change in sedimentation style occurs from deposition of net progradational sandstone packages to primarily aggradational sand deposition. A representative southwest-northeast-trending strike section across the field area is illustrated in Fig. 11. Reservoirs in the middle and lower Frio sections consist of multiple stacked pay sandstones. Interpretations supported by SP log profiles and whole core studies indicate that the dominant reservoir lithofacies are fluvial channel-fill deposits. Individual reservoir sandstones (5th order units) within each zone are

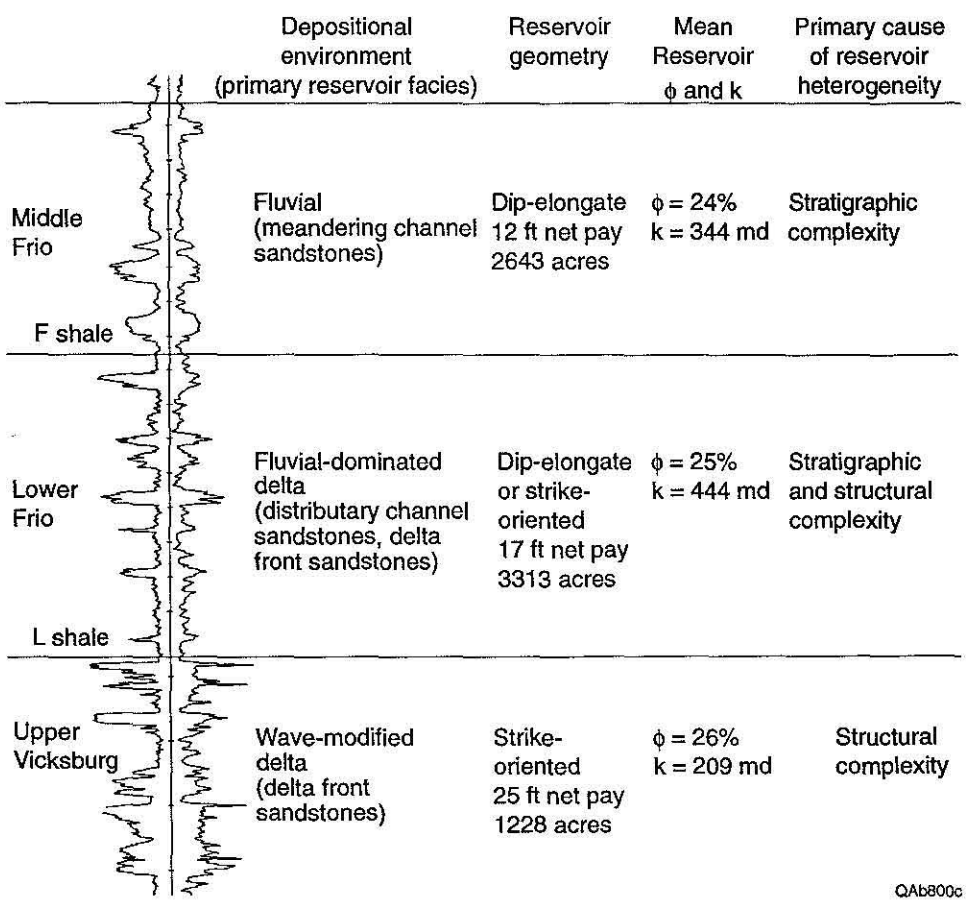

Figure 10. Depositional systems and reservoir attributes of the Rincon field reservoir section.

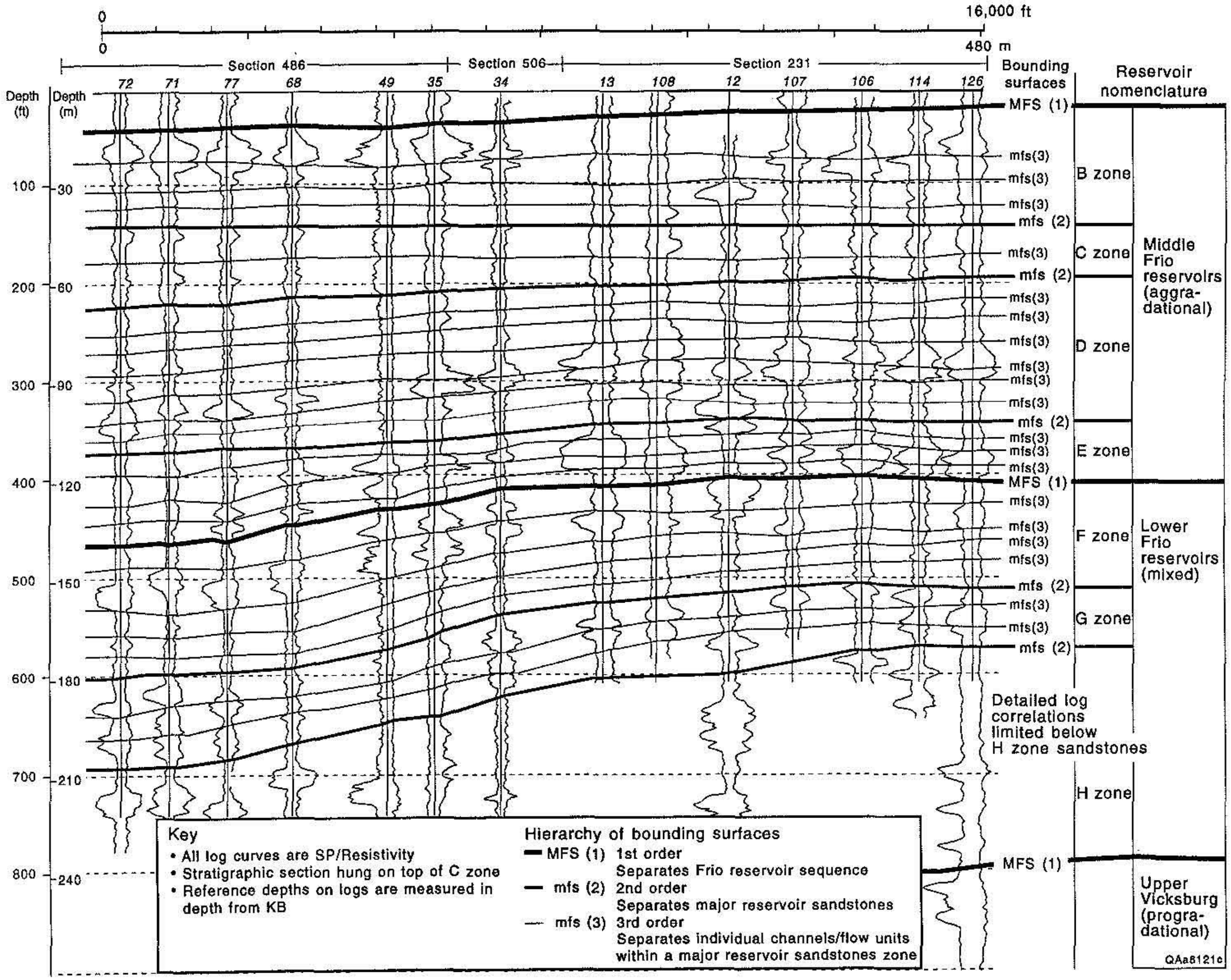

Figure 11. Regional stratigraphic strike cross section across Rincon field study area. Line of section is identified as A–A′ on the map shown on Fig. 7. Datum is the top of Frio B sandstone, which also marks the top of the productive oil reservoir interval in the field.

commonly 5- to 30-ft-thick channel-fill units and have lateral dimensions ranging from 1,000 to more than 6,000 ft. The major cause for reservoir complexity and compartmentalization of hydrocarbons is a result of this variability in sandstone geometry and the multilateral and multistacked nature of these individual reservoir units. Characteristics specific to each stratigraphic reservoir interval are discussed in more detail below.

Upper Vicksburg Reservoirs

Vicksburg reservoirs in Rincon field include the L sandstone unit shown in the lower portion of the log interval illustrated in Fig. 10. These reservoirs consist of thick progradational (seaward-stepping) deltaic sandstone deposits that occur in units 50 to 150 ft thick and are separated by 50- to 200-ft-thick intervals of mudstone. Primary reservoir facies are channel-mouth-bar sandstones that are interbedded with prodelta mudstone and siltstone (Fig. 12). Individual upward-coarsening channel-mouth-bar deposits are generally less than 50 ft thick and stack to produce repetitive cycles that can reach 150 to 200 ft in thickness.

Vicksburg reservoirs in Rincon field are not presently targets for resource delineation and additional recovery through our studies, which emphasize characterization of stratigraphic heterogeneity. This is because their deposition was strongly influenced by faulting associated with the development of the Vicksburg Fault Zone (Coleman and Galloway, 1990, 1991), and correlations necessary to document depositional heterogeneity and stratigraphic compartmentalization in these reservoirs are difficult. Our reservoir studies are focusing on the structurally uncomplicated Frio reservoir interval where there is better potential for identifying lateral facies heterogeneity and stratigraphic compartmentalization, and there are also much more data available.

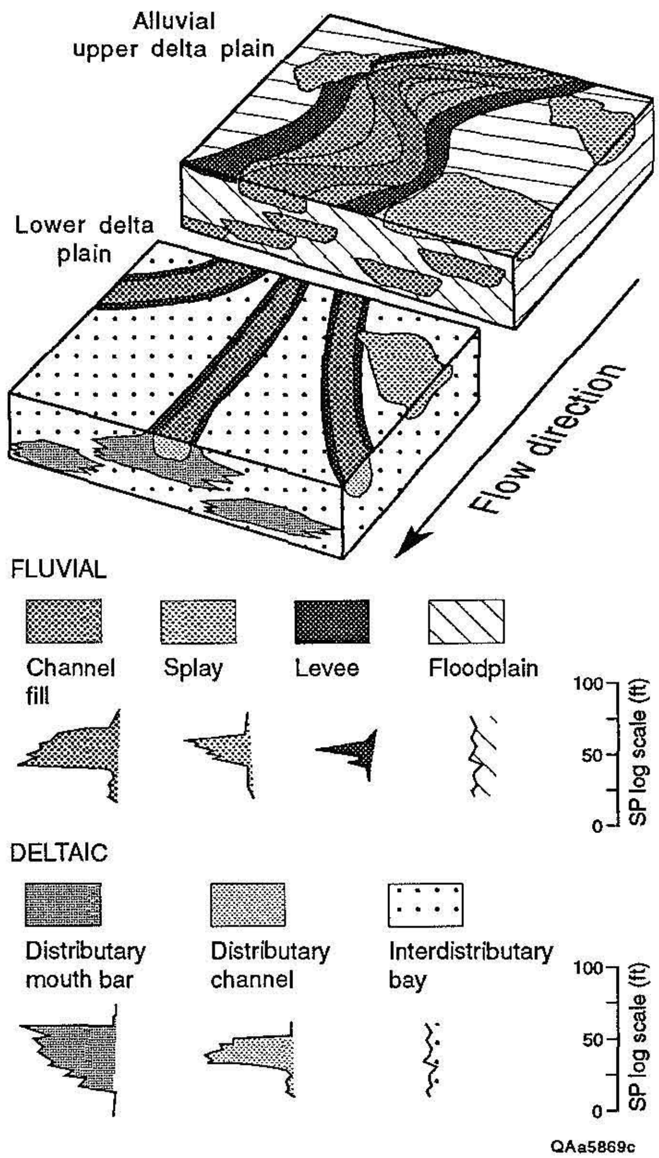

Figure 12. Schematic block diagram illustrating general three-dimensional relationships and characteristic SP log responses in fluvial reservoir and nonreservoir facies (modified from Galloway, 1977).

Lower Frio Reservoirs

In Rincon field, the lower Frio stratigraphic interval appears to represent deposition in an aggradational to mixed aggradational and progradational setting within the Gueydan fluvial system. The lower Frio reservoir interval shown on the log in Fig. 10 and the stratigraphic cross section in Fig. 11 are interpreted to correspond to an interval of mixed progradational and aggradational sedimentation. The F shale is taken to mark the boundary between the mixed aggradational and progradational reservoirs in the lower Frio section and the purely aggradational deposition that characterizes the middle Frio section.

Reservoir facies in the lower Frio interval are interpreted to represent predominantly fluvial channel and delta-plain distributary-channel sandstones. Channel units are distributed as elongate, dip-parallel belts. Individual, upward-fining channel sandstone units expressed as bell-shaped SP log profiles, range from 5 to 20 ft thick and commonly stack to produce amalgamated units that have vertical thicknesses of 10 to 50 ft. These stacked sandstone units commonly display an upward-thickening trend. Although sandstone units are, on average, thicker than in middle Frio reservoir zones, sandstone body continuity is generally less than in middle Frio fluvial channels. This may be because distributary channel-fill sandstones are commonly narrower and are flanked laterally by sand-poor interdeltaic facies. Low-permeability mudstone facies locally encase and compartmentalize or isolate individual reservoir sandstones and create reservoir compartments that are the primary targets for additional oil recovery in the lower Frio interval.

Middle Frio Reservoirs

The depositional pattern in the middle Frio interval in Rincon field is characterized by sedimentation dominated by fluvial aggradation. Deposition in dip-elongate channel systems developed across the low-relief Oligocene Gulf Coastal Plain toward the shoreline in a direction from northwest to southeast (Fig. 5). Middle Frio reservoir facies consist primarily of dip-elongate fluvial channel-fill sandstones and are separated by nonreservoir facies that include levee siltstones and floodplain mudstones. Productive middle Frio reservoirs in Rincon field occur as both individual narrow channel-fill units isolated vertically and laterally by low-permeability overbank and floodplain facies and as large channel complexes with multiple sandstone lobes. Sandstones have individual thicknesses ranging from 5 to 30 ft but are commonly stacked into composite units with gross thicknesses between 20 and 60 ft. Low-permeability subfacies within the channel fill are responsible for the development of multiple reservoir compartments that may represent significant opportunities for additional recovery.

Selection of Reservoirs with High Potential for Incremental Recovery

The Frio D and E sand series are the two most highly prolific reservoir zones in Rincon field. Sandstones within this combined interval have produced more than 22 MMbbl of oil since production began in 1940 (Table 4). The Frio E sandstone consists of four individual sandstone units and has produced nearly 12 MMSTB of oil since production began in 1940. Secondary

Table 4. Summary of reservoir data for the Frio D and E zones in Rincon field.

	Frio D Sandstone	**Frio E Sandstone**
CURRENT STATUS:	95% of completions abandoned	85% of completions abandoned
DEPTH INTERVAL:	3700–3800 ft	3800–3900 ft
RESERVOIR UNITS AND GEOMETRY:	D-3,4,5,6 zones: fluvial channel system with dip-oriented geometry	E-1,2,3,4 zones: fluvial channel system with dip-oriented geometry
PETROPHYSICAL ATTRIBUTES: (Wireline core data)		
Mean porosity:	25% (range 21–26%)	26% (range 22–28%)
Geometric mean permeability:	50 md (range 23–91 md)	59 md (range 31–116 md)
Mean initial water saturation:	40.5%	37.5%
TOTAL PRODUCTION (1940–1990):	>9.8 MMBO	>14.0 MMBO
SECONDARY PRODUCTION:	200 MBO from waterflooding (2% total D production)	2.5 MMBO from waterflooding (21% total E production)
ORIGINAL ESTIMATED OOIP:	33.85 MMBO	37.04 MMBO
RECOVERY EFFICIENCY: (Operator data)	29% *(based on 27.5% ϕ, 40.5% S_w)*	38% *(based on 26.5% ϕ, 37.5% S_w)*
ESTIMATED RESIDUAL OIL:		
@ 50% probability:	15.4 MMBO (45% OOIP)	16.0 MMBO (43% OOIP)
@ 95% probability:	20.8 MMBO (61% OOIP)	21.7 MMBO (58% OOIP)
EST. REMAINING MOBILE OIL:		
@ 50% probability:	8.7 MMBO (26% OOIP)	7.0 MMBO (19% OOIP)
@ 95% probability:	3.3 MMBO (10% OOIP)	1.4 MMBO (4% OOIP)

waterflooding in the Frio E reservoir zone successfully accounted for 2.5 MMSTB of additional production. Using average reservoir values of 26.5% porosity and 37.5% water saturation, Frio E sandstones are estimated to have an overall recovery efficiency of 38%.

The main productive Frio D reservoir zone also consists of four stratigraphic units that have produced nearly 10 MMSTB oil. Frio D sandstones have similar reservoir attributes as Frio E reservoirs (average porosity of 25.2%, S_W of 40.5%, and estimated OOIP of approximately 35 MMSTB) but a significantly lower recovery efficiency of 28%. Waterflooding attempts in this reservoir zone accounted for secondary recovery amounting to only 2% of total D production. These disappointing results were attributed by the field operator to the heterogeneous nature of the D sandstone interval.

The stratigraphic complexity of this interval of vertically stacked and laterally coalescing sandstone lobes provides ideal conditions for the isolation of oil accumulations in multiple reservoir compartments, many of which are now incompletely drained or completely untapped. Significant additional reserves may be identified through integrated geologic and engineering studies that characterize the heterogeneity of the various reservoir facies.

Geologic Characterization of Frio D and E Reservoirs: Determination of Reservoir Architecture

The identification of additional oil resources in Frio D and E reservoir sandstones was pursued through the evaluation of existing oil production trends, facies mapping, and analysis of abundant petrophysical data from wireline cores and geophysical logs. Mapping sandstone thicknesses and facies distribution will identify the dimensions of individual flow units and provides critical insight into the reasons these reservoirs have experienced different production histories. Reservoir mapping was integrated with petrophysical models developed from the evaluation of core data and geophysical well logs to delineate original oil in place and the distribution of remaining hydrocarbon saturation. Specific locations of untapped and/or incompletely drained reservoir compartments with significant remaining oil resources may then be identified and targeted for incremental recovery.

Internal Reservoir Facies and Sedimentology

Detailed core studies were conducted on conventional core cut from the T. B. Slick A133 and A149 wells, located in lease block 231 near the center of the field study area (Fig. 13). A total of 155 ft of core was examined. Core descriptions from both wells, along with porosity and permeability profiles derived from conventional core analysis data, are illustrated in Figs. 14–16.

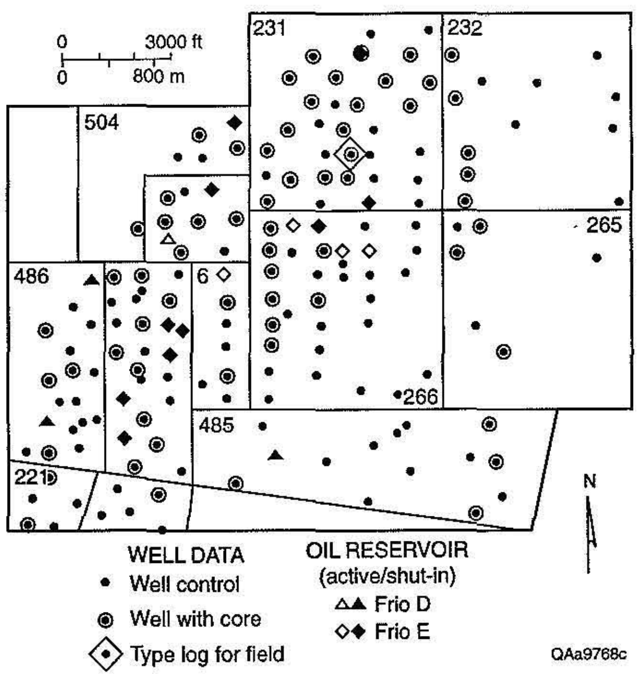

Figure 13. Detailed data map of area selected for study within Rincon field showing distribution of wells and available core data. The study is located within the central and northern portion of greater Rincon field and includes nearly 200 wells.

Unfortunately, the quality of the SP log for well A133 is very poor, and there is no SP log for well A149. Because the vast majority of log data available from wells in the study area are pre-1950 electric logs (SP, resistivity curves only), it was an original objective of this study to be able to calibrate core facies observed in these two wells to SP log response. Because of the lack

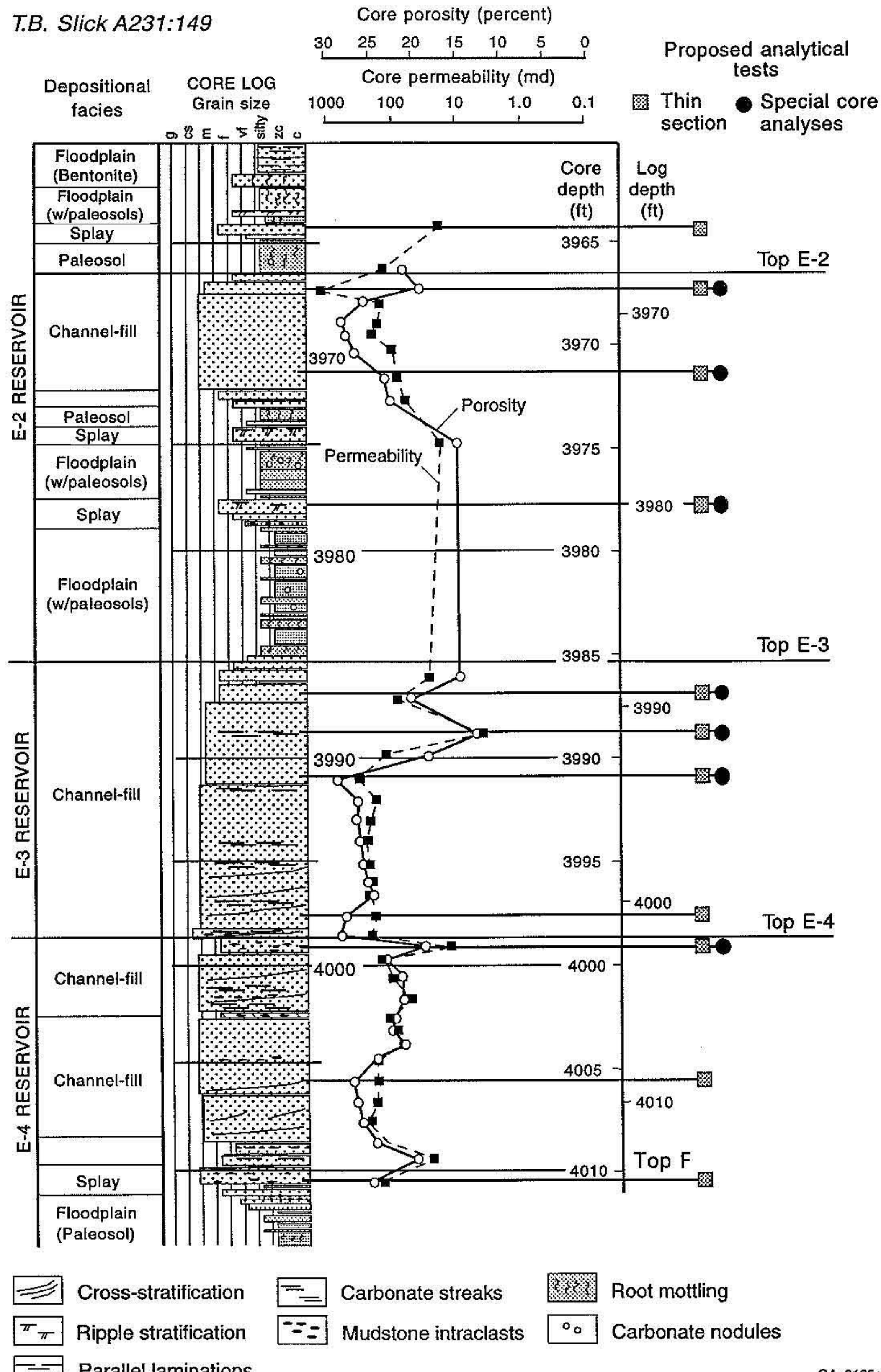

Figure 14. Graphic core log for the T.B. Slick 231:149 well over the Frio E reservoir zone, along with corresponding facies interpretations, core analysis data for porosity and permeability, and location of samples selected for petrographic and special core analyses.

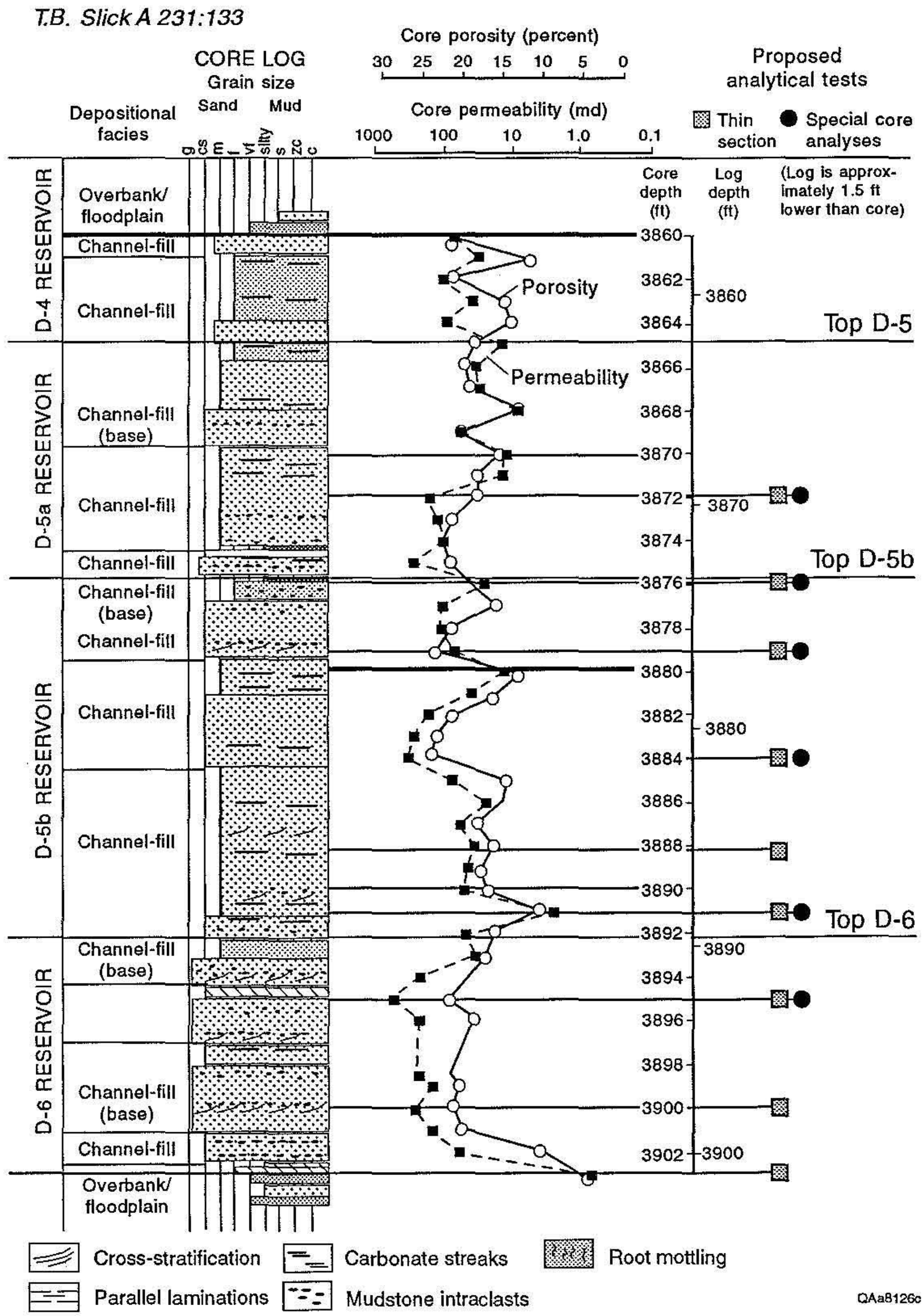

Figure 15. Graphic core log for the T.B. Slick 231:133 well over the Frio D reservoir zone, along with corresponding facies interpretations, core analysis data for porosity and permeability, and location of samples selected for petrographic and special core analyses.

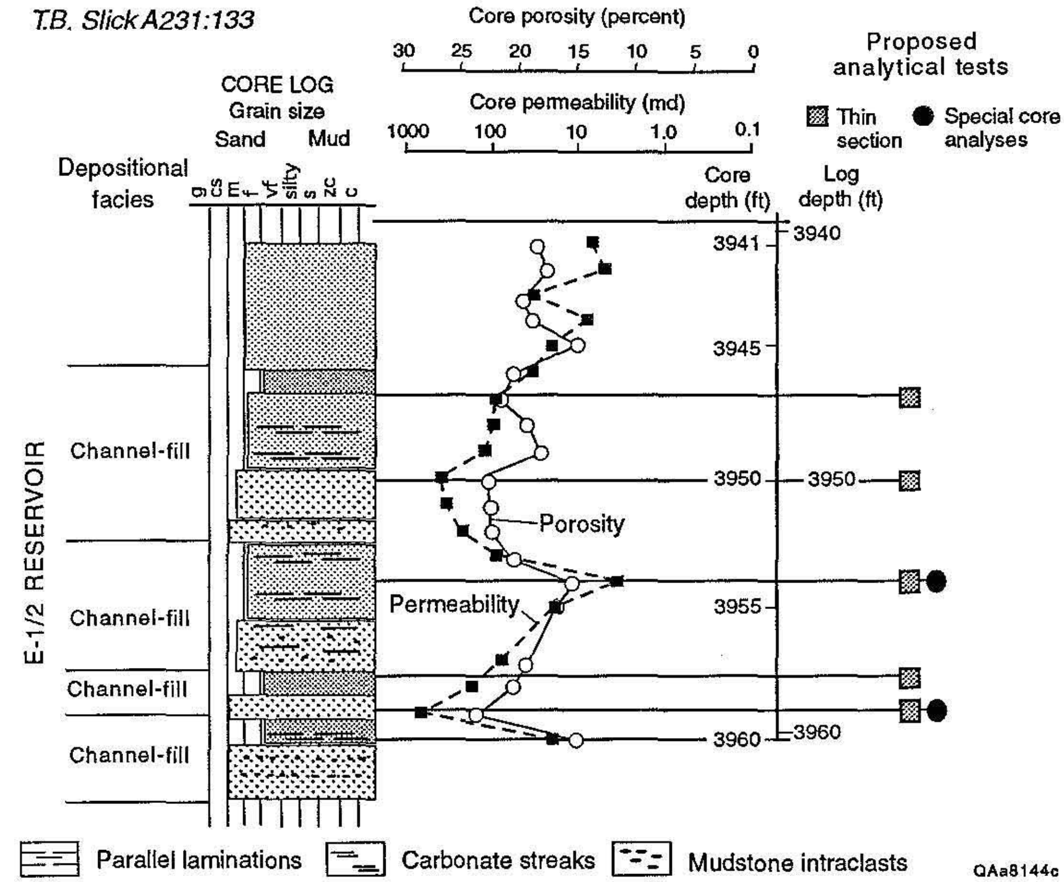

Figure 16. Graphic core log for the T.B. Slick 231:133 well over the Frio E reservoir zone, along with corresponding facies interpretations, core analysis data for porosity and permeability, and location of samples selected for petrographic and special core analyses.

of SP log data in both these wells, this was not possible. Core studies therefore focused on detailed description, identification of depositional facies, and sampling for petrographic study and special core analysis (Fig. 17). The core preserved from well 133 was not continuous and consisted of individual 1- to 6-inch-long pieces of slabbed 4-inch-diameter core each representing 1-ft core interval. Based on core description information, these pieces are assumed to be representative for the lithology of the entire 1-ft interval. Locations of samples selected for these additional studies are annotated on the core graphic logs shown in Figs. 14–16.

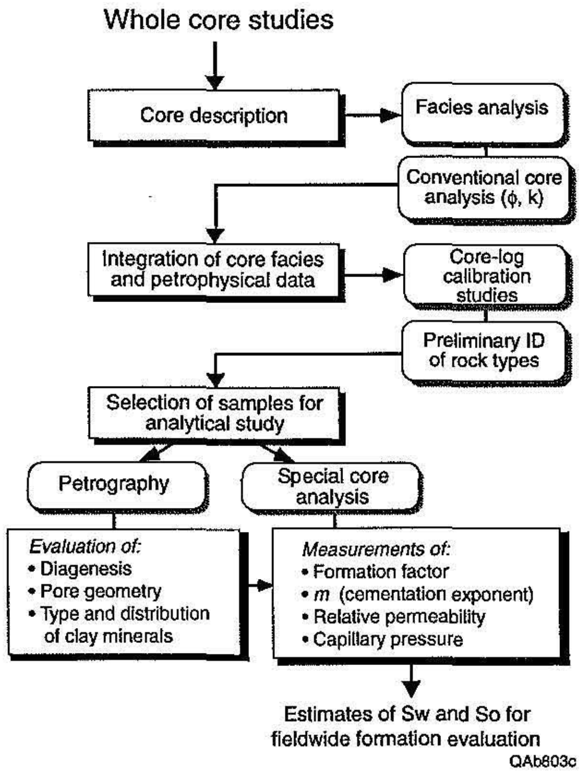

Figure 17. Workflow diagram for studies of Rincon field whole core samples.

Detailed core description and sampling were limited to the two reservoir zones selected for detailed characterization studies: the Frio D and E sandstones. The core from well 149 includes the stratigraphic interval through most of the E reservoir zone (Fig. 14), and the well 133 core represents the depth interval through the D reservoir and the top portion of the E reservoir (Figs. 15 and 16). Based on core observations, there are no obvious distinctive differences in sandstone mineralogy, textures, or facies types between the Frio D and E reservoir zones. Vertical facies sequences of channel-fill sandstones, splay sandstones, and floodplain mudstone units recognized in both cores support our interpretations of fluvial depositional environments determined from electric log correlations and reservoir mapping.

Mudstones

Floodplain units present between sandstone facies consist of red-brown mudstone, silty mudstone, and siltstone commonly exhibiting color variegation and various degrees of bioturbation, root molds, and calcareous nodule development that are all diagnostic of alteration associated with soil-forming processes. Caliche formation and the reddish coloration of the mudstones reflect deposition in well-drained and sparsely vegetated floodplains and suggest semiarid climatic conditions. The abundance of pedogenic features also indicates that interchannel areas were subaerially exposed and drowned only during infrequent flooding. The mudstone intervals between successive channel sandstone units range in thickness from 0 to 100 ft.

Darker gray and laminated mudstones with a conspicuous lack of pedogenic features that characteristically indicates abandoned channel facies were not observed in core. Because of the very limited whole core available, this is not surprising. Abandoned channel facies are interpreted to be present within the field study area, but cannot be distinguished solely on the basis of electric log signature. Mudstones that cannot be correlated between wells may be inferred to represent abandoned channel facies.

Some floodplain mudstones are green-gray and possess a mottled waxy texture typical of an altered bentonite (e.g., 3,960–3,961 ft, Fig. 14). Volcanic activity was occurring in northeastern Mexico throughout the Oligocene, and other workers have noted the presence of bentonites and high concentrations of volcanic glass in the Frio reservoir section in other South Texas fields (Kerr and Jirik, 1990, Grigsby and Kerr, 1993).

Sandstones

Both channel-fill sandstones and crevasse splay sandstone facies were observed in core. Individual channel-fill sandstones range from 5 to 12 ft thick, and all exhibit upward-fining textures. Splay sandstones were less than 1 ft thick (e.g., 3,964 ft, 3,974 ft, 3,980 ft, Fig. 14) and appear more uniform or slightly upward coarsening in grain size. The thin (<2 ft) nature of these splay facies suggests that crevasse development was localized and did not provide a significant contributor to sand deposition.

In addition to these primary facies distinctions, three channel subfacies—basal, middle, and upper channel-fill—could be identified on the basis of texture and sedimentary structures. The basal channel-fill facies refers to the lowermost portion of the channel-fill unit, is commonly coarser grained than the rest of the channel fill (medium- to coarse-grained sand), and may include a gravel lag consisting of intraformational clasts of mudstone and calcareous nodules (e.g., 3,997 ft, 4,010 ft, Fig. 14; 3,875 ft, 3,894 ft, Fig. 15). The thickness of the basal facies of the channel fill is typically less than 1 ft. The middle channel-fill facies comprises the majority of the channel-fill unit and has a grain size that normally ranges from medium to fine. Evidence of cross-stratification is very faint or unobservable in core. The upper channel-fill facies consists of the top few feet of a channel-fill unit, is finer grained than the underlying middle channel-fill sandstone (fine to very fine sand to silty sand), and has rare evidence of ripple-drift stratification.

Vertical profiles of porosity and permeability values are plotted alongside each of the described cores to assist in the identification of different petrophysical rock types present in the various depositional facies. These profiles also illustrate the comparison of reservoir properties between channel-fill sandstones and splay sandstones and among the various channel subfacies. Channel-fill sandstones have lower permeability in the basal channel fill, where there is commonly a well-developed mud chip zone (e.g., 3,997 ft, 4,009 ft, Fig. 14; 3,876 ft, 3,891 ft, Fig. 15). Porosity and permeability systematically increase upward through the middle portions of the sand unit and then are typically reduced near the top of a sand where there is a reduction in grain size (e.g., 3,970 to 3,967 ft, 4,009 to 4,003 ft, Fig. 14; 3,876 to 3,870 ft, Fig. 15). Thin sandstones that are interpreted to represent crevasse splays or perhaps distal channel margins are generally finer grained than channel-fill facies and therefore possess lower porosity and permeability (e.g., 3,964 ft, 3,974 ft, Fig. 14).

Commonly two sandstone units are stacked together, and the presence of a mud chip zone at the base of the upper sandstone unit results in a significant reduction of permeability (e.g., 3,997 ft, Fig. 14; 3,875 ft, Fig. 15). Another rock type that has not been designated a separate facies consists of middle or upper channel facies sandstones that contain abundant carbonate cement. Thin (<1 ft) cement zones observed in core appear to be a localized phenomenon but, where present, correspond to lower porosity and permeability values (e.g., 3,989 ft, Fig. 14; 3,871 ft, Fig. 15).

Definition of Stratigraphic Unit Geometries and Distribution of Depositional Facies

Subdivision of the Frio D and E reservoir interval consisted of defining correlation surfaces that are interpreted to represent a series of time slices through the reservoir zone. A primary goal in detailed reservoir characterization is to subdivide a productive reservoir interval so that any nonpermeable unit (usually mudstone) that may form a continuous barrier between two or more wells is associated with a bounding surface. In fluvial sandstone reservoirs, this objective is most often achieved by correlating mudstone units, representing primarily interchannel floodplain facies, from well to well. In many instances, floodplain mudstones units are not continuous across more than a few wells, and where equivalent mudstone is not preserved in adjacent wells, the position of a bounding surface must be defined within an interval of sandstone. Some of the mudstones used as correlation surfaces occur throughout the entire field study area. Most mudstones are more restricted in areal extent and occur over only a portion of the study window. Some were observed in only a few wells. Identifying the distribution of all shale barriers is very important, as they are probably the most significant cause of heterogeneity in fluvial reservoirs and are responsible for the isolation and compartmentalization of parts of the reservoir and preventing sweep by injected fluids.

A total of 10 primary correlation surfaces were used to subdivide the Frio D–E reservoir zone. There are eight productive sandstone-rich reservoir zones defined within these primary surfaces. Correlation of an additional two less easily recognizable surfaces was also attempted within the thicker D-5 and E-2 genetic units in order to better understand the architecture of these complex zones. The depth of each correlation surface was defined in every well so that each surface could be interpolated throughout the study area for use in the development of a reservoir model.

Sandstone Geometry and Depositional History of Frio E Reservoir Units

A series of maps were constructed on each of the Frio D and Frio E reservoir subunits using net sandstone values based on shale volume calculations from SP logs for each well and depositional facies interpreted from electric log signature. Geologic data from mature Frio reservoirs in South Texas consist primarily of pre-1950 electric logs and very limited whole core, and facies studies must rely heavily on stratigraphic correlations using only these older vintage electric logs.

The Frio E reservoir zone includes strata from the F shale marker to the E shale marker (Fig. 18). The entire zone is composed of four predominantly upward-fining units divided by three low-resistivity marker beds. Each unit between two shale markers represents a depositional parasequence that together makes up a larger-scale, backstepping or retrogradational cycle that took place during deposition of the entire E zone.

The onset of sand deposition in the Frio E stratigraphic interval is represented by the E-4 unit (Fig. 19h). Log facies and net sandstone thickness patterns reveal the development of two to three discrete through-going fluvial channels oriented along directional dip from northwest to southeast. Individual log facies patterns of these channels exhibit blocky and upward-fining responses representing channel-fill facies. The next depositional unit, the E-3 sandstone (Fig. 19g), is characterized by thicker development of sandstone, reflecting an increase of sediment supplied to this portion of the depositional system. The dip-elongate channel patterns observed in the underlying E-4 unit are still apparent. The channels are distinctly separated by floodplain facies in the downdip portion of the map area, but in the updip portion, the channels appear to be better connected, suggesting some flow communication would be present between

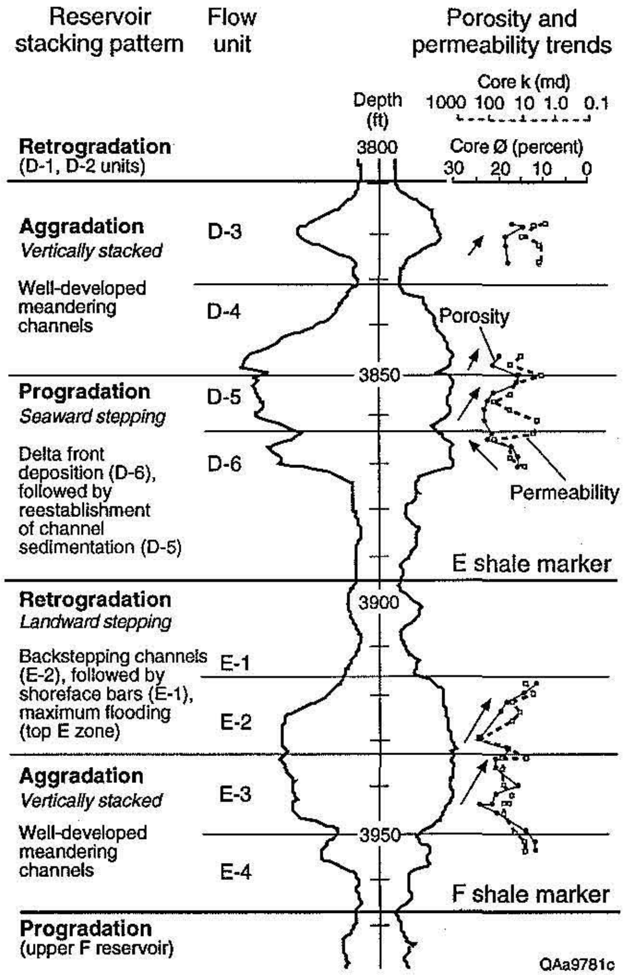

Figure 18. Representative log illustrating succession of stacking patterns that are developed within the Frio E and D reservoir units. Conventional core analysis data posted on the right illustrate porosity and permeability trends commonly observed in each subunit that generally correspond to SP and resistivity bell and funnel curve shapes indicative of upward-fining channel sandstones and upward-coarsening bar sandstones, respectively.

the two. Higher up section in the E-2 unit (Fig. 19f), dip-oriented NW to SE channel geometries still predominate. In the updip portions of these channels, some minor strike-oriented features are apparent, and maximum sand thicknesses have stacked up in a more updip position relative to earlier deposition, indicating a backstepping pattern caused perhaps by relative sea-level rise.

A significant change in the amount and distribution of sandstone is observed at the top of the E zone. In the E-1 unit (Fig. 19e), mudstone facies predominate, and the majority of sandstone is distributed in strike-oriented bodies that are limited in areal extent. These small

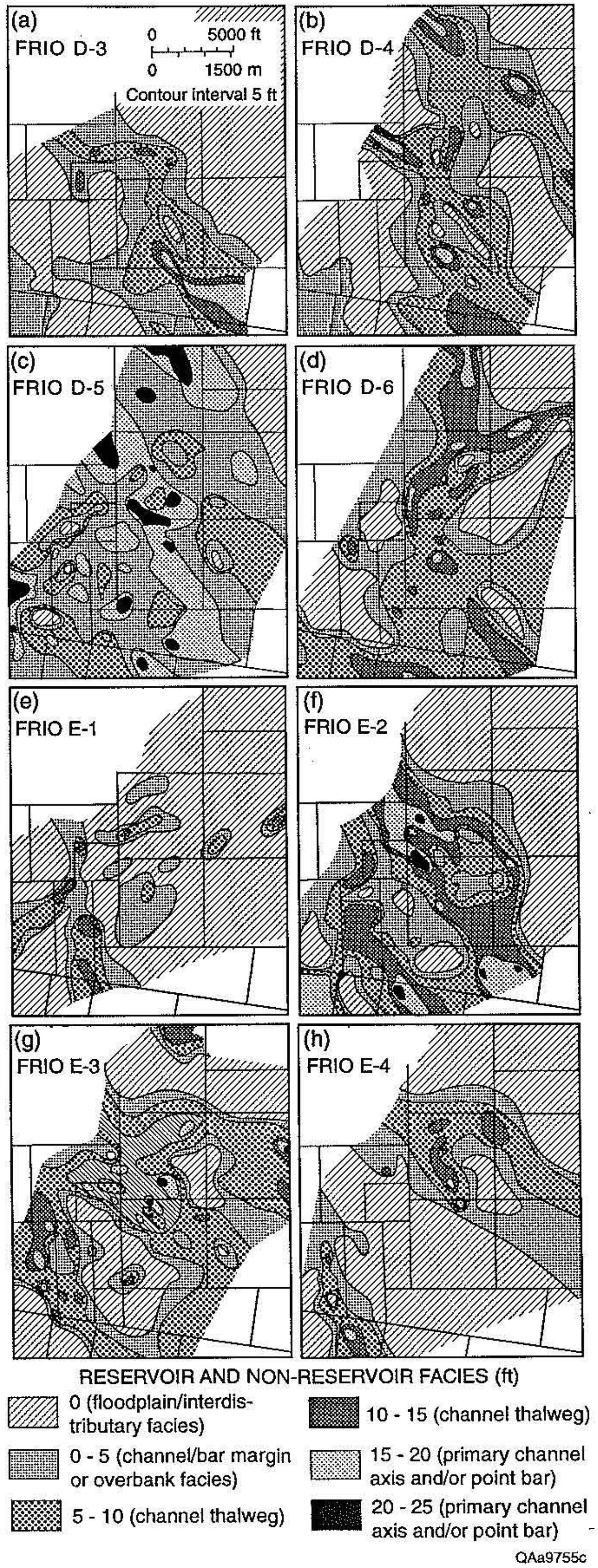

Figure 19. Series of net sandstone isopach and facies maps showing changes in the distribution of facies and sandstone facies geometry for the Frio E-4, E-3, E-2, and E-1 reservoir units and Frio D-6, D-5, D-4, and D-3 reservoir units. See text for discussion.

strike-oriented sandstone deposits are interpreted to represent the development of minor shoreface bars associated with continued backstepping or retrogradation. A narrow dip-elongate channel, perhaps a narrow tidal channel, is present in the far southwestern corner (bottom left of Fig. 19e) of the map area. The advance of a laterally extensive flooding surface marks the end of E zone deposition.

Depositional History of Frio D Reservoir Units

The productive D reservoir interval also consists of four discrete depositional parasequences divided by three low-resistivity shales (Fig. 18). These are identified as the D-3, D-4, D-5, and D-6 units, and together they form a larger scale depositional sequence that includes both progradational and aggradational units. Located above the E flooding surface, the D-6 unit is the lowermost sandstone of the D reservoir zone and follows a relatively extended period of predominantly mud deposition. The strike-elongate sandstone pattern in the D-6 unit (Fig. 19d) is believed to reflect initial progradation and development of a thin delta front. Upward-coarsening and blocky log responses in many of the electric log profiles of D-6 units are further evidence that delta-front sand facies make up this strike-oriented sand body. Dip-elongate channel deposition appears to be present in the northern portion of the study area, as well as across the center of the map where the strike elongate delta-front sandstone is dissected by narrow upward-fining channel facies.

Progradation continues during deposition of the D-5 unit (Fig. 19c). The overall sandstone geometry in the D-5 consists of northwest-southeast-trending, dip-parallel channel facies. Because of the greater thicknesses of mapped sandstone patterns, it is difficult to distinguish boundaries between individual channels. The thickest development of sandstone is present as a relatively narrow channel feature that runs from northwest to southeast across the study area. The D-5 zone also has evidence of some reworked strike-oriented delta-front remnants, and log correlation in some areas indicates this unit may be mapped as two discrete episodes of channel deposition. The uppermost Frio D reservoir subunits represent a return to more discrete channels and aggradational sedimentation. Both the D-4 and D-3 units are dominated by dip-elongate fluvial channel deposition. Sediment load being carried by these channels appears to be reduced from earlier D-5 deposition, as evidenced by thinner development of sandstone and more clearly identified channel margins. The two channel systems mapped in the D-4 unit (Fig. 19b) appear to be in communication in the updip portion of the map area. The D-3 unit (Fig. 19a) consists of a single, relatively broad channel system. In addition to the blocky and upward-fining log patterns that characterize channel-fill facies, serrate and thin coarsening upward responses diagnostic of levee and crevasse splay facies are also observed adjacent to channel margins in these two units.

Petrographic Reservoir Description, D and E Intervals: Controls on Porosity Distribution

Petrographic studies on Rincon Frio sandstone samples were conducted to determine framework compositions, textures, and cement types and distribution to evaluate the degree to which diagenesis is controlling reservoir quality in the Frio D and E reservoir sandstones in Rincon field. General descriptions of pore geometry of these sandstones were also completed to supplement results from special core analyses.

Methods

The guiding approach to petrographic analyses was to conduct them within the context of the reservoir stratigraphic framework. Twenty-two representative samples from core in both wells were selected to provide good data coverage of each of the various reservoir facies and petrophysical rock types present within the Frio D and E reservoir zones in the two wells (Figs. 14–16). Samples selected from the T. B. Slick 231/149 well were taken from the end trims of 1-inch-diameter core plugs so that petrographic parameters viewed in thin section could be directly compared to laboratory-derived porosity and permeability values. Several of these plugs were also selected for special core analyses. There are core analysis data for the T. B. Slick 231/

133 core, but the original plugs from which these measurements were taken were not available. New core plugs were drilled from adjacent available core material for selected additional core measurements, and thin section chips were taken from the ends of these new core plugs.

Composition of Frio D and E reservoir sandstones was determined by standard thin-section petrography supplemented by SEM using an energy dispersive X-ray spectrometer (EDX). Petrographic characteristics, including texture (grain size, sorting), detrital mineralogy, authigenic cements, and porosity type and distribution were observed and quantified by point counts of 21 of the 22 thin sections. A total of 200 counts were made on each thin section. Thin sections were stained for potassium feldspar and carbonates. Major categories of whole-rock volume counted include (1) primary detrital framework grains (quartz, feldspars, and rock fragments), (2) authigenic cements, (3) accessory minerals, (4) detrital clay matrix, and (5) pore space. Size estimates of framework grains were performed by visually comparing thin sections to standardized grain-size charts. Both potassium feldspar (orthoclase) and plagioclase grains were categorized as fresh, leached, calcitized, or vacuolized/sericitized. Authigenic cements were identified by mineral composition and categorized according to their distribution within intergranular pores or within secondary pores formed by dissolution of preexisting framework constituents. Porosity was identified as primary or secondary according to similar criteria. Primary and secondary porosity was identified in the context of the inferred diagenetic history of the samples. SEM and EDX analysis of samples enabled visualization of mineral and pore morphology and precise identification of clay mineralogy.

Texture

Frio sandstone samples from Rincon field range from lower fine grained (0.15 mm) to pebbly lower medium grained (0.3 mm), with most samples being in the upper fine to lower medium sandstone range (0.21 to 0.3 mm). The mean grain size of all samples is 0.25 mm, the size that marks the border between the fine and medium sand categories. Sorting ranges from very poor to moderate; most samples are poorly sorted. Sand grains are angular to subrounded.

Framework Mineralogy

All Frio sandstones examined are mineralogically immature, and most samples are classified as feldspathic litharenites by the sandstone classification of Folk (1974) (Fig. 20a). The dominant framework constituents of most Frio Rincon samples are rock fragments, which on average compose one-half of all framework grains. The average composition of essential framework grains (normalized to 100 percent) from all 21 core samples is 17 percent quartz, 33 percent feldspar, and 50 percent rock fragments ($Q_{17}F_{33}R_{50}$). Compositions of samples from Rincon field generally coincide with compositions of other shallow (3,500 to 6,000 ft) Frio

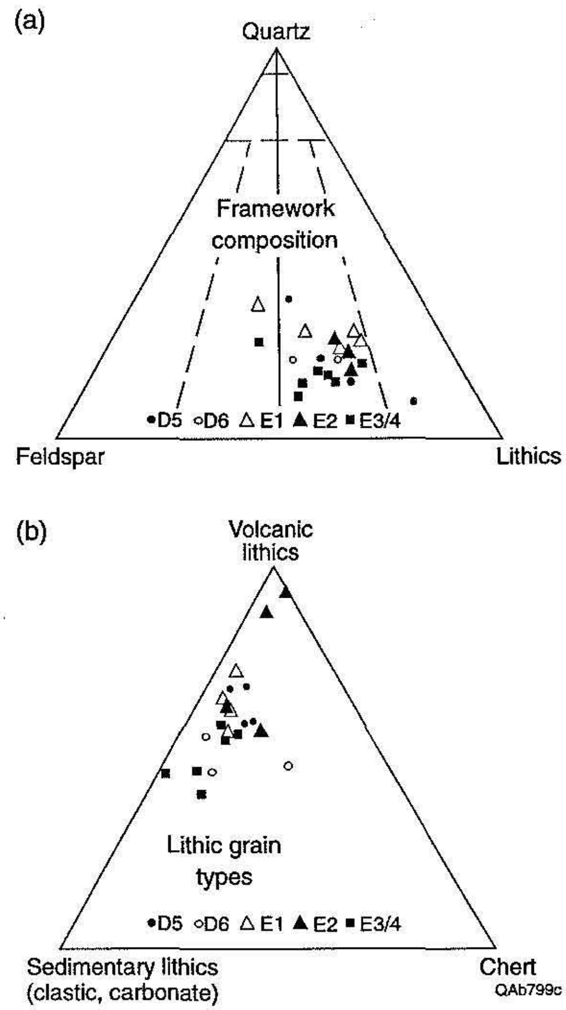

Figure 20. Ternary diagrams showing composition of Rincon D and E reservoir sandstones from thin-section petrography. (a) Percentages of quartz, feldspar, and lithic fragments. (b) Composition of lithic fragments, which included volcanic rock fragments, sedimentary rock fragments, and chert.

reservoir sandstones of the lower Texas Gulf Coast (Grigsby and Kerr, 1993). Deep (6,000 to 18,000 ft) Frio samples of the lower Texas Gulf Coast tend to be richer in quartz grains than the shallow Rincon samples, probably owing to the greater degree of dissolution of feldspar and feldspar-rich rock fragments in the deep samples and resulting relative enrichment in quartz (Bebout and others, 1978; Loucks and others, 1986).

Most lithic fragments in the Frio Rincon samples are volcanic rock fragments (VRFs) (Fig. 20b), which compose an average of 59 percent of all rock fragments (range: 10 to 94 percent) and 18.7 percent of whole-rock volume (range: 6.5 to 26.0 percent) (Table 5). Coarser grained VRFs contain either plagioclase or predominantly orthoclase within a fine-grained groundmass and were derived from contemporaneous active volcanic areas in northern Mexico and West Texas (Loucks and others, 1986). Lindquist (1976) determined that most Frio VRFs from the Rio Grande Embayment are rhyolite and trachyte clasts, although we also observed numerous VRFs of basic composition, such as basalt clasts. In the outcrop equivalent to the Frio, sandstones contain VRFs of felsic and intermediate compositions as well as basalt grains (McBride and others, 1968). Rare VRFs in coarsest samples preserve original vesicular volcanic texture, with chert spherules now filling vesicles. Many isolated well-rounded chert and rare chalcedony grains within the Frio Rincon samples are probably vesicle fills. Sedimentary rock fragments (SRFs), which constitute an average of 41 percent of all rock fragments in Frio Rincon samples (14.7 percent of whole-rock volume), include carbonate rock fragments (CRFs), chert, and rare shale, siltstone, and sandstone clasts. CRFs and chert predominate, with only minor to trace amounts (<2 percent of whole-rock volume) of the other lithic types. CRFs are micritic and are interpreted to have been derived from caliche (Lindquist, 1976). Frio Rincon samples also contain trace amounts of metamorphic rock fragments (MRFs), generally phyllite or slate.

Plagioclase is by far the most abundant feldspar in the samples, composing an average of 82 percent of all feldspars and 17.6 percent of whole-rock volume (range: 12.0 to 27.0 percent) (Table 5). Frio samples contain an average of 3.9 percent (whole-rock volume) orthoclase (range: 1.0 to 11.0 percent). Both plagioclase and orthoclase grains occur in several states of alteration

Table 5. Summary of petrographic data for Rincon sandstones.

Depth	Res. zone	Depositional facies	Gr. size (mm)	Phi size	Framework constituents (counts) Q	F	R	Lithic grain compositions (counts) Vrf	Srf	Cht	$CaCO_3$ cement	Visual porosity estimates 1° Ø (cts)	2° Ø (cts)	Total Ø (cts)	% total 2°
3872.0	D-5a	Channel-mid	0.15	2.75	11	30	59	68	26	5	7.5	1.5	20	21.5	93
3876.0	D-5a	Channel-base													
3879.0	D-5b	Channel-mid	0.21	2.25	16	41	43	69	22	9	4	0	27	27	100
3884.0	D-5b	Channel-mid	0.3	1.75	16	30	54	60	25	15	4.5	4.5	17.5	22	80
3891.0	D-5b	Channel-base	0.3	1.75	25	27	48	59	27	13	14	0.5	16.5	17	97
3895.0	D-6	Channel-mid	0.30	1.75	11	35	54	47	42	11	15	2	14	16	88
3900.0	D-6	Channel-base	0.30	1.75	13	30	57	56	38	6	22.5	2	4	6	67
3945.0	E-1	Channel-top	0.15	2.75	7	45	48	73	22	4	7.5	1	14.5	15.5	94
3950.0	E-1	Channel-mid	0.30	1.75	12	36	52	63	29	8	4.5	3.5	15	18.5	81
3954.0	E-1	Chan-mid (cc)	0.30	1.75	14	37	49	66	28	5	32.5	0	1.5	1.5	100
3959.0	E-1	Channel-base	0.30	1.75	10	43	47	58	32	10	14	2	14.5	16.5	88
3964.0	E-2	Splay	0.21	2.25	21	46	33	94	0	6	0	0	2.5	2.5	100
3967.3	E-2	Channel-top	0.21	2.25	30	43	27	58	24	18	10.5	12.5	4.5	17	26
3969.3	E-2	Channel-mid	0.30	1.75	23	34	43	89	7	4	4	18.5	8	26.5	30
3974.6	E-2	Splay	0.21	2.25	15	27	58	64	29	7	24.5	5	7	12	58
3987.0	E-3	Channel-top	0.21	2.25	18	29	53	46	51	2	8.5	2.5	25.5	28	91
3988.7	E-3	Chan-mid (cc)	0.21	2.25	21	30	49	55	33	11	25	1	5.5	6.5	85
3990.9	E-3	Channel-mid	0.21	2.25	19	28	53	59	32	9	9	12.5	13.5	26	52
3997.5	E-3	Channel-mid	0.25	2	21	23	56	57	30	14	8	12.5	9.5	22	43
3999.6	E-3	Channel-base	0.25	2	16	34	50	47	44	9	5.5	3.5	18	21.5	84
4008.3	E-4	Channel-mid	0.30	1.75	23	25	52	41	46	13	9	11.5	18	29.5	61

Key: Q-quartz, F-feldspar, L-lithics, Vrf-volcanic rock fragment, Srf-sedimentary rock fragment (clastic), Crf-carbonate rock fragment (intraformational), 1° Ø-primary porosity, 2° Ø-secondary porosity, Total Ø-total visual porosity (1° + 2°), all values in counts (total 200 cts/sample), 2° Ø (% total)-percentage of total visual porosity that is secondary.

(in order of abundance): fresh, vacuolized/sericitized, leached, and calcitized. Leaching of entire feldspar grains was a prominent stage in the diagenetic evolution of the Frio Rincon reservoirs, and partially and wholly leached grains contribute to reservoir porosity and permeability. Both topics are discussed more fully in subsequent sections.

Quartz grains are third in relative abundance of all framework grains (average of 10.6 percent of whole-rock volume; range: 4.5 to 16.5 percent) (Table 5). Most quartz grains are single crystals. Rare grains in each sample, however, are polycrystalline, indicating, along with the sparse MRFs, a minor metamorphic source terrane for Frio Rincon samples.

Accessory minerals in Frio Rincon samples include, on average, only trace amounts of muscovite and biotite, and nearly 1 average whole-rock percent of patchy organic material. Pyrite is only locally finely disseminated in matrix and organics.

Detrital Clay Matrix

Frio Rincon reservoir rocks are low in clay matrix content, which is an insignificant factor in controlling reservoir quality. Samples contain an average whole-rock volume of 2.2 percent clay matrix (range: 0 to 9.0 percent) (Table 5). Illite and/or illite/smectite are the dominant clay minerals. One Frio Rincon sample (3,964.1 ft) is notable in its abundance of detrital illite and/or illite/smectite matrix. This sample contains 48.5 whole-rock percent matrix, which is interpreted to be the alteration product of volcanic ash in a bentonite bed. Because this bed does not represent reservoir rock, its matrix content was not included in computations of the average content of the reservoir facies. Volume of pore-filling matrix (detrital clay) and clay cements is consistently low in the samples and is not considered to be a significant influence on reservoir quality.

Cements

Authigenic cements collectively constitute a range of 4.0 to 32.5 percent of the whole-rock volume in the Frio Rincon samples, with a mean value of 11.6 percent (Table 5). Authigenic cements include (in order of abundance) nonferroan calcite, chlorite, and kaolinite. There are also trace amounts of quartz and feldspar overgrowths and illite/smectite grain-rimming cement. Calcite dominates other cements, with an average of 11.2 percent, close to the average sample content of all cements. Chlorite and kaolinite constitute an average of 0.4 and 0.1 percent of all cements, respectively.

Calcite cement occurs as an intergranular cement with a sparry, nonpoikilotopic crystal habit. Most samples are only sparsely cemented and contain abundant, commonly oversized (as much as 0.45 mm in greatest dimension), pores. Isolated patches of sparry calcite with locally crenulate (corroded) rims are characteristic of most samples. In heavily calcite-cemented samples (low porosity), cemented areas are commonly as much as two framework-grain diameters wide and four grain diameters long. Some partially leached feldspar grains and VRFs contain calcite within intragranular dissolution voids; however, such grains were point-counted as calcitized feldspar and VRF, respectively, and are relatively rare. Calcite is a significant Frio cement phase in other fields of the lower Texas Gulf Coast (Lindquist, 1977; Bebout and others, 1978; Loucks and others, 1986; Grigsby and Kerr, 1993).

The whole-rock volume of chlorite cement varies from 0 to 4.0 percent. Chlorite and illite/smectite are mostly grain-rimming cements but also fill a small percentage of intergranular pore space. Chlorite crystal morphology typically takes the form of platelets. Kaolinite, a decomposition product of feldspar, is present in only 6 of the 21 Frio Rincon samples and occurs as a patchy intergranular cement.

Quartz overgrowths are sparsely distributed in some samples and absent in others. Where present, overgrowths are consistently thin and poorly developed and probably represent incipient quartz cementation in these shallow Frio samples. Loucks and others (1986) noted that quartz overgrowths first developed in Frio sandstones between depths of 5,000 and 6,000 ft, deeper than the 3,870- to 4,000-ft range of the Rincon field samples. In Seeligson and Stratton fields of South Texas, minor amounts of quartz overgrowths occur in Frio samples from 4,000 to 6,500 ft deep (Grigsby and Kerr, 1993). In their comparative study of Tertiary sandstones along the entire Texas Gulf Coast, Loucks and others (1986) also observed that quartz overgrowths are more abundant in samples having more quartz grains. Moreover, quartz grains are consistently the least abundant of framework grains in Frio samples from the lower Texas Gulf Coast (Bebout and others, 1978). Therefore, minimal overgrowth development in the Frio Rincon samples may also be in part due to their low quartz content. Feldspar overgrowths are rarer than quartz overgrowths in Frio Rincon samples. However, this cement is characteristic of other Frio reservoirs and is inferred to have developed at shallow depths (<4,000 ft) (Loucks and others, 1986).

Porosity

Total porosity observed in thin section varies from 2.5 to 29.5 percent of whole-rock volume, with an average value of 17.3 percent (Table 5). Secondary porosity composes most of visible thin-section porosity in the Frio Rincon samples. It varies considerably from 2.5 percent of whole-rock volume in heavily calcite-cemented samples to 28.0 percent in heavily leached samples (average: 15.7 percent). Secondary porosity is developed as voids within partially dissolved framework grains (mainly feldspars and VRFs) and as oversized pores that once contained framework grains and/or calcite cement. Little primary porosity (average: 1.5 percent) is preserved in the samples. It exists as small intergranular voids at least partially lined with chlorite or calcite crystals growing into the voids within areas of closely spaced framework grains. However, in most cases it is difficult to identify primary porosity because such textural relations are not present. The Rincon samples underwent at least two stages of dissolution of framework constituents and calcite, the dominant pore-filling cement (Fig. 21). Therefore, textural relations typically cannot be used to confidently establish whether observed porosity is original.

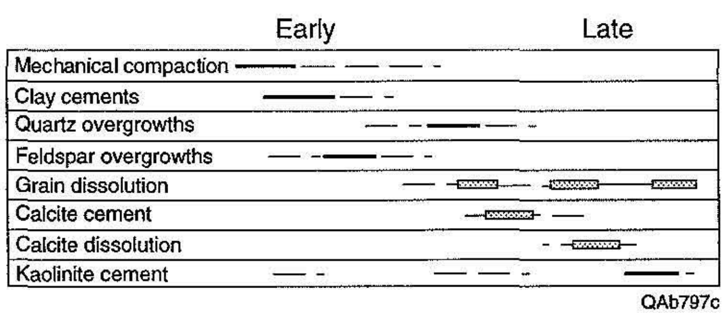

Figure 21. Diagenetic sequence diagram for Rincon D and E reservoir sandstones.

Diagenetic Sequence

The primary diagenetic events in the burial history of Frio Rincon sandstones were (1) early mechanical compaction, (2) precipitation of clay (chlorite, illite/smectite) grain-rimming cements, (3) development of quartz and feldspar overgrowths, (4) dissolution of primarily feldspar and feldspar-rich VRFs (probably contemporaneous with step 3 and steps 5–8), (5) calcite cementation, (6) dissolution of calcite cement, (7) migration of hydrocarbons through the reservoir rock, and (8) precipitation of kaolinite cement (Fig. 21).

The diagenetic sequence of mineralization of the Frio Rincon samples was deduced from textural relations among the framework grains and cements observed in thin section. Where quartz and feldspar overgrowths are present, chlorite and illite/smectite grain-rimming cements lie, at least partially, between the grain and the overgrowth, thus indicating that overgrowth formation postdated clay cementation. Feldspar overgrowths probably predate, or are in part contemporaneous with, quartz overgrowths in these shallow Frio samples, although direct textural evidence is lacking. However, other studies of Frio diagenesis inferred these same temporal relations (Bebout and others, 1978; Lindquist, 1977; Loucks and others, 1986). Dissolution of the least chemically stable framework grains and rock fragments (feldspars, VRFs) began with deeper burial and continued throughout the burial history of the Rincon reservoirs. There were probably discontinuous periods of enhanced dissolution (Fig. 21), perhaps coinciding with episodes of migrating pore fluids. Loss of detrital grains from sandstones represents one of the volumetrically most important diagenetic processes that has occurred and is occurring in the Frio Formation (Milliken, 1989). In the few heavily calcite-cemented samples examined, calcite cement fills voids that are one to several grain diameters in size and are a replacive component of partially leached framework grains, all evidence that calcite cementation followed significant grain dissolution in the Rincon reservoirs. However, most Rincon samples exhibit abundant porosity due to subsequent dissolution of most of the calcite cement, as indicated by characteristic residual patches of sparry cement with corroded edges. Where calcite-cement volume is low owing to dissolution and creation of porosity, sample porosity is higher

(Fig. 22). Calcite dissolution was a significant diagenetic stage that was magnified by the preceding and contemporaneous leaching of framework grains, particularly feldspars and VRFs. Sparse patchy kaolinite cement fills voids created by the loss of calcite cement. However, earlier kaolinite cementation is also inferred.

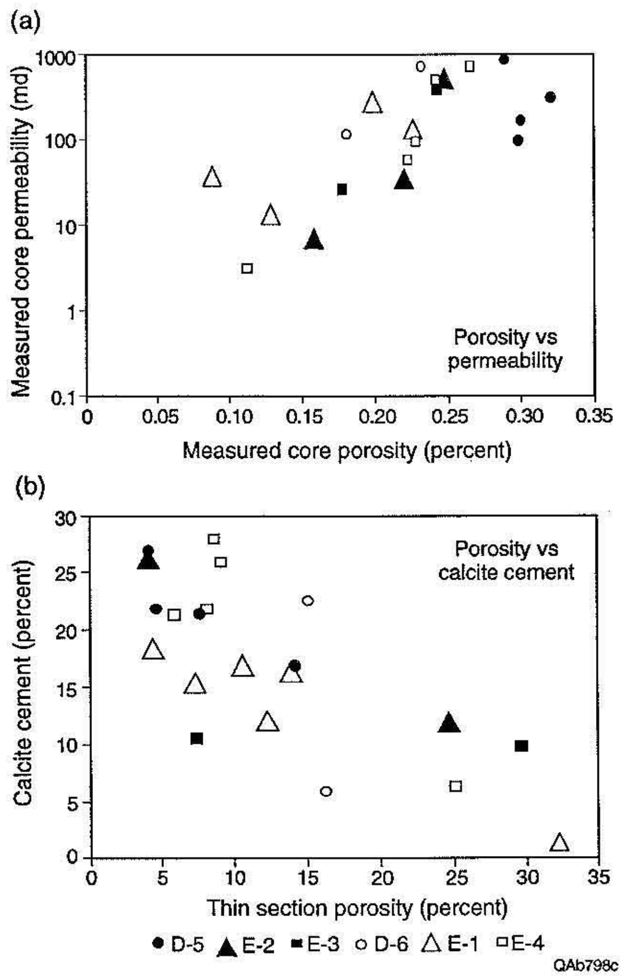

Figure 22. Relationships of (a) porosity and permeability from routine core analysis and (b) porosity and calcite cement for Rincon samples. See text for discussion.

The petrology and ultimately the diagenesis of these Frio sandstones are primarily a function of source area and, secondarily, of original depositional environment. The presence of volcanic source terrains in northern Mexico and West Texas controlled the large volume of VRFs and feldspars in the Frio Rincon sandstones. Leaching of these abundant framework constituents created the porosity in which calcite cement precipitated and from which the cement was subsequently largely leached. Depositional environment had a secondary but important influence on porosity and permeability. Because of the fluvial depositional setting of the Rincon reservoir facies, these sands were poorly sorted and experienced minimal winnowing of the more chemically unstable and softer framework grains, such as plagioclase and VRFs. Therefore, the high percentage of volcanic grains were preserved prior to burial and diagenesis.

Petrophysical Evaluation, D and E Intervals

The purpose of reservoir petrophysical analyses was to quantify the volumes of reservoir rock, water, and hydrocarbons and to determine the ability of the fluids to flow through the rock. Well log, wireline core, special core analyses data, and petrographic identification of the type and distribution of clay minerals were used to (1) establish net sandstone values, (2) calculate reservoir porosity, (3) identify porosity–permeability relationships to predict permeability from well logs, (4) determine water saturations, and (5) tabulate remaining mobile oil.

Because the bulk of reservoir development within Rincon field was done during the 1940s and 1950s, very little modern well log data are available. Only six wells in the study area have modern log suites that include porosity and acoustic log curves. Two of these wells also have abundant routine core analysis data and available wireline core material. These two wells, T. B. Slick A149 and 133, located near the center of the study area, were established as reference data sets, and special core analysis data were obtained to supplement existing information. For the remainder of the wells, porosity values derived from resistivity and porosity values from the two reference wells were used as a quality control check. Porosity–permeability relationships established on a facies-by-facies basis from the abundant routine core analysis data were then used to calculate permeability in wells where no core data were available.

Samples for special core analyses were selected from the continuous core of the E reservoir in well 149 (Fig. 14) that represent the range of petrophysical rock types identified from core description and porosity–permeability data from conventional core analysis. Samples were chosen to demonstrate differences (if any) in measured values (1) between the base and top of a single-story sandstone unit, (2) between the base and top of a multistoried/stacked channel unit, and (3) in a thin crevasse splay sandstone. Samples from channel base/top pairs in the core from well 133—three in the Frio D and two in the E sandstone (Figs. 15 and 16)—were also selected. Samples from this well will provide our only rock data from the D sandstone, and the results from the E sandstone in well 133 can be compared with results in the same E reservoir zone measured in well 149. Petrographic thin sections were prepared from all plugs selected for special core analyses in order to identify clay mineralogy and habit.

Special core analysis tests included FRF, which allowed calculation of the cementation exponent, m, resulting in a more confident assessment of water saturations. Capillary pressure and core flood tests were also done to constrain irreducible water saturations and residual oil saturations, respectively. Both of the latter values can be subtracted from the original oil saturation to determine the original saturation of mobile oil within a reservoir. Results of special core analyses are reported where applicable in the sections "Water Saturation Calculations" (p. 72) and "Calculation of Original Mobil Oil Saturation" (p. 75).

Calculation of Net Sandstone Volumes

In reservoirs within the Frio Fluvial-Deltaic Play, the location and volume of reservoir rocks are coincident with volumes of net sandstone. Volumes of net sandstone were calculated by subtracting volumes of shale (V_{sh}), identified in well logs, from total reservoir interval thicknesses. The model used to calculate V_{sh} (see "Determination of Porosity" [p. 56]) was based on SP log data, primarily because there are very few wells with gamma-ray logs in the field. The SP index of shale volume (I_{SP}) is defined as:

$$I_{SP} = \frac{SP - SP_{min}}{SP_{max} - SP_{min}} \qquad (1)$$

where SP is the log value for a given depth, SP_{min} is the log value determined for clean sandstone, and SP_{max} is the SP log value designated as the shale baseline. Before calculating shale volumes, all logs were depth adjusted to corresponding core data, if available. After an appropriate shale baseline was identified for the reservoir interval in question, all logs were normalized to that standard shale baseline. This facilitated calculations in log intervals where the shale baseline was shifted.

The relationship between V_{sh} and net sandstone thickness was based on the standard Gulf Coast model that uses a 67% cutoff value. Visual inspection of available conventional core from two wells in Rincon field confirms that this assumption is reasonable. Values of net sandstone and percentage sandstone derived from these calculations were used in reservoir mapping.

Determination of Porosity

Both core porosity and resistivity porosity values were used to develop a porosity model. Because only six wells in the study area have modern log suites that include porosity and acoustic log curves, it was necessary to derive reservoir porosity completely from SP and resistivity log data for the bulk of the wells.

An example of core and porosity log data over the E reservoir in the T. B. Slick A149 well is shown in Fig. 23. This is one of two wells for which we have whole core, abundant conventional core analyses, and a modern log suite including gamma ray, deep induction, density, and compensated neutron log curves. There is no SP log for this well, and this is most unfortunate, because virtually all of the other wells in the field have SP logs (and no gamma ray), and therefore no whole core–SP log calibration can be made. Comparisons of the (1) resistivity

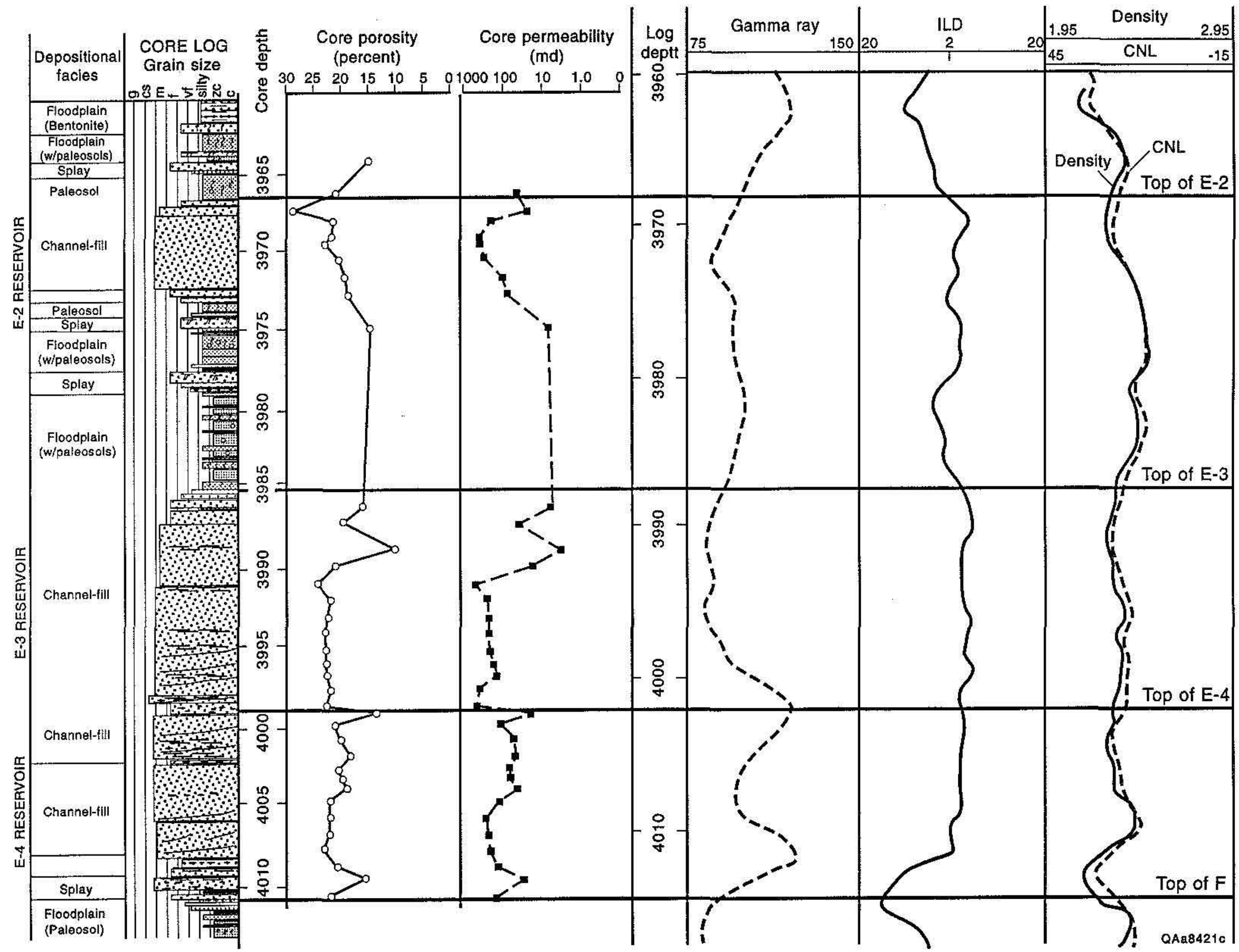

Figure 23. Core graphic log; porosity and permeability data; and gamma-ray, induction, and porosity logs for well T. B. Slick 231:149. Refer to Fig. 14 for legend explanation.

curve with the (2) core graphic log and with (3) porosity and (4) permeability data measured on core samples show a reasonable correlation between resistivity, core facies, and porosity–permeability. Sandstones with reduced porosity and permeability correspond to locations described in core as basal channel facies, or they are carbonate cemented. These permeability variations are not readily recognizable from the log data alone.

Relationships between log resistivity and porosity were studied in order to develop a model to determine porosity from electric log data. Relationships determined for porosity and resistivity were subsequently used to calculate permeability using the appropriate porosity–permeability relationship that has been identified for each reservoir facies type.

Porosity Model from Modern Well Logs

Modern well logs are uncommon in Rincon field. However, it is important to develop a methodology for their analysis because they provide data critical to the evaluation of the success of potential infill wells. A log suite including gamma ray, resistivity, density and compensated neutron porosity along with core data from three wells was analyzed in order to develop a strategy for wireline petrophysics.

The workflow scheme for analyzing modern logs includes depth shifting core data to wireline depths, determining a bulk shale volume indicator (Vsh), and developing a porosity algorithm. On the basis of correlation with other wells and the significant presence of radioactive lithic fragments within the sandstone, it was determined that the gamma-ray log is not a good indicator of shale volume. Instead, the neutron log (CNL) is used as a shale indicator to calculate the shale fraction. Equation 2 is used to determine the shale volume:

$$V_{sh} = ((CNL * (CNL - CNL\ sand)) / DI)^{**}\ 0.5 \qquad (2)$$

where DI = CNL shale * (CNL shale - CNL sand), V_{sh} = bulk shale volume, CNL = CNL log value, CNL sand = the clean sand value read from the CNL log, and CNL shale = the pure shale value read from the CNL log. Shale determination is based on adjusting the CNL log reading between a pure sandstone and pure shale measurement. The clean sand and the pure shale values are respectively picked from local (Frio E reservoir) minimum and maximum values of the CNL log. For the particular well example the neutron clean sand value is 0.283 and the neutron shale value is 0.534, read directly from CNL log (Fig. 24).

Porosity can be determined from the standard density neutron crossplot applying a bulk volume shale correction. When calculating porosity, a clay density of 2.124 g/cc and a neutron clay response of 0.534 were chosen. These values were determined from density and neutron logs where the pure shale volume (100% of shale) occurs. It is noted that the value for the density of clay (2.124 g/cc) corresponds closely to the published value of 2.120 for montmorillonite. The neutron log value for clay (0.534) is not very much different from the published value of 0.6 for montmorillonite and is close to the published value of between 0.519 and 0.500 for wet clay.

Correction for bulk volume shale is critical in determining correct porosity. The computed results for porosity without shale correction and shale corrected crossplot porosity have been compared with core porosity. Figure 25 clearly shows that shale-corrected crossplot porosity better represents core porosity than uncorrected crossplot data and that uncorrected data predict overly optimistic porosity values. The shale-corrected crossplot porosity log ($\phi_{crossplot}$) generally agrees with the core porosity from E2 through E4 zones (3,974–4,015 ft); however, it underestimates porosity by 4 to 10 percent compared to the core porosity in the E1 reservoir (3,962 ft–3,974 ft).

Porosity Model from Old Well Logs

Resistivity measurements are used to determine porosity from wireline logs where modern porosity logs are not available. Several steps are needed to ascertain the resistivity-derived porosity ($\O s_n$), which is a function of the volume of clay (V_{cl}), the near-borehole mixing-zone resistivity (R_z), and the measured short normal resistivity (R_{sn}).

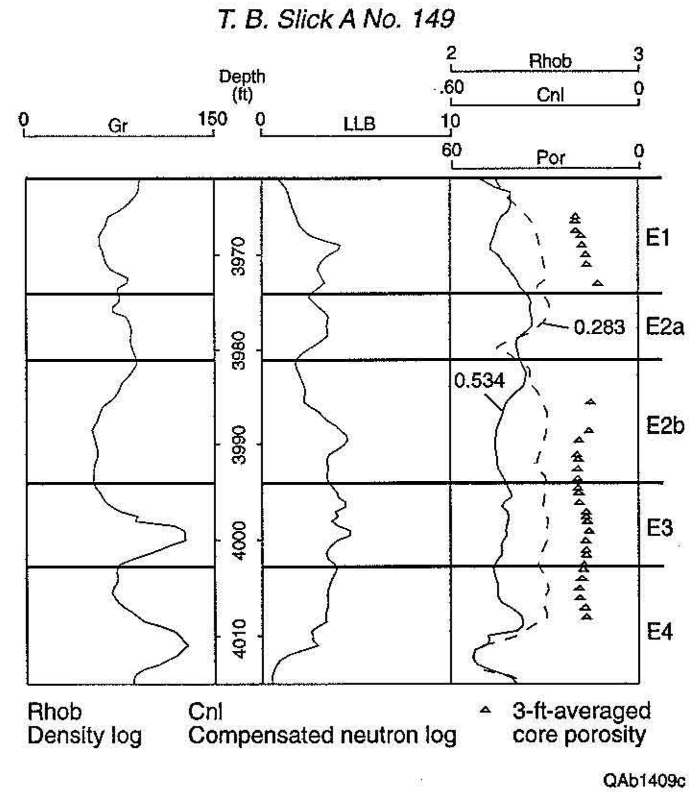

Figure 24. Logs and core porosity from well T. B. Slick No. 149 in E reservoir from depth of 3,962 to 4,015 ft.

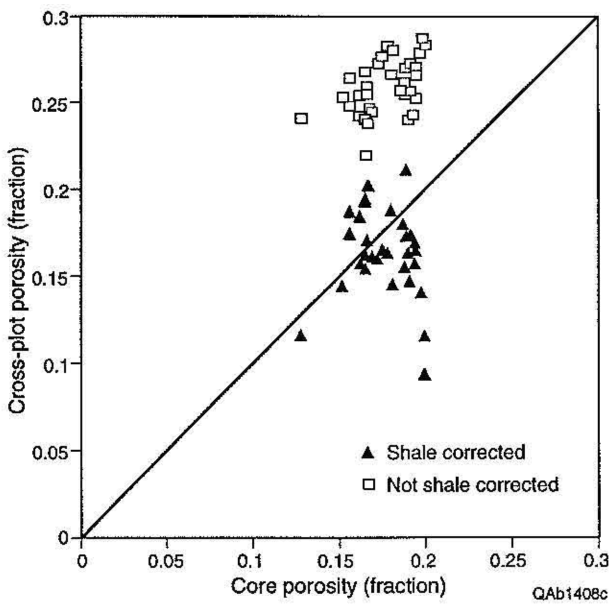

Figure 25. Comparison of shale-corrected and uncorrected cross-plot porosity versus core porosity.

The first step in determining the bulk volume of shale is to calculate a clean sandstone SP response (SSP) for separate reservoirs. The need to derive a separate SSP for each reservoir is the result of each reservoir having a different R_w value. Before this can be done, however, an accurate mud filtrate resistivity (R_{mf}) may have to be calculated if it is not available from the well header, as is the case in many older logs. A value for R_{mf} is derived through Eq. 3, using mud resistivity (R_m) and a constant, C, which is equal to 0.847, when mud weight is less than 10.8 pounds.

$$R_{mf} = C^*(R_m)^{1.07} \quad (3)$$

The R_{mf} value is then used in Eq. 4, along with the measured SP response, to determine SSP. When applying Eq. 4, Rw and Rmf must be at reservoir conditions, and T_r represents reservoir temperature. The SSP value must then be tested to make sure it does not exceed the minimum measured SP response. If this discrepancy occurs, the variables in the equation must be adjusted to make the minimum SP equal to the SSP.

$$SSP = ((0.133^*Tr)+60)^*\log(Rw/R_{mf}) \quad (4)$$

Having a reservoir specific SSP allows the accurate determination of bulk volume shale (V_{cl}) from the SP wireline curve. The simple calculation is made using Eq. 5.

$$V_{cl} = 1-(SP/SSP) \quad (5)$$

The near-borehole mixing-zone resistivity (Rz) is determined at formation temperature from formation water resistivity (R_w) and R_{mf}. For shallow invasion, R_z is calculated from Eq. 6.

$$Rz = 1/((0.1/R_w)+(0.9/R_{mf})) \quad (6)$$

When values for V_{cl} and R_z have been calculated, resistivity-derived porosity (ϕ_{sn}) can then be derived from Eq. 7.

$$\phi_{sn} = (R_z/R_{sn})^{0.5} * (1/V_{cl}) \quad (7)$$

This more accurate resistivity from older logs is then used to calculate reservoir compartment and drainage volumes in those portions of the reservoir where core or modern well logs are unavailable. The subsequent volumetric analysis and resulting evaluation of original in place and remaining resources are more accurate and reliable. Such accuracy is invaluable in reducing the uncertainty associated with predicting the economic risk of recompletions and targeted infill wells.

Identification of Facies-Based Porosity—Permeability Relationships

To accurately characterize porosity and permeability and to determine their distribution within a hydrocarbon reservoir are keys to understanding past production history and are of obvious importance in designing future incremental recovery strategies to maximize resource development. Because it can be directly related to fluid transmissivity and therefore productivity, permeability values can provide a direct means to allocate total hydrocarbon production to specific geologic units. In many older reservoirs, such as in Rincon field, production has been combined and reported for multiple sandstone units, and characterizing the vertical permeability distribution within wells and lateral distribution of permeability between wells is possible only when abundant data from routine core analyses are available. Rincon field is unusual among mature South Texas oil fields in its abundance of core data. The field was extensively cored during its early drilling phase, and although these wireline cores were not preserved, core analysis data exist from more than 100 wells within the general field study area (Fig. 13).

The standard technique used by many operators for estimating porosity and permeability is to combine all routine core data from a reservoir to derive a general porosity–permeability relationship and then use this derived relationship, along with porosities calculated from well logs, to estimate permeability in uncored wells and intervals. This method is obviously inappropriate in heterogeneous reservoirs. Using a single relationship between porosity and permeability may result in underestimating the possible permeability contrasts present within a reservoir interval, and this will subsequently lead to incorrect calculations of original oil-in-place volumes and inaccurate predictions of future production potential.

Rincon conventional core analysis data were grouped by reservoir subunit and by reservoir facies in order to identify variations in porosity and permeability values between individual reservoir zones and facies (Fig. 26). These data groups provide the basis for the identification of means and distribution of values (heterogeneity) for the reservoir attributes of porosity and permeability for sandstone reservoir units and reservoir facies within Rincon field.

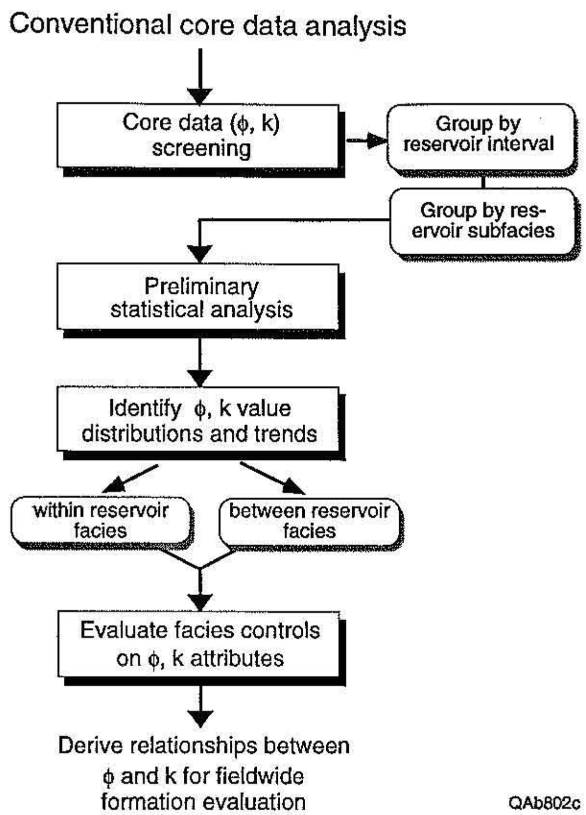

Figure 26. Workflow diagram for establishing relationships between porosity and permeability on the basis of routine core analysis from Rincon D and E reservoirs.

Porosity and Permeability Distribution for Primary Facies Types

Measured porosity and permeability values from wireline cores were analyzed with their sample depths and corresponding reservoir subunit and facies types identified from patterns on sandstone isopach maps and electric log signatures, respectively. Log facies and sandstone distribution for each of the reservoir subunits reveals three primary depositional facies types: (1) channel (dip-elongate) sandstone reservoir units, (2) bar (strike-oriented) sandstone reservoir units, and (3) overbank (levee and crevasse splay) units. Basic descriptive statistics, including histograms and linear regressions of porosity vs. permeability, were calculated for each different subgroup of data. Frequency distributions of core porosity and permeability values grouped according to the three general facies types are illustrated in Fig. 27. Channel units, on average, possess higher values of porosity and permeability (21% mean Ø, 61 md mean k) than the bar sandstone units (mean Ø of 18%, mean k of 24 md). Overbank facies have lower porosities (mean 18%) and substantially lower permeabilities (mean 12 md) than either channel or bar sandstones. Mean permeability values for thin upward-coarsening log patterns interpreted to be

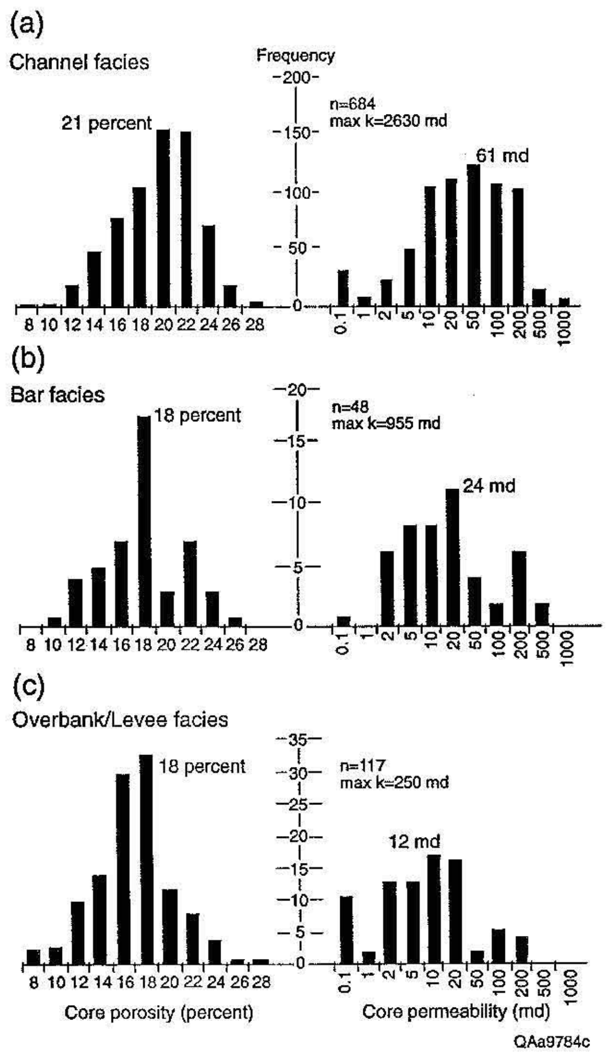

Figure 27. Histograms illustrating the distribution of porosity and permeability values according to each of the mapped reservoir facies: (a) aggradational channels, (b) retrogradational bars, and (c) overbank (splay and levee) facies.

crevasse splays are 25 md (range 0.3–199 md) and are 5 md (range 0.1–54 md) in units with serrate log responses classified as levee facies. These poorer quality overbank facies are generally insignificant reservoirs.

The relationship of porosity and permeability between channel and bar facies is distinctly different. In the E-1 and D-6 units, the predominant reservoir facies types are strike-oriented shoreface bar and delta-front sandstones, and the distributions of core data values have different slopes than those observed in the other channel-dominated reservoir units. Petrographic studies indicate that the bar sandstone facies have, on average, a higher abundance of calcite cement that appears to be the cause of lower porosity and wider variability. Mean values of porosity and permeability for bar sandstone facies in the E-1 and D-6 reservoir subunits and for all channel facies types in the other reservoir units were cross plotted, and a standard linear regression was performed for each group (Fig. 28). The resulting equations for the regression lines demonstrate the different porosity–permeability relationships between these reservoir types. Similar porosity values have a lower corresponding permeability for channel sandstone facies than for bar sandstone facies. These two different relationships will be incorporated into the petrophysical model.

Porosity and Permeability Variability within Channel Facies

Potential Significance of Basal Channel Facies

Profiles of porosity and permeability core data from individual wells typically show a vertical profile that reflects grain size variations commonly observed within a fluvial channel. Permeability, in particular, appeared to exhibit a consistent vertical trend for channel facies with lowest values at channel bases (mean: 6 md, range: 0.1–157 md), where development of a mud chip lag is common. Permeability increases upward through midchannel (mean: 60 md, range: 0.1–1,530 md) and then decreases at channel tops (mean: 14 md, range: 0.1–185 md) where grain size decreases (Figs. 14–16).

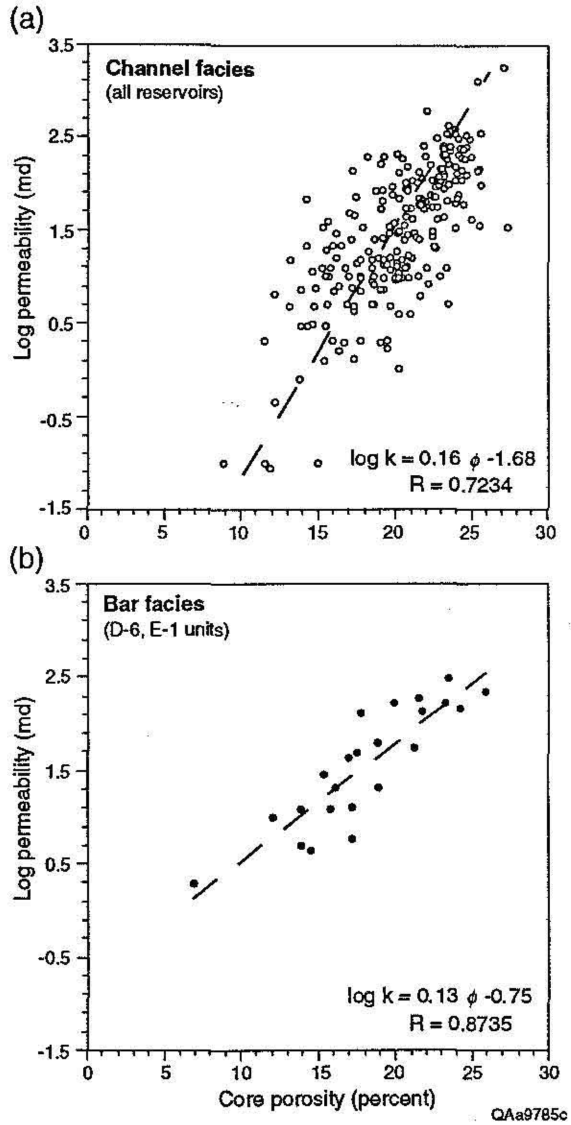

Figure 28. Cross plots reveal different porosity–permeability relationships for the two primary reservoir facies: (a) channel facies and (b) bar facies.

Commonly two sandstone units are stacked together, and the presence of a mud chip zone at the base of the upper sandstone unit may result in a sufficient reduction of permeability to provide a partial or even complete barrier to flow between these two sandstones. Accurate characterization of the petrophysical attributes of channel bases is therefore critical in assessing whether two vertically adjacent sandstone units are in flow communication. As a consequence, particular attention was paid to quantifying the reduction in permeability at the bases of channels to gain insight into how much of a potential baffle or barrier to flow these mud-clast-rich basal channel units may be.

Histograms comparing the distribution of porosity and permeability values from basal and midportions of channel sandstones are shown in Fig. 29. Basal units have much lower mean values of porosity and permeability, and lower maximum values as well. The spread in values, indicated on the Ø-k cross plots, suggests, however, that not all basal units are of poor reservoir quality. The evaluation of whether two vertically stacked sandstones are in communication must

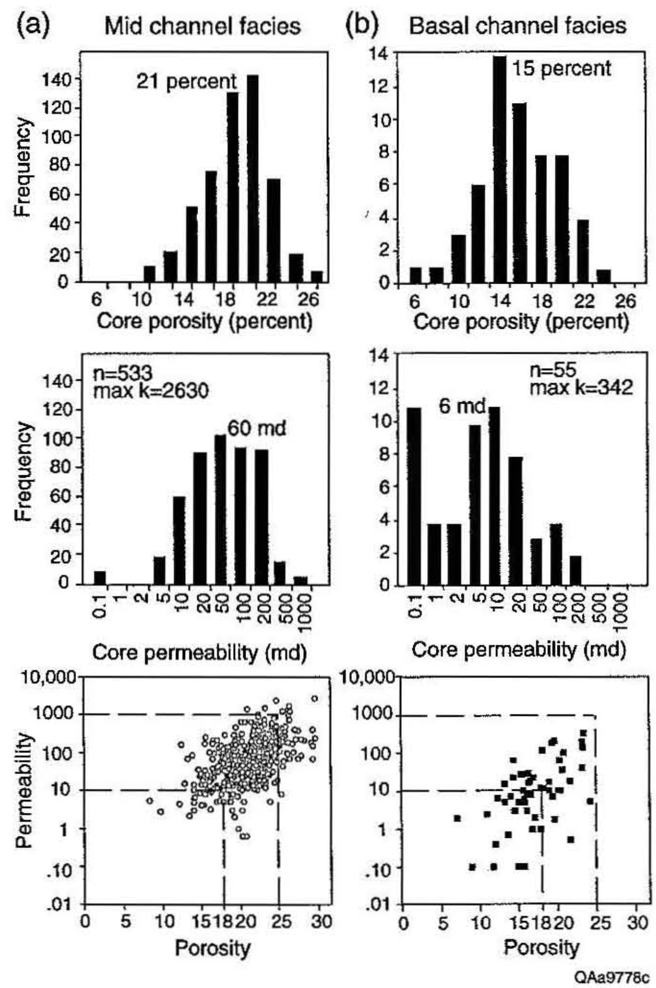

Figure 29. Comparison of core porosity, core permeability, and well log porosity for (a) midchannel facies and (b) basal channel facies.

be considered on a case-by-case basis and must also take into account the lateral persistence of reduced permeability basal facies as well as the presence, thickness, and lateral extent of interchannel mudstones. This task is quite difficult when these interpretations are based solely on subsurface electric log correlations.

Lateral Permeability Structure within Channel Units

During the course of our evaluation of porosity and permeability data for individual reservoir facies, it was observed that core data from thin sandstones located immediately adjacent to floodplain facies had consistently lower permeability values than data measured from sandstones located within the primary channel area. To explore this apparent discrepancy further, channel units within each reservoir subunit were classified as belonging to either channel thalweg facies, identified as the mapped area along the primary channel axis with thicker development of sandstone, or channel margin facies, located adjacent to the primary channel region and arbitrarily defined, for simplicity, as the area between the 0 and 5 ft isopach on the net sandstone map (Fig. 30). Frequency distributions of porosity and permeability values for each facies type for both the Frio D and Frio E reservoir zones are shown in Fig. 31. Mean porosity values range from 16 to 18% in channel margin facies and 20 to 21% in the channel thalweg. Mean porosity values for both facies types are slightly higher for Frio E units than for Frio D units for each facies type. Permeability differences between the two reservoirs are more significant. Mean permeabilities for channel margin units are 10 md for both the D and E reservoirs, but Frio E reservoirs have much higher mean and maximum permeability values in channel thalweg/point bar facies than their counterparts in the Frio D reservoir zone (Fig. 31). Higher permeability values in the upper Frio E reservoir zone may be a result of the retrogradational sedimentation pattern that characterizes deposition of these E reservoir subunits. Decrease of sediment supplied to these channel units may have been responsible for relative backstepping of dip-oriented channel deposition shown by the E-2 unit (Fig. 19f) and subsequent reworking of sediment deposited previously in channels into strike-oriented bars, as shown by

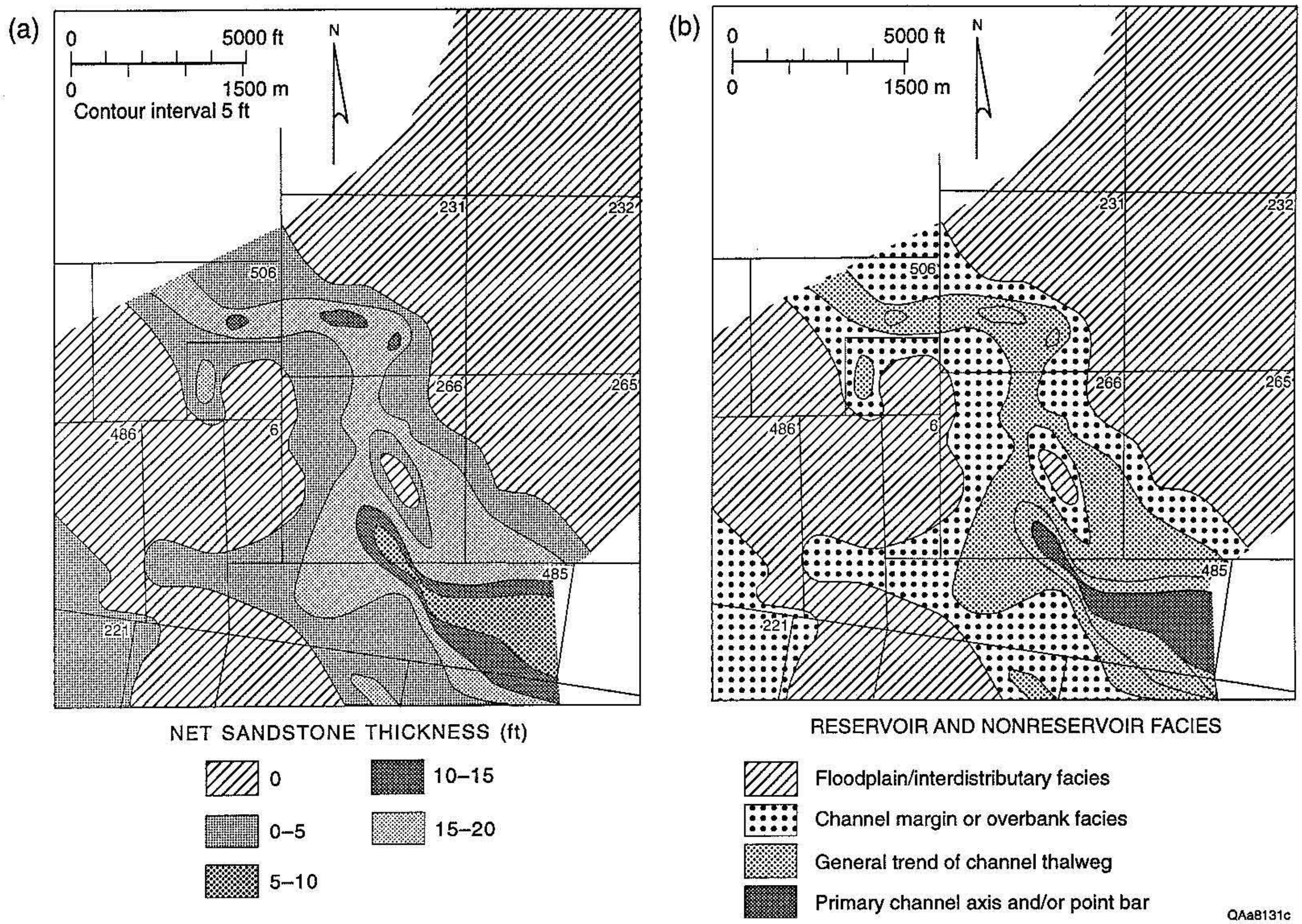

Figure 30. Example of net sandstone isopach map (a) for the D-3 reservoir with corresponding reservoir and nonreservoir facies (b) nomenclature.

the E-1 unit (Fig. 19e). Initial sediment reworking of E-3 and E-2 reservoir subunits may have cleaned up these sands and may explain the statistically higher permeability values measured in these reservoir units.

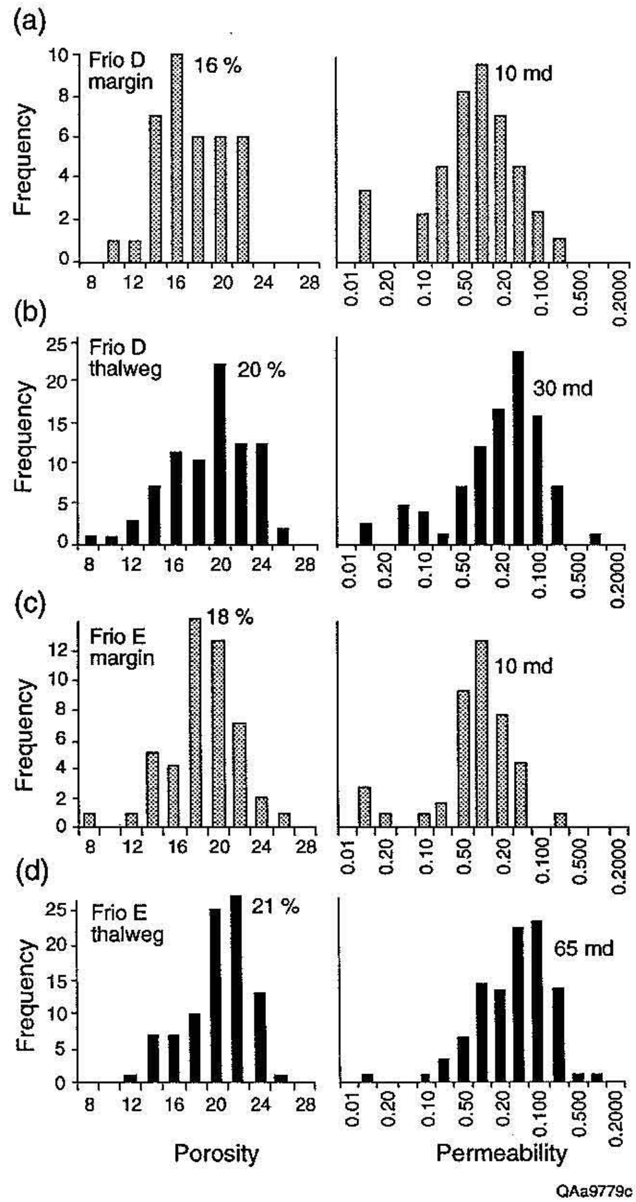

Figure 31. Histograms comparing distribution of porosity and permeability values among channel-margin and channel thalweg data sets for Frio D and E units. (a) Frio D channel margin facies, (b) Frio D thalweg facies, (c) Frio E channel margin facies, and (d) Frio E thalweg facies.

The systematic bankward decrease in permeability from channel center to channel margin has been well documented in both modern rivers and in outcrop studies (Pryor, 1973; Dreyer and others, 1990; among others). Our analysis of lateral permeability variability from abundant core data indicates this trend is also present, at least on a gross scale, within these Frio channel units and suggests that channel facies types defined from subsurface mapping may be used to reasonably predict permeability in the absence of other core or geophysical log data.

Water Saturation Calculations

Calculating water saturations is critical to determining original oil in place and detecting depletion that might be indicated by wells late in the life of the reservoir. Accurate water saturation calculations require reliable values for porosity, resistivity, cementation exponent, m, and saturation exponent, n. Following the calculation of porosity, the most poorly constrained values in this relationship are m and n. The cementation exponent, m, was calculated using FRFs measured during special core analysis, and n was estimated on the basis of published values.

Cementation and Saturation Exponents

Formation resistivity measurements were conducted to define the cementation exponent, m, which is used in the Archie equation to calculate formation water saturation. It has been documented in studies on the sensitivity of variables used in the Archie equation (Archie, 1942) that, unless reservoirs are characterized by low porosity (which these Frio reservoirs are not), variations in m will affect calculated water saturation values much more than values of n, the saturation exponent (Chen and Fang, 1986). Reported data on m values from the Frio in South Texas are very limited and range from 1.6 to 1.8 (Dewan, 1988). Reported Frio values are all less than the value 2.0, which is the standard default value generally used in the Archie equation for sandstones characterized by intergranular porosity. Higher values of m result in higher calculated water saturation values, which will in turn result in lower estimates for oil in place. Accurate estimates of water saturation are critical to delineating reasonable volumes of oil in place, and measurements of m on Rincon core samples were required in order to provide the best possible estimates of values and variations in Sw in these Frio reservoir rock types.

Formation resistivity factors (FRFs) were analyzed from lab measurements. A total of 14 measurements were obtained to determine the character of FRFs. The samples analyzed represented the total range of pay as defined by porosity and permeability. Porosity of these samples ranges from 9 to 32 percent, and permeability ranges from 0.4 to 747 md. Measured FRF values are also consistent with published data ranging from 12.5 to 45.8. Converting FRF to m values, assuming in the Archie equation that a=1, the values range from a minimum of 1.67 to a maximum of 2.4 and have a median of 1.81 (Table 6). This median is consistent with the average published m values in Table 6.

Table 6. Summary of measured petrophysical values of porosity, permeability, formation resistivity, and calculated cementation exponent (m) for Rincon field reservoir units. Values for measured porosity and m for aggradational D sandstones are significantly higher than those measured from underlying E reservoir units. High formation resistivity corresponds to low-porosity samples heavily cemented with calcite.

Unit	Depth	Visual porosity	Measured porosity	Measured perm. (md)	Formation resistivity factor	Cementation exponent (Archie m)	Calcite cement % volume
D-5a	3872	0.22	0.30	172	13.85	2.18	7.5
D-5a	3876		Disintigr.	--	--	--	--
D-5b	3879	0.27	0.30	102	13.64	2.40	4.0
D-5b	3891	0.17	0.32	320	15.52	2.40	14.0
D-6	3895	0.16	0.18	121	19.69	1.73	15.0
E-1	3950	0.19	0.22	130	14.78	1.80	4.5
E-1	3954	0.02	**0.09**	0.4	**45.79**	1.57	**32.5**
E-1	3959	0.17	0.20	370	14.15	1.82	14.0
E-2	3967.3	0.17	0.22	36.5	16.25	1.83	10.5
E-2	3974.6	0.12	**0.16**	7.2	**25.20**	1.74	**24.5**
E-3	3987.0	0.28	0.22	61	14.57	1.78	8.5
E-3	3988.7	0.07	**0.11**	3.3	**44.58**	1.73	**25.0**
E-3	3990.9	0.26	0.26	747	12.51	1.90	9.0
E-3	3999.6	0.22	0.23	98	16.82	1.90	5.5
E-4	4008.3		0.18	27.5	20.47	1.74	--

Modeling FRF for use in the Archie equation was accomplished by assuming that porosity, permeability, and FRF are all interrelated. The tortuosity that the electrical path measured by FRF is a function of both porosity and permeability. Relatively high porosity but poor permeability could have a larger FRF value than a lower porosity with relatively higher permeability. Thus modeling FRF by applying both porosity and permeability has the potential to determine more accurate values.

Both porosity and permeability display power relationships with FRF. Exponential, logarithmic, and power functions were applied with porosity and permeability as the independent variable and FRF as the dependent variable. A porosity power function was determined to have a superior correlation coefficient (r^2) of 0.86, and a permeability power function had a superior correlation coefficient of 0.82. Because both porosity and permeability strongly predict FRF, a multiple nonlinear regression is possible.

A robust multiple nonlinear regression model for the prediction of FRF was developed. The model in Eq. 8 predicts FRF with porosity and permeability as input independent variable. The correlation is strong, displaying a multiple r of 0.95 and an F statistic of 53 compared to a significant F of $2.3 \times 10\text{-}6$. The predictive capability is illustrated in Fig. 32. Actual versus predicted values cluster closely around the 1 to 1 line with the exception of one data outlier. This outlier is a data point that displays a higher FRF for the measured porosity and permeability.

$$FRF=10^{(1.029 - 0.58*\log(porosity) - 0.095*\log(permeability))} \quad (8)$$

As mentioned, water saturation calculations are much less sensitive to the saturation exponent, n, than they are to *m*. As a consequence, an estimate of *n* based on published values for reservoirs in this trend was deemed sufficiently accurate for use. As shown in Table 7, values for *n* in this trend range from 1.66 to 1.8 and average 1.73. A rounded value of 1.7 was used for *n* in all water saturation calculations for the D and E reservoirs.

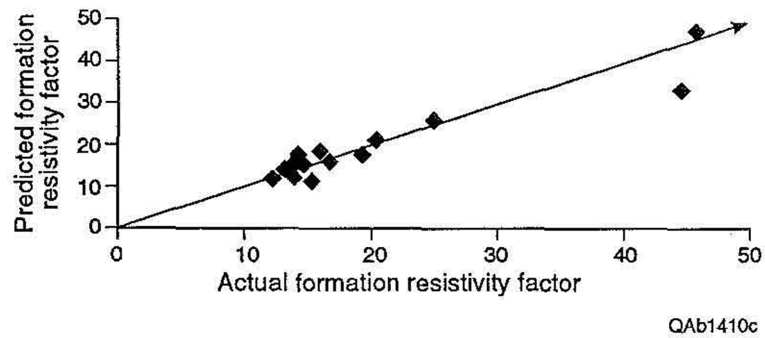

Figure 32. Results of the multiple nonlinear regression model for predicting FRF. The strong predictive capability is displayed by the clustering of the data around the 1-to-1 line.

Table 7. Representative saturation exponents from the Frio Fluvial-Deltaic Sandstone Play (*from Dewan, 1988; **from Ambrose and others, 1992).

Field	Cementation exponent	Saturation exponent
*Frio, South Texas	1.80	1.8
*Agua Dulce	1.71	1.66
*Hollow Tree	1.84	1.665
**Seeligson	1.89	1.79
Average	**1.81**	**1.729**

Calculation of Original Mobile Oil Saturation

An accurate calculation of the volume of mobile oil in the reservoir at the time of discovery is required for a determination of the amount of mobile oil remaining. The original mobile oil saturation, S_{om}, is related to the total oil saturation determined from log analysis, S_o, by Eq. 9:

$$S_{wirr} + S_{or} + S_{om} = S_o \tag{9}$$

where S_{wirr} = irreducible water saturation and S_{or} = residual oil saturation. Irreducible water saturations were determined through capillary pressure testing, and residual oil saturations were obtained through core flood experiments.

Irreducible Water Saturations

The primary objective of the mercury-injection capillary pressure measurements was to determine the distribution of pore throat sizes present in each sample and to ascertain any differences in pore types among the various rock types identified from core description and evaluation of conventional core analysis data. Thin sections were prepared for each sample selected for capillary pressure studies to provide visual description of pore geometries and estimates of pore sizes. The mercury-injection technique is the most commonly used and fastest method of capillary pressure measurement and yields the maximum number of data values. Pore geometry identified from these measurements provides insight into heterogeneity present within individual samples.

Pore throat size derived from capillary pressure tests formed the basis for estimates of irreducible water saturation. Values of irreducible water saturation vary widely from 15 to 37 percent (Table 8). Carbonate-cemented intervals had the highest values (36–37 percent). Values for channel-base sandstones varied widely from 15 percent in the E-1 and E-3 to 36 percent in the D-5b. Values in channel-middle sandstones varied from 18.8 to 30 percent, with D sandstones generally having higher values.

These estimates of S_{wirr} will in turn be used in subsequent resource calculations. Capillary pressure results may also be used to estimate reservoir efficiency.

Residual Oil Saturation and Relative Permeability

Core flood tests were conducted on 15 core plugs to acquire data on residual oil saturation (S_{or}) and end point relative permeability. There is no good available residual oil saturation data for these reservoirs, and values for S_{or} reported for reservoirs throughout the Frio play range widely from 10 to 38% (Holtz and McRae, 1995a). S_{or} data are obviously critical to obtaining reasonable estimates of remaining mobile oil.

Table 8. Comparison of reservoir units and corresponding depositional facies identified from core descriptions with irreducible water and residual oil saturations determined from mercury-injection capillary pressure measurements and core flood tests. Higher water saturations are present in the upper E and Frio D reservoir units, as well as in calcite-cemented sandstones. Smaller pore-throat size distributions are characteristic of finer grained top channel facies and samples with abundant carbonate cement.

Unit	Depositional facies	Sample depth	Residual oil sat. (S_{or})	Irreducible water sat. (S_{wi})	Med. pore-throat size (microns)	PHI size	Perm. (md)	Cement. exponent (Archie m)
D-5a	Channel-mid	3872.0	0.26	30.0	50	0.299	172	2.18
D-5b	Channel-mid	3879.0	0.393	30.0	15	0.297	102	2.40
D-5b	Channel-base	3891.0	0.154	36.0	21	0.319	320	2.40
D-6	Channel-mid	3895.0	--	25.0	85	0.179	121	1.73
E-1	Channel-mid	3950.0	0.453	20.0	80	0.224	130	1.80
E-1	Chan-mid (cc)	3954.0	0.624	37.0	3	0.087	0.4	1.57
E-1	Channel-base	3959.0	0.147	15.0	118	0.234	370	1.82
E-2	Channel-top	3967.3	0.244	23.5	21	0.218	36.5	1.83
E-2	Splay	3974.6	0.194	17.0	39	0.157	7.2	1.74
E-3	Channel-top	3987.0	0.189	21.0	70	0.221	61	1.78
E-3	Chan-mid (cc)	3988.7	0.286	36.0	10	0.111	3.3	1.73
E-3	Channel-mid	3990.9	0.227	18.8	200	0.264	747	1.90
E-3	Channel-base	3999.6	0.298	15.0	72	0.226	98	1.90
E-4	Channel-mid	4008.3	--	27.0	40	0.176	27.5	1.74

Relative permeability is defined as the ratio of effective permeability of a fluid to the absolute permeability of the rock and therefore is directly dependent on saturation (Honarpour and Mahmood, 1988). Relative permeability is very closely related to pore size distributions, and the results from relative permeability measurements conducted on the cores provide a cross-check on the distribution of pore sizes determined from capillary pressure measurements.

Evaluation of General Trends of Past Oil Production

Areal patterns of reservoir development identified by isoproduction contours reveal the general distribution of hydrocarbon storage capacity and degree of flow communication within a productive reservoir zone. These maps also may indicate areas where there are significant production contrasts that may be a direct result of flow barriers created by stratigraphic heterogeneity. Most well completions in a given reservoir include a stratigraphic interval that spans more than one flow unit, and, as a result, cumulative production data on a per well basis do not often provide insight into the stratigraphic distribution of production or the vertical efficiency of the recovery process. The data in Rincon field are no exception, and the results from petrophysical modeling efforts, specifically the identification of permeability structure, will be used to allocate production stratigraphically and create a three-dimensional understanding of the remaining mobile oil present in these reservoirs.

As a first step in identifying the general distribution of oil production, structural isopach maps (Fig. 33a and 33b) and cumulative production isopach maps (Fig. 33c and 33d) were constructed for both the Frio D and E reservoir zones. Composite net sandstone thicknesses were calculated for the Frio D and Frio E reservoirs to serve as a comparison to the total reservoir production maps (Fig. 33e and 33f). The cumulative production map for the E reservoir shown in Fig. 33c illustrates the trend of high production following along the crest of the structure. In addition to structural position, another control on cumulative production appears to be differences in net thickness. The composite E reservoir net sandstone isopach map shows greatest sandstone thicknesses occurring in the updip portion of channels, and comparison with the production map indicates that higher production roughly corresponds to areas of thicker net sandstone that generally follow along channel depositional axes (Fig. 33e).

Maps comparing the distribution of oil production in the D zone with structure show a similar pattern as was observed in the E reservoir zone, with production "hot spots" oriented along strike parallel to the crest of the anticlinal structure (Fig. 33b and 33d). Areas of high production within the D reservoir appear to be much more isolated than those observed on the E cumulative production map (Fig. 33c). The total net sandstone thickness map for the combined D interval shown in Fig. 33f illustrates the strongly dip-oriented pattern of the composite D sandstone interval. The stratigraphic complexity of this interval of vertically stacked and laterally coalescing sandstone lobes provides ideal conditions for isolation of oil accumulations in multiple reservoir compartments, many of which may be incompletely drained or completely untapped. Detailed characterization of each individual reservoir subunit should reveal causes of stratigraphic heterogeneity that have resulted in compartmentalization of oil volumes. The results should lead us to understand better how reservoir architecture may be controlling recovery efficiency and to identify areas with high potential for containing undeveloped resources that may be targeted for incremental recovery.

Integrated Analysis of Reserve Growth Opportunities

Effect of Sandstone Geometry on Oil Production

The Frio D and E reservoir interval illustrates a systematic evolution of sediment transport styles and stratigraphic stacking patterns (Fig. 18): (1) aggradation in the lower Frio E-4 and E-3 reservoir units, (2) retrogradation in the upper Frio E-2 and E-1 units (3) progradation in the lower Frio D-6 and D-5 units, and (4) a return to aggradation in the upper Frio D-4 and D-3 units. These different styles of deposition directly affect the reservoir geometry present within each sandstone unit (Fig. 19). Aggradational and progradational channel sedimentation create dip-oriented channel sandstones that may or may not be in communication with one another. Strong dip-oriented geometry in the D units and development of successively more laterally isolated channels during aggradation reduce communication between units that may be directly responsible for lower recovery efficiency. Retrogradational units such as those present in the E reservoir, in contrast, allow reworking of previously deposited sediment into long strike-oriented features that have potential for increased flow communication. Individual map patterns suggest that the strike-oriented distribution of sandstone located in the updip portions of the map area in the E-3 and E-2 units, combined with the relative broadness (3,500–7,000 ft) and lower sinuosity of individual channel units, may lead to greater interconnectedness of channels and increased communication between reservoir flow units. The updip stacking of sandstone thickness and lateral connectivity between E units may be controlling factors in the relatively high recovery efficiency (38%) of this reservoir zone.

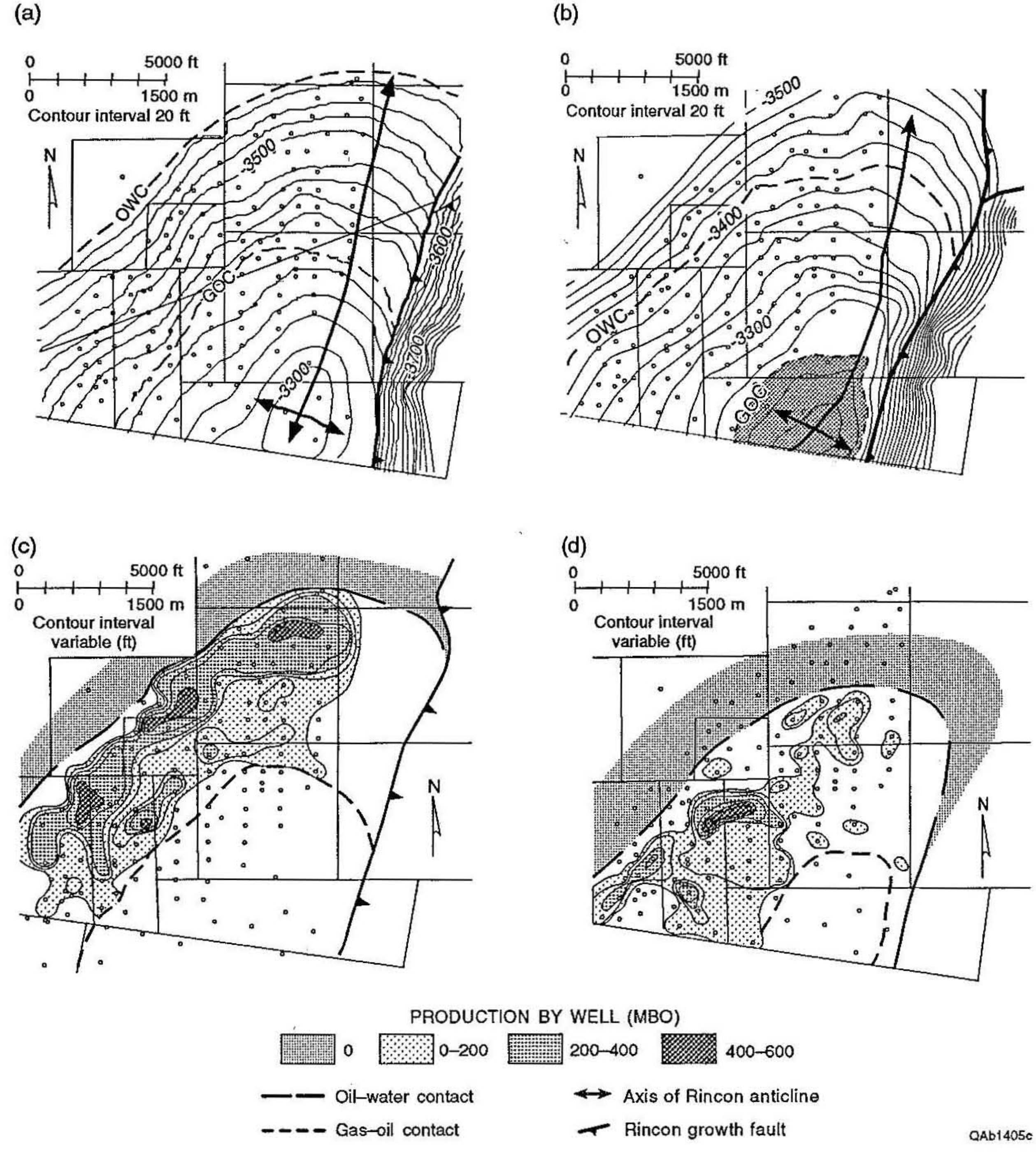
(a)
0
5000 ft
0
1500 m
Contour interval 20 ft
N
OWC
GOC
3500
3600
3700
3300
(b)
0
5000 ft
0
1500 m
Contour interval 20 ft
N
3500
3400
OWC
3300
GOC
(c)
0
5000 ft
0
1500 m
Contour interval variable (ft)
N
(d)
0
5000 ft
0
1500 m
Contour interval variable (ft)
N
PRODUCTION BY WELL (MBO)
0
0–200
200–400
400–600
Oil–water contact
Gas–oil contact
Axis of Rincon anticline
Rincon growth fault
QAb1405c

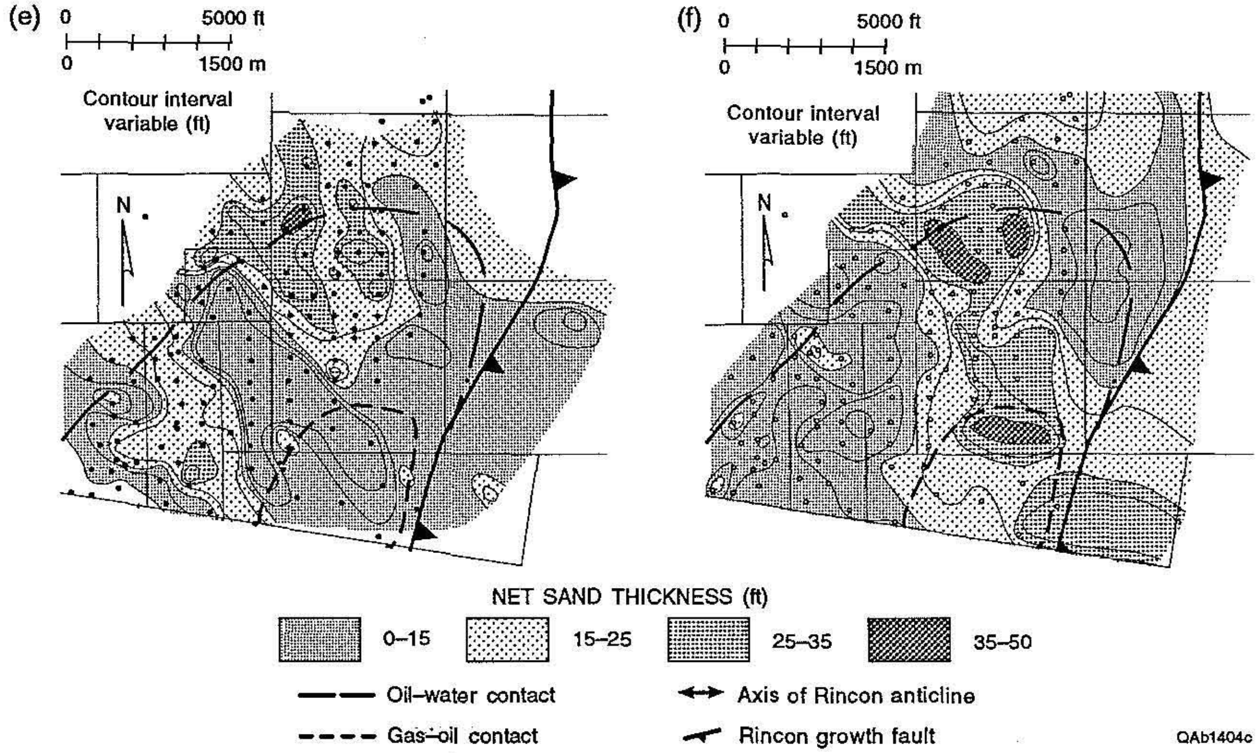

Figure 33. Comparison maps illustrating differences in overall reservoir geometry and distribution of production for the Frio D and E reservoir zones. Maps on the left for the Frio E reservoir show (a) representative structure contoured on the top of the Frio E unit, showing the anticlinal pattern of the Rincon structure and location of the down-to-the-east Rincon growth fault; and (c) cumulative oil production for the combined Frio E reservoir; and (e) isopach map from the total E sandstone reservoir zone, showing distribution of net sandstone thickness and depositional geometry. The stacking of greater sandstone thicknesses in the updip portion of map area may have created increased flow communication between adjacent channels along the crest of the structure and be responsible for the relatively high recovery efficiency of the E reservoir. Maps illustrating structure (b), distribution of cumulative oil production (d), and total net sandstone thickness (f) are presented on the right for the Frio D reservoir. In contrast to the Frio E zone, the strong dip-elongate depositional pattern and narrower geometry of Frio D channels make this reservoir appear more compartmentalized and may explain lower overall recovery efficiency.

Controls on Reservoir Production within Individual Reservoir Units

Reservoir Development Patterns within the Frio E Reservoir

The Frio E sandstone is the most prolific reservoir zone in the field and has produced nearly 12 MMSTB of oil since production began in 1940. The E zones are individually mapped as the E-1, E-2, E-3, and E-4 sands. Stratigraphic correlation and production data from the operator indicate that the E-1 and E-2 sands are commonly in fluid communication, as are the E-3 and E-4 sand zones. Secondary waterflooding in the Frio E reservoir zone accounted for 2.5 MMSTB, or nearly 21% of total E zone production. An overall recovery efficiency of 38 percent was calculated for the combined E zone using average reservoir values of 26.5% porosity and 37.5% water saturation.

Net sandstone isopach data were combined with log facies interpretations to create maps for the E-4 through E-1 units to document the distribution of sandstone and depositional facies within each reservoir subunit. Reservoir development within each unit was indicated by identifying wells with completions within the stratigraphic interval that comprises each unit. In addition, wells were identified that were unperforated within the mapped zone but that were completed in a reservoir subunit stratigraphically above or below the mapped unit that may have been in partial or complete vertical communication. The series of reservoir geometry/development maps prepared for the E reservoir units are shown in Figs. 34–37.

The Frio E-4 unit has the least number of completions of the three E reservoir units (E-4, E-3, and E-2) that are characterized predominantly by channel sedimentation. This unit consists of two discrete dip-oriented channel bodies that are separated laterally by at least 3,000 ft of nonreservoir floodplain facies (Fig. 34). The channel located in the southwest portion of the map area is narrow (1,000–1,500 ft) and contains a relatively thin channel-margin facies as interpreted from net sandstone isopachs. The channel system located in the central portion of the map area consists of two main channel tracts defined by thicker development of sandstone, and these are probably in flow communication. The updip, connected portion of this channel system is

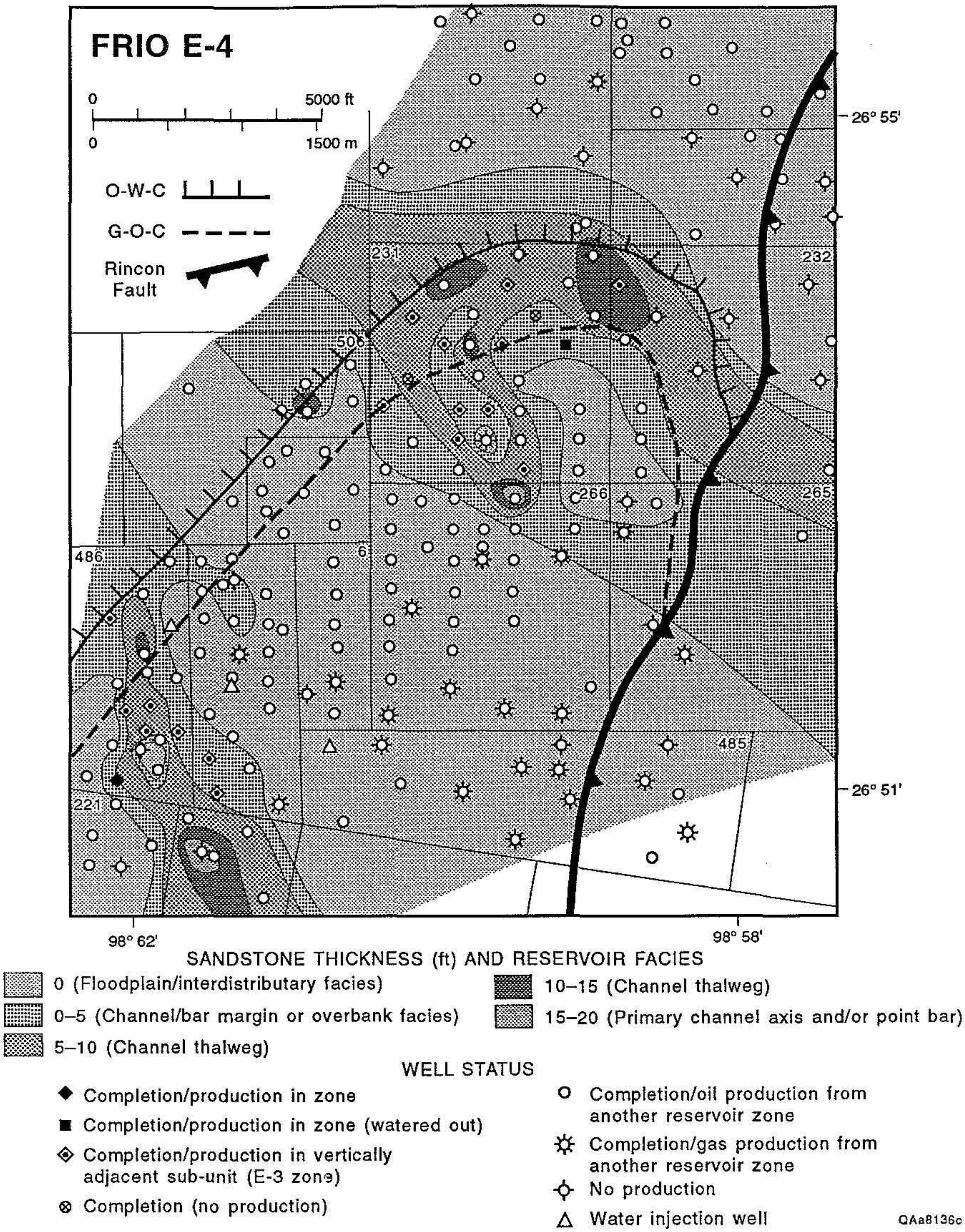

Figure 34. Map illustrating sandstone thickness distribution, corresponding reservoir facies geometry, productive limits, and level of development in the Frio E-4 reservoir unit.

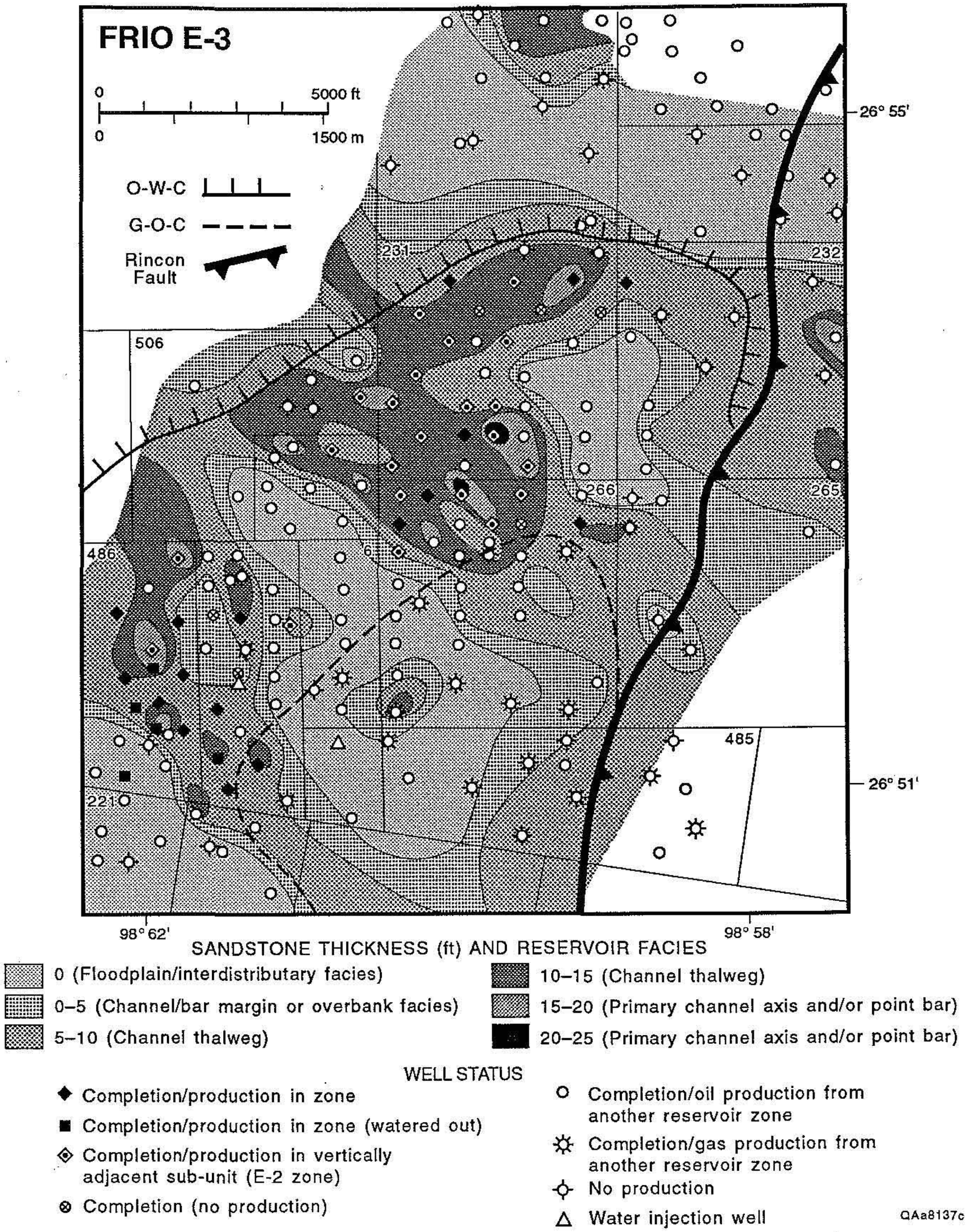

Figure 35. Map illustrating sandstone thickness distribution, corresponding reservoir facies geometry, productive limits, and level of development in the Frio E-3 reservoir unit.

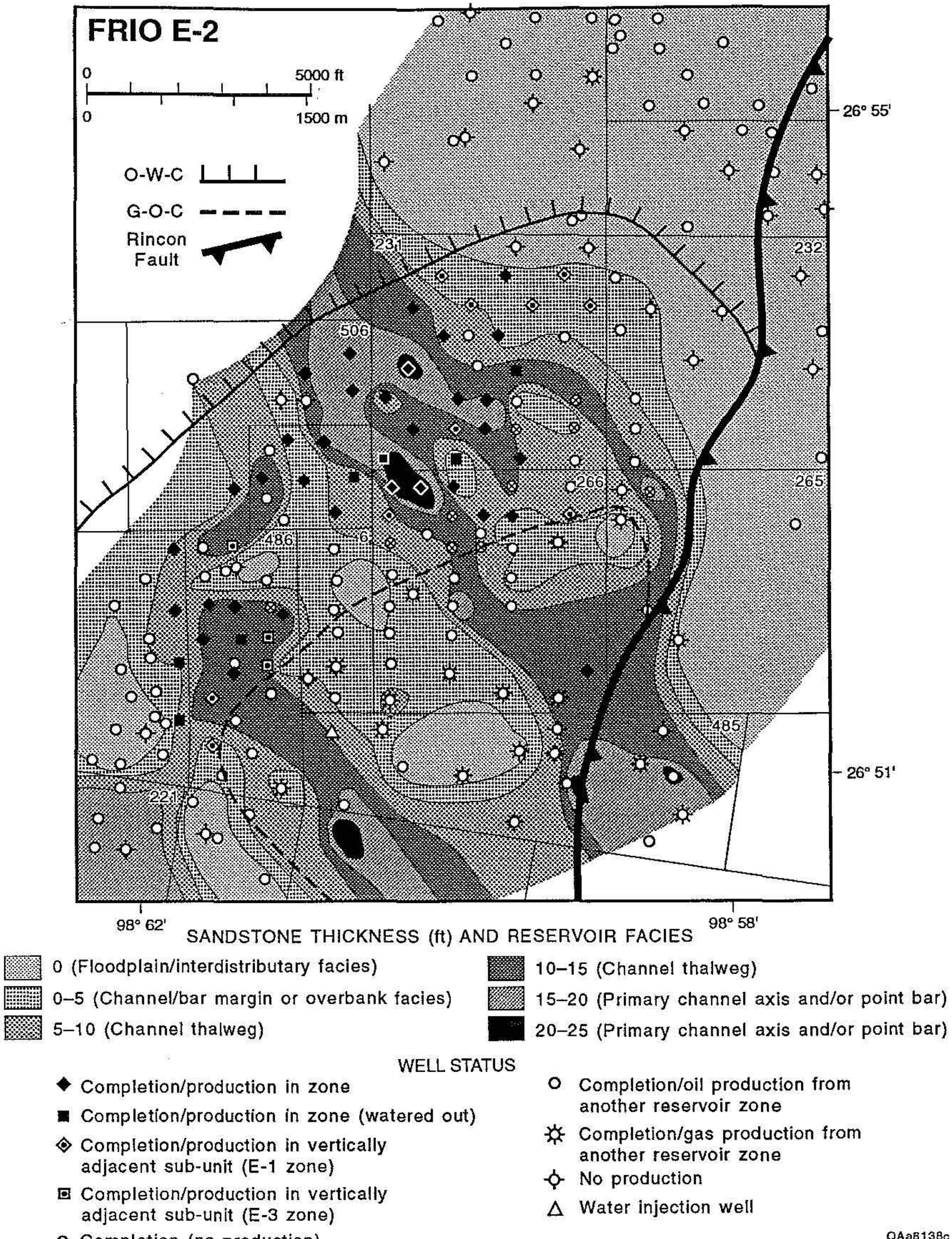

Figure 36. Map illustrating sandstone thickness distribution, corresponding reservoir facies geometry, productive limits, and level of development in the Frio E-2 reservoir unit.

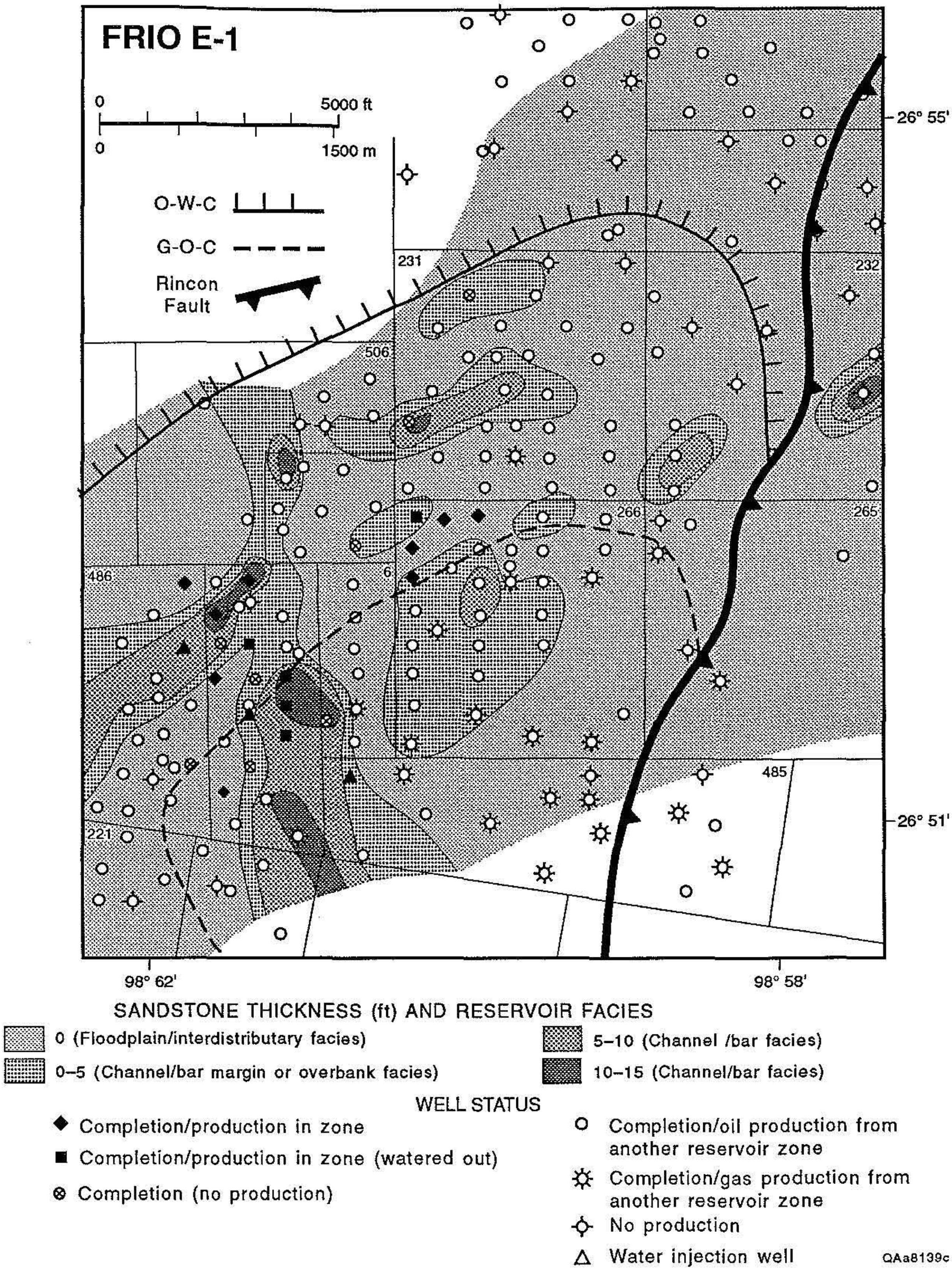

Figure 37. Map illustrating sandstone thickness distribution, corresponding reservoir facies geometry, productive limits, and level of development in the Frio E-1 reservoir unit.

approximately 3,500 ft wide and narrows to 2,000 to 2,500 ft farther downdip, where it appears to bifurcate into two separate channel units. Forty-nine wells penetrate sandstone facies in the E-4 reservoir, and only 21 of these have been completed. Many of these completed wells may have associated production, but actual volumes are not known because all E-4 production reported by the operator was assigned to the combined E-3 and E-4 reservoir zone.

E-3 unit reservoirs appear to consist of three separate channel systems oriented northwest to southeast across the field study area (Fig. 35). The location of the oil–water contact indicates that it is likely that the southwesternmost channel is not in communication with the two channels located to the north. The two northern channels appear connected, in part, and are probably in lateral communication. The southwestern channel is approximately 2,500 ft wide and has 50 completions and 21 producing wells. The majority of completions and producing wells are located in these two northern channels. Many additional wells have been completed in a vertically subadjacent zone, primarily the overlying E-2 reservoir, and have produced oil, some of which may be properly allocated to the E-3 unit. More than 3 MMBO of production has currently been assigned to E-3 reservoir.

The Frio E-2 reservoir unit possesses the greatest number of completions (64) and producing wells (46) of all E reservoir subunits. The mapped sandstone geometry (Fig. 36) shows two primary dip-oriented channels that are probably only in partial communication because of the floodplain facies and lower permeability channel-margin facies developed between the two channel areas. The primary channel area in the E-2 unit is relatively broad (4,000–6,000 ft) and contains sandstone facies that have some of the highest permeability values (1,250 md+) measured in the field. Present production allocation indicates that the E-2 unit is also by far the most prolific oil reservoir sandstone in Rincon field, with more than 7.5 MMBO currently reported.

The uppermost E reservoir sand, the E-1 unit, has the fewest completions of all E subunits. Part of this is attributable to the fact that the E-1 and E-2 sandstones were developed as though they were usually in flow communication, and extensive development in the E-2 reservoir has likely produced much of the E-1 oil. Sandstone isopach mapping and evaluation of log facies in this study suggest that the E-1 sandstone was deposited in a retrogradational cycle where preexisting channel units have been eroded and reworked into a series of strike-elongate bar sands that cover most of the mapped study area (Fig. 37). Well data and log facies interpretations indicate that these bar units are thin (mean thickness of 6 ft) and not very laterally continuous (width dimensions from 1,500 to 3,000 ft). This facies interpretation indicates that there may be less vertical communication between E-2 and E-2 reservoir units than previously assumed. A summary of characteristics, including reservoir facies, sandstone geometry, petrophysical attributes, and key production data for E reservoirs is provided in Table 9.

Reservoir Development Patterns within the Frio D Reservoir

Frio D reservoirs have produced nearly 10 MMSTB oil since 1940. The main productive D sand interval consists of four units correlated as the D-3, D-4, D-5, and D-6 sands (Fig. 18). These

Table 9. Summary of production characteristics for the Frio E reservoir subunits.

	E-4	E-3	E-2	E-1
Reservoir sedimentology				
Dominant facies type	Channels	Channels	Mixed	Bars
Sedimentation style	Aggradation	Aggradation	Mixed	Retrogradation
Reservoir geometry				
Wells with >0 net sandstone	49	102	109	39
Mean net sandstone thickness	7	10	10	6
Maximum net sandstone thickness	21	24	30	16
Petrophysical attributes				
Mean sandstone porosity	19.7	20.8	20.1	19.2
Geometric mean permeability	26	43	25	18
Max permeability	135	411	1253	299
Reservoir development				
Completed zones	21	50	64	14
Producers	1	21	46	6
MBO produced	3	3100	7517	881
Ratio of well completions/ sandstone penetrations	**0.43**	**0.49**	**0.59**	**0.36**

units are correlated as individual sandstones that combine into a complex stratigraphic channel system that covers more than 2,000 acres in the northern half of the field. Frio D sandstones have similar reservoir attributes as Frio E reservoirs (average porosity of 25.2%, Sw of 40.5%, and estimated OOIP of approximately 35 MMSTB) but a lower recovery efficiency of 29%. Waterflooding attempts in this reservoir zone accounted for secondary recovery amounting to only 2% of total D production. These disappointing results were attributed by the field operator to the heterogeneous nature of the D sandstone interval.

Composite maps illustrating the distribution of reservoir sandstone, facies patterns, and level of development for each of the D reservoir subunits are presented in Figs. 38–41, and a summary of important reservoir characteristics determined for each of the four D reservoir units is provided in Table 10. As discussed previously, the lowermost D reservoir unit, the D-6 sand, has been interpreted to represent part of a progradational cycle of sedimentation during which strike-elongate sandstone bars deposited during the previous retrogradational cycle are being eroded and transected by a dip-oriented channel system that trends across the center of the map area. (Fig. 38). Upward-coarsening profiles observed on electric logs indicate the presence and northeast-to-southwest distribution of the bar sandstone facies that appear to be in the process of being dissected by the northwest-to-southeast-oriented channel. The D-6 unit has relatively few completions (14), and although some of these completions were productive, all production was originally assigned to the composite D-5 reservoir zone.

As illustrated in Fig. 39, the depositional geometry of the Frio D-5 subunit is very complex. The isopach map pattern reveals the presence of a primary axis of deposition, indicated by the thickest development of sandstone, running from northwest to southeast across the center of the map area. The relatively thick sandstone throughout this reservoir zone obscures much of the depositional pattern. The D-5 zone has more completions (60) and productive wells (39) than all other D reservoir units combined, and production reported for the composite D-4, D-5, and D-6 reservoir zone totals more than 6 MMBO. The permeability distribution within the D-5 unit suggests that there are several areas where these flow baffles or barriers may exist, and this

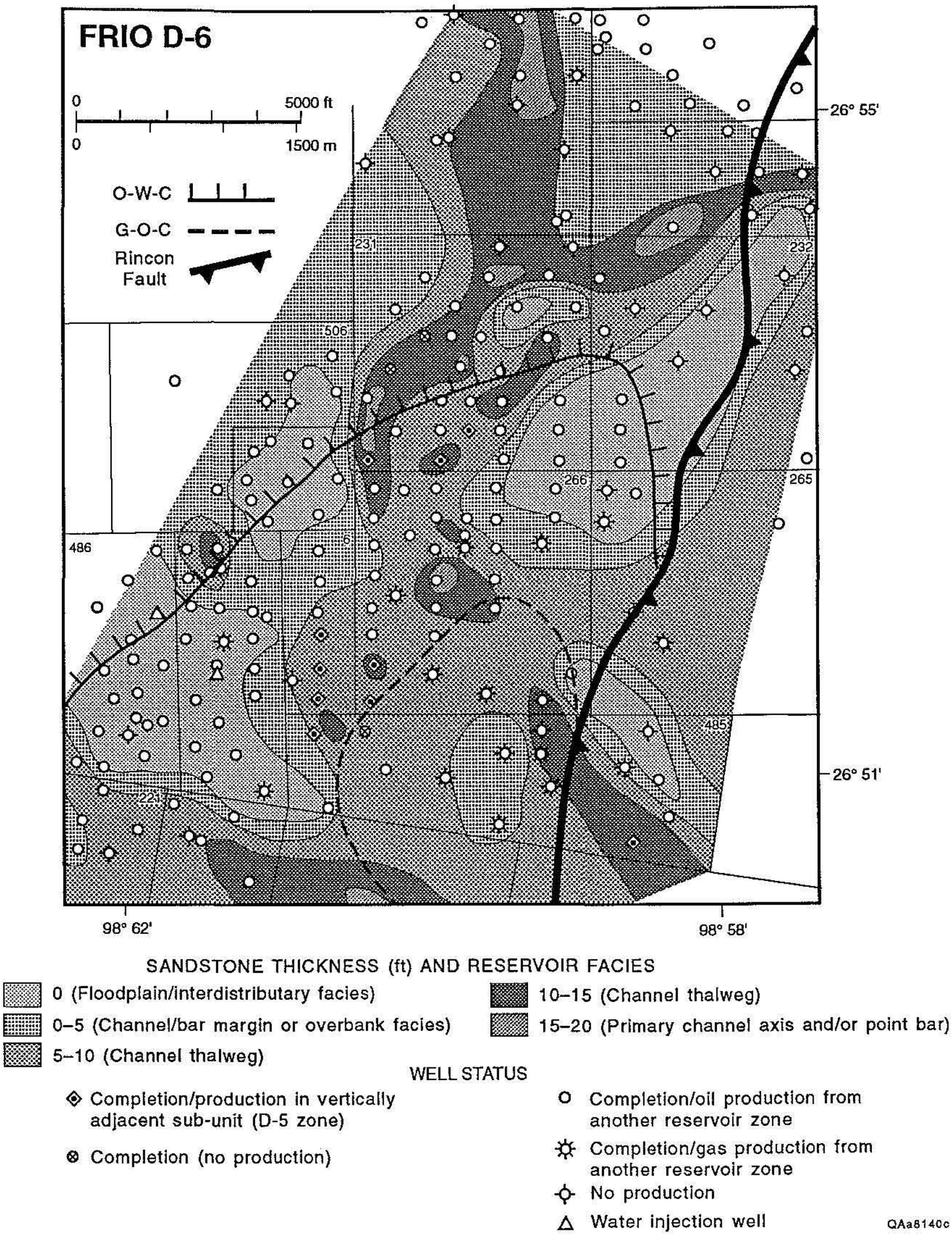

Figure 38. Map illustrating sandstone thickness distribution, corresponding reservoir facies geometry, productive limits, and level of development in the Frio D-6 reservoir unit.

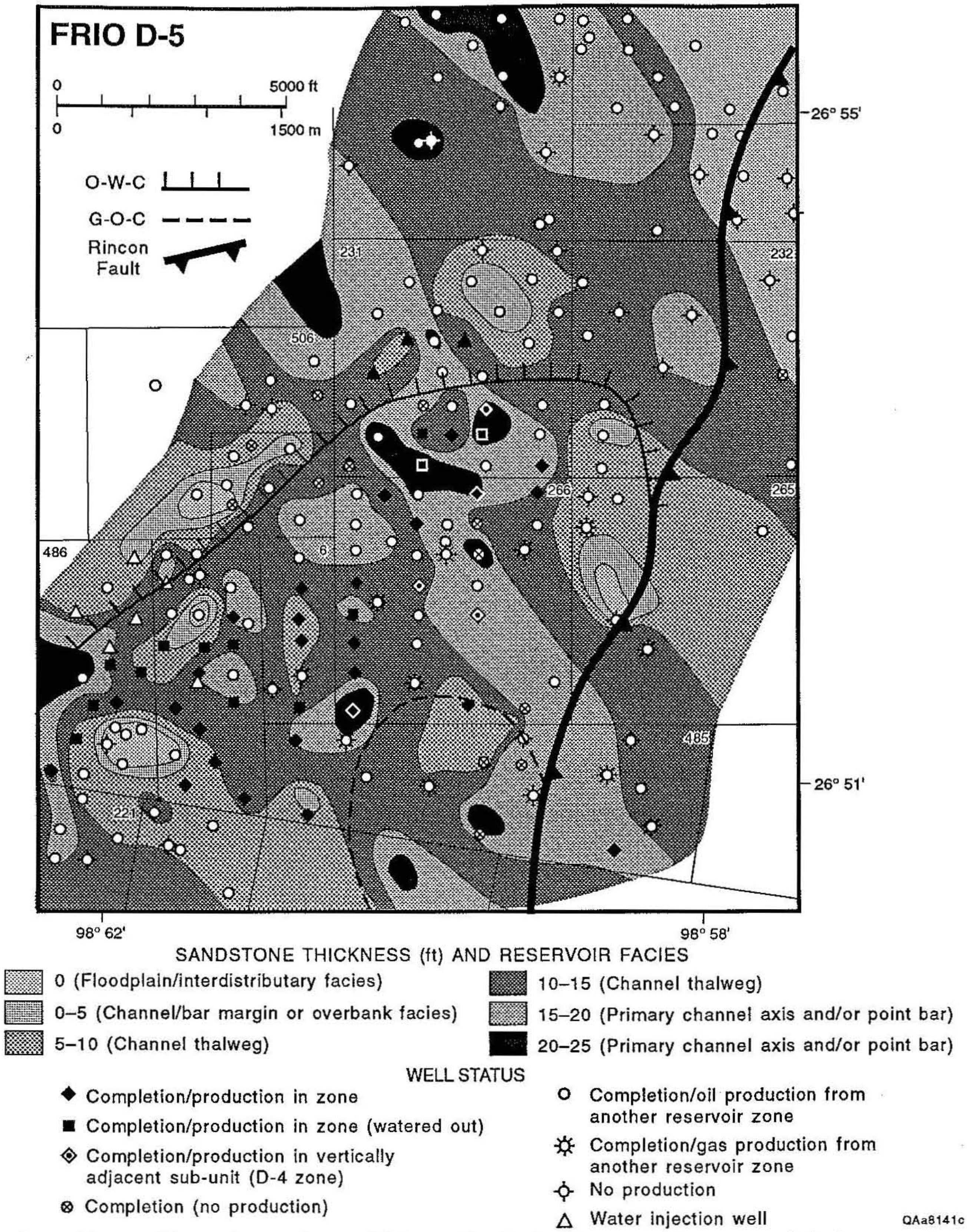

Figure 39. Map illustrating sandstone thickness distribution, corresponding reservoir facies geometry, productive limits, and level of development in the Frio D-5 reservoir unit.

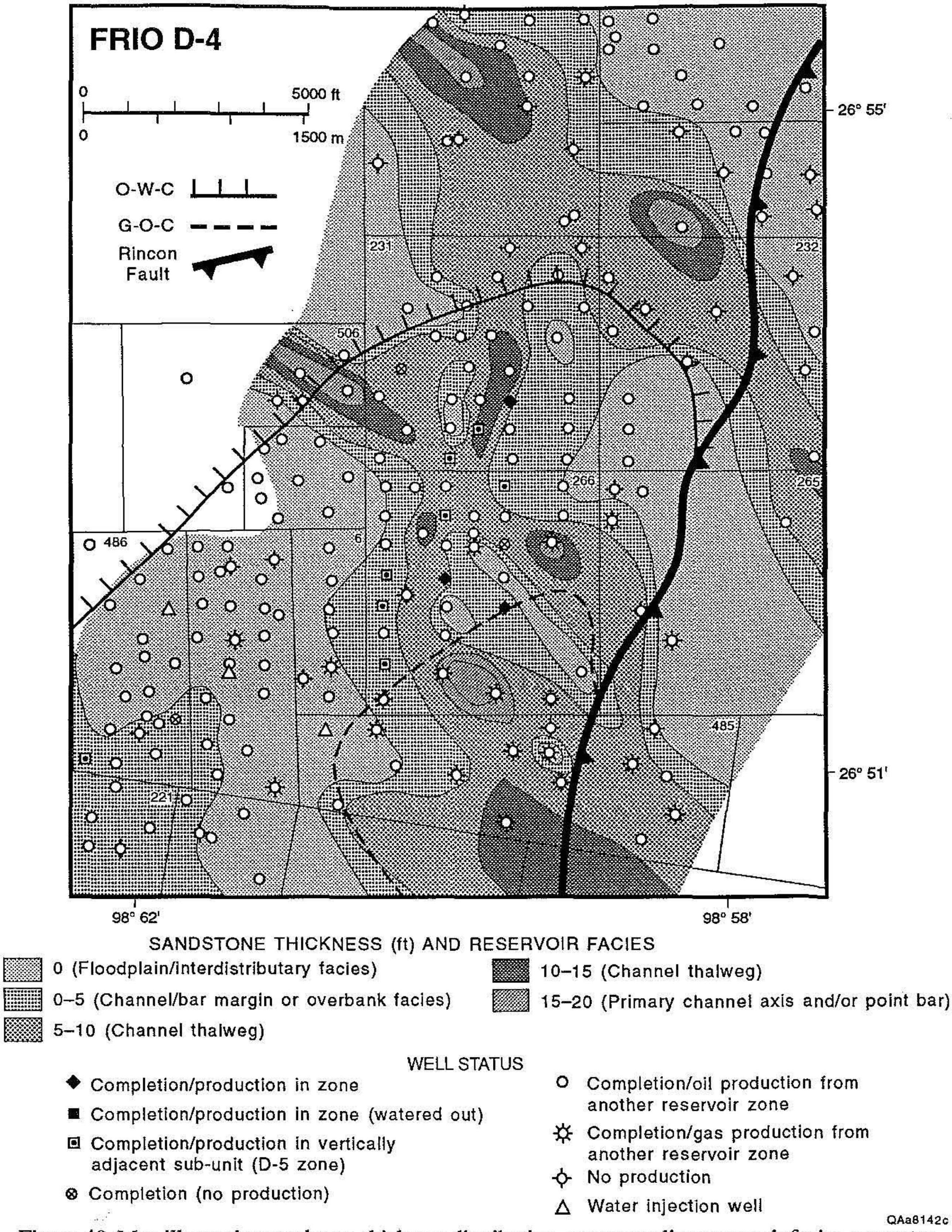

Figure 40. Map illustrating sandstone thickness distribution, corresponding reservoir facies geometry, productive limits, and level of development in the Frio D-4 reservoir unit.

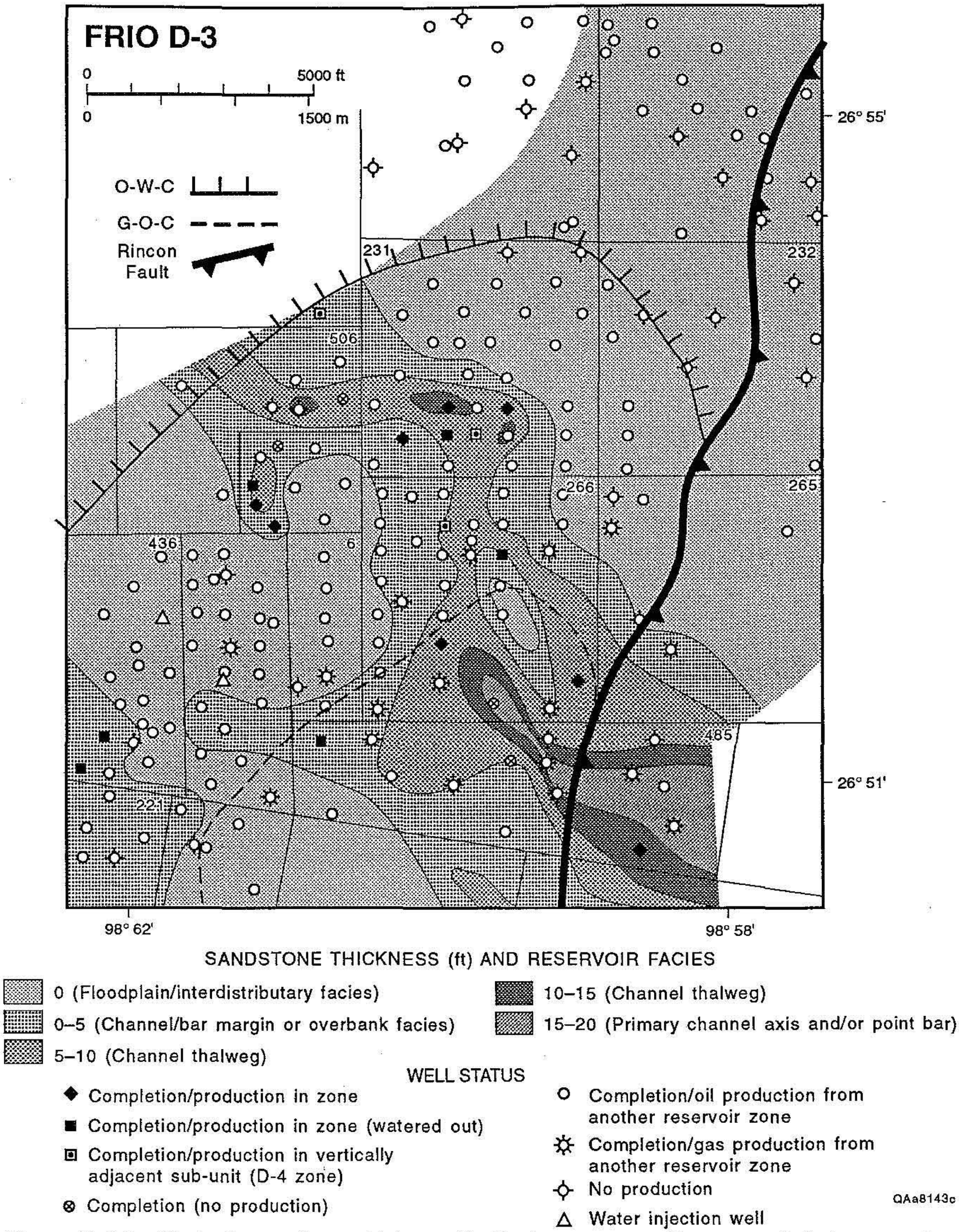

Figure 41. Map illustrating sandstone thickness distribution, corresponding reservoir facies geometry, productive limits, and level of development in the Frio D-3 reservoir unit.

Table 10. Summary of key reservoir characteristics for the Frio D reservoir zone.

	D-6	D-5	D-4	D-3
Reservoir sedimentology				
Dominant facies type	Bars/channel	Mixed	Channels	Channels
Sedimentation style	Progradation	Mixed	Aggradation	Aggradation
Reservoir geometry				
Wells with >0 net sandstone	77	132	127	57
Mean sandstone porosity	19.8	20.5	19.6	18.9
Mean sandstone permeability	49	30	37	14
Max permeability	241	390	199	137
Mean net sandstone thickness	9	13	7	6
Maximum net sandstone thickness	23	24	19	20
Level of development				
Completed zones	14	60	16	22
Producers	/	39	3	10
MBO produced	6205	5866	339	746
Ratio of well completions/ sandstone penetrations	**0.18**	**0.45**	**0.13**	**0.39**

heterogeneous unit probably represents the best potential for identifying incompletely drained or completely undeveloped reservoir compartments.

The D-4 reservoir unit consists of a series of two to three dip-oriented channel units that appear to be connected in their updip portion of the map area, and they therefore are likely in lateral communication with each other (Fig. 40). Channel boundaries are clearly defined, and width dimensions range from 2,000 to 3,500 ft. The number of completions within the D-4 unit (16) is few compared to those in the D-5. Vertical communication between D-4 and D-5 sandstones is probable, and it is assumed that many D-5 completions have also produced oil from the D-4 unit. Actual oil volumes produced from the D-4 unit will be allocated after completion of volumetric calculations and petrophysical modeling efforts.

Reservoir geometry in the D-3 unit is also clearly defined and mapped as a single channel that transects across the center of the field area (Fig. 41). The channel dimensions are relatively narrow in the updip region (2,500 ft) but broaden significantly downdip to the southeast to more than 6,000 ft wide. The D-3 unit has reported production from 10 wells of nearly 750 MBO, but some production associated with 12 additional completions has been assigned to the D-5 composite reservoir zone in wells where the D-3, D-4, and D-5 units have been considered to be in communication.

Allocation of Past Production for Individual Flow Units

Methodology

The potential for infield resource additions is a function of original oil-in-place volumes, present level of development, and the degree of internal geologic complexity of the reservoir being produced. Studies on the Frio D and E reservoirs in Rincon field have documented that reservoir geometry within each stratigraphic reservoir interval is variable and provides important controls on the level of flow communication within a single reservoir unit. Stratigraphic heterogeneity and variability in reservoir quality exhibited within these reservoirs are directly responsible for the distribution of original oil in place, and they are also primary controls on present recovery efficiencies. The wide range of oil volumes produced from wells completed in the same reservoir is an additional indication of the presence of interwell-scale heterogeneity.

Completion of volumetric calculations for each reservoir subunit, followed by modeling of permeability distribution and apportioning of cumulative oil production to each subunit, is required to identify the stratigraphic distribution of oil and to fully understand controls on its accumulation and subsequent production.

Calculation of kH

Reservoir areas were measured for each of the eight mapped subunits, and original oil-in-place volumes were calculated using the following values:

porosity (Ø):	variable for each flow unit, statistical mean from core data
Acre/ft:	variable for each flow unit, gridded acre/ft map calculation
Water saturation (Sw):	constant for D (.32) and E (.20) zones, based on results of capillary pressure measurements on selected cores
Residual oil saturation:	constant (.30), from early fieldwide estimates
Formation volume factor (Boi):	constant (1.20), from Rincon field fluid studies

Cumulative production was apportioned by estimating fluid transmissivity, using permeability-feet (kH) calculations for productive completions within individual flow units. Footage values were derived from net sandstone thicknesses calculated from log analysis. In cored wells, permeability values were derived from the statistical means of measured petrophysical analyses, and where core data were unavailable, representative mean permeability values were substituted for each designated facies type (channel margin, D channel thalweg, E channel thalweg, shoreface/delta-front bar, and overbank facies) (Fig. 42).

The results are illustrated on the log shown in Fig. 43. The E reservoir has an overall greater recovery efficiency than the D reservoir, and individual flow units within the E zone exhibit a systematic increase in both original oil-in-place volumes and recovery efficiency from the lower, aggradational units to the backstepping retrogradational units in the upper part of the reservoir. In the D unit the opposite trend is present, with higher original oil-in-place volumes and recovery efficiency in the lower progradational reservoir units to lower original oil volumes and lower recovery efficiency in the overlying aggradational reservoir units. In addition, Frio E reservoirs have successfully produced from completions over more of the channel area (50–60% of

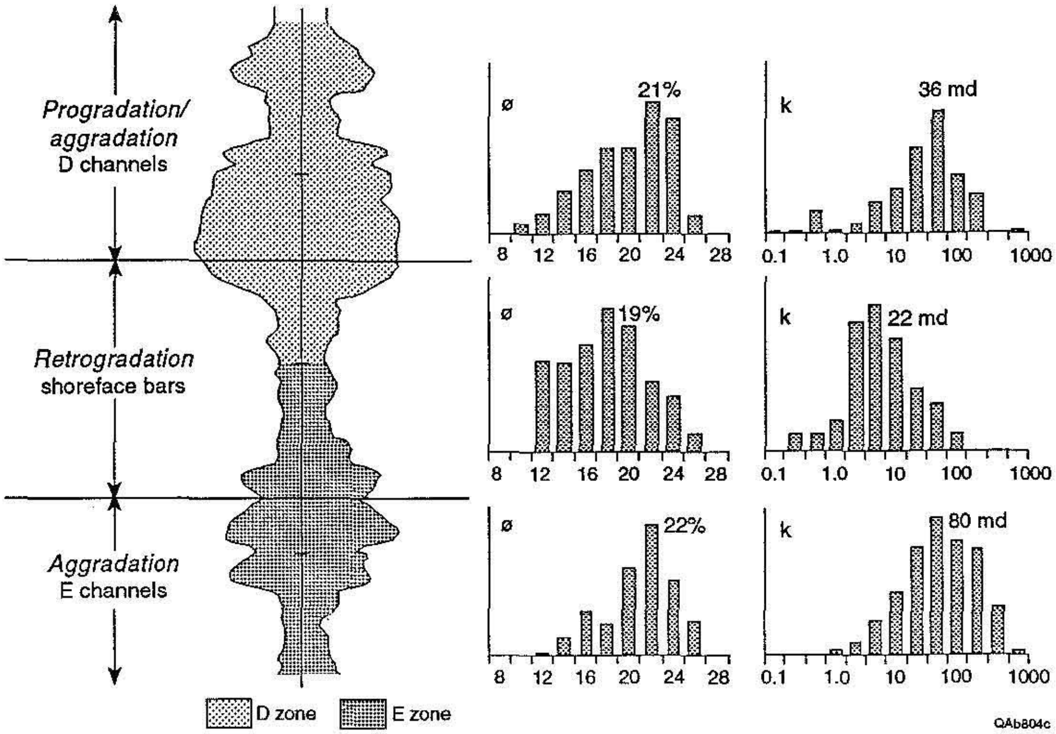

Figure 42. Frio reservoir unit attributes (porosity and permeability) by stratigraphic position.

completions are within channel thalweg facies), whereas in the D unit, production is more limited to the central portions of the channel, with more than 90% of productive completions occurring within the designated central portions of the channel (Table 11). There are key differences in reservoir architecture between the D and E reservoirs and their apparent importance on oil production. Identification of the stratigraphic position of a reservoir unit, as well as the evolution of reservoir architectural styles within an entire reservoir sequence, is critical to understanding heterogeneity in production behavior and an important tool to predict reservoirs with the highest potential for incremental recovery.

Preliminary Assessment of Remaining Reserves

A preliminary assessment of the probable remaining mobile oil resource in each of the Frio D and E reservoirs was performed by using mean values of acre/ft, porosity, S_W, and Boi specific to each reservoir to calculate an estimate of original oil in place. The playwide probability

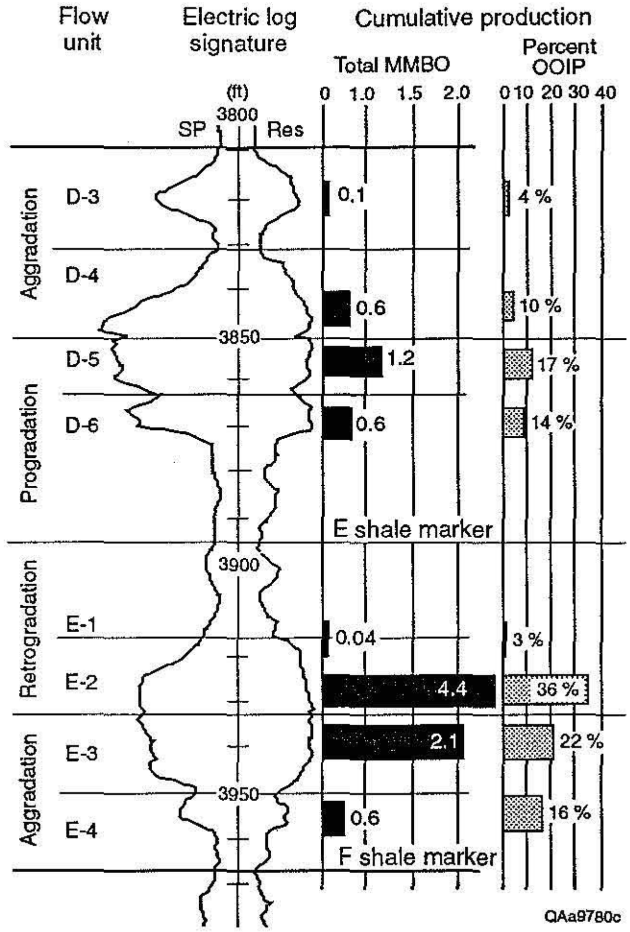

Figure 43. Representative log for Frio D–E flow units showing stratigraphic distribution of production and recovery efficiency.

distribution of S_O values was then used to generate a range of possible residual oil values. Cumulative production was subtracted from this residual oil distribution to predict the range of the remaining mobile oil resource that may be present in these reservoirs. The mean results of this simulation (at 50% probability) shown in Fig. 44 suggest that more than 15 MMBO of additional recoverable mobile oil may be present in Frio D and E reservoirs (Table 4). A more conservative estimate at the 95% probability level indicates that nearly 5 MMBO of mobile oil is remaining. At least 10% of the volume of original oil in place for the stratigraphically heterogeneous Frio D sandstone zone, or more than 3.3 MMBO, is expected to be present as remaining mobile oil. This significant remaining oil resource is the target of further delineation studies within these reservoirs.

Table 11. Comparison of sandstone geometry and oil production among Frio D and E reservoir flow units.

	E-4	E-3	E-2	E-1	D-6	D-5	D-4	D-3
Sandstone architecture								
Stacking pattern	A	A	A-R	R	P	P-A	A	A
Mean net sand thickness	8.0	7.1	8.3	6.0	8.8	10.5	7.1	6.2
Reservoir acres	532	1843	1931	462	975	1734	532	294
Percent reservoir (acre/ft) in primary channel facies	77	92	83	---	---	99	78	57
Reservoir development								
Allocated MBO production (based on kH calculations)	486	1405	3453	23	583	2129	712	492
Number of completions	21	35	39	17	11	30	14	15
Percent completions in primary channel facies	50	71	62	---	---	68	71	73
Percent total oil produced from primary channel facies	96	91	66	---	---	94	93	99
Percent total oil produced from reservoir zone	7	31	51	1	19	62	16	3

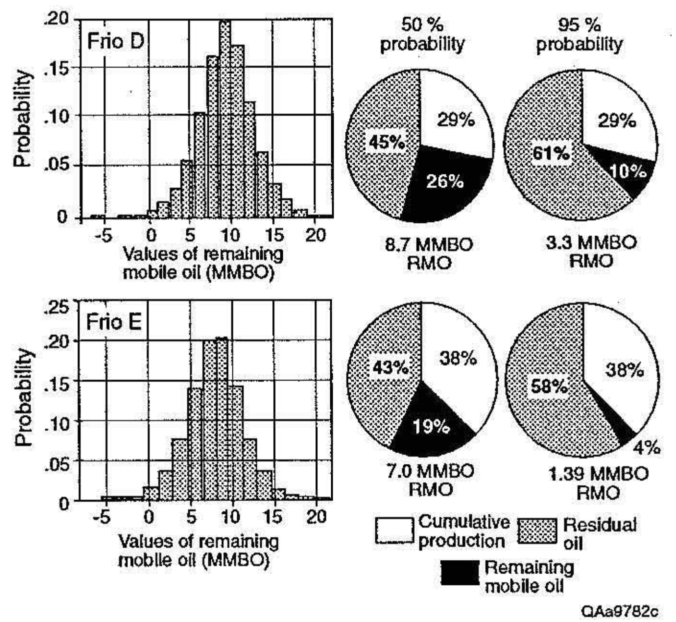

Figure 44. Mean (50% probability) and conservative estimates (95% probability) of remaining mobile oil present in Frio E reservoir sandstones in Rincon field. Mean (50% probability) and conservative estimates (95% probability) of remaining mobile oil present in Frio D reservoir sandstones in Rincon field. The highly heterogeneous Frio D sandstone zone has recovered nearly 10 MMBO to date, but has potential for recovering over 3 MMBO of additional oil that is presently residing in untapped and incompletely drained compartments.

Reserve-Growth Opportunities

Although preliminary estimates of volumes of remaining mobile oil indicate the scope of reserve-growth opportunities, it is the reservoir thickness/completion maps (Figs. 35–42) that provide information regarding the location of specific opportunities. Figs. 35–42 show the location of wells completed within a flow unit or within adjacent flow units. Penetrations that are located in areas of thick reservoir above the oil–water contact and at least two locations distant from production in a unit or adjacent unit represent recompletion opportunities. Areas of reservoir meeting these criteria but lacking penetrations or containing only abandoned well bores represent opportunities for targeted infill drilling.

These first-order assessments focus attention toward obvious opportunities. The risk associated with recompletions or infill wells based on such an analysis can be further reduced through a complete evaluation of petrophysical data. In such a case, production allocated to a completion in a flow unit can be distributed into a drainage radius around the well bore using Soøh maps. These volumes can be subtracted from calculated original mobile oil in place to ascertain the distribution of remaining mobile oil. This mapping process will determine more accurately the volume of reserves recoverable from each recompletion of infill well.

The potential for infield resource additions is a function of the original oil-in-place volume, the present level of development, and the degree of internal geologic complexity of the reservoir being produced. Studies of the Frio D and E reservoirs in Rincon field have identified the current level of development in individual reservoir units and documented that reservoir geometry within each stratigraphic reservoir interval is variable and provides important controls on the level of flow communication within a single reservoir unit. Stratigraphic heterogeneity and variability in reservoir quality exhibited within these reservoirs are directly responsible for the distribution of original oil in place and have also been a primary control on present recovery efficiencies. The wide range of oil volumes produced from wells completed in the same reservoir is an additional indication of the presence of interwell-scale heterogeneity.

Frio D reservoir sandstones have more complex facies patterns and a greater degree of stratigraphic variability, and, as a result, the composite reservoir zone has a significantly lower recovery efficiency than do E series reservoirs. The relatively poor recovery efficiency of the Frio D reservoir zone is caused by the fact that current well spacing is greater than the size of reservoir compartments that collectively make up the total storage space of the mobile oil resource in the Frio D reservoir zone. Documenting stratigraphic heterogeneity and identifying of the presence of flow barriers within and between individual Frio D reservoir units are the primary goals of continuing studies to understand styles of reservoir compartmentalization and to delineate the location of incompletely drained and undeveloped reservoir compartments. Results from calculations of reservoir areas and volumes for each reservoir subunit will be combined with results from petrophysical modeling of water saturations to generate more accurate original oil-in-place calculations for each of the reservoir units. Cumulative production reported for entire reservoir zones will subsequently be reapportioned to individual reservoir subunits based on the permeability distribution established for each subunit, and these volumes will be subtracted from the OOIP calculations to identify remaining volumes of oil. Areas that contain large volumes of OOIP and little or no cumulative production will represent prospective targets that may contain significant remaining oil.

Engineering studies in progress to estimate drainage radii of productive wells will support stratigraphic studies documenting the geometry of reservoir flow units to identify the locations of remaining mobile oil that will be the targets for incremental recovery. Geological, petrophysical, and production studies will be integrated and used to construct maps that will be the key to planning strategies for additional recovery and reserve growth. Maps of porous hydrocarbon volumes will be constructed following petrophysical modeling, and general areas of opportunity will be identified by comparing maps of cumulative production with maps of Soøh and remaining oil. Optimum advanced recovery will focus on targeting depositional trends that are coincident with the location of the largest volumes of remaining mobile oil.

Strategies for Optimizing Reserve Growth

The result of the integration process is a map for each flow unit of remaining mobile oil, as well as information regarding effective drainage radii for each flow unit. This information can be combined to determine areas of remaining mobile oil that can be drained by existing well bores (recompletion opportunities) and those areas that must be reached with new well bores through geologically targeted infill drilling. These opportunities can be ranked in terms of estimated profitability by calculating the volume of oil recoverable from each possible recompletion or infill and dividing by the cost of the completion.

Many single completions can drain large areas because they are situated where vertically adjacent flow units are in good communication, thereby necessitating the completion of only a short interval of the well bore. Other single completions may drain comparatively small volumes because that particular flow unit is internally heterogeneous. In many cases of reserve-growth opportunities in mature fields, an opportunity requiring infill drilling to reach a single zone may not be economically justifiable on its own. However, an infill well that is designed such that it targets that opportunity and another opportunity in a similar area but in a different flow unit may rise above the economic hurdle. As a consequence, the best strategy for optimizing reserve-growth opportunities is to overlay maps of infill drilling opportunities and plan a directional infill well, if necessary, that penetrates as many opportunities as feasible. An extreme case of this might occur when a single flow unit contains many laterally isolated, untapped, or incompletely drained compartments that are adjacent. In this case, a horizontal, or nearly horizontal, well might be planned that economically targeted just a single flow unit.

CONCLUSIONS

Assessing the potential for incremental reserve growth in mature fields, such as those producing from Frio reservoirs in South Texas, requires identifying the location and volume of the remaining resource in the reservoir (Tyler and Finley, 1991). Detailed interwell-scale studies of selected reservoirs serve to characterize reservoir flow-unit architecture and determine the controls reservoir characteristics exert on the distribution of original oil volumes, present production trends, and locations and volumes of unrecovered mobile oil in untapped and incompletely drained zones. With an estimated 1.6 Bbbl of remaining recoverable oil, Frio reservoirs in South Texas represent a significant resource worthy of these efforts.

Different Frio reservoir architectural styles possess characteristic geometries and permeability distributions that directly impact their ability to produce hydrocarbons. Studies of the Frio D and E reservoir zones in Rincon field demonstrate that sandstone architecture is a primary control on recovery efficiency. The architectural styles exhibited by the D and E reservoirs in Rincon field include aggradational, retrogradational, and progradational stacking patterns. The D and E reservoir sequence records an evolution from aggradational, vertically stacked, and more laterally isolated units in the lower E zones to retrogradational, landward-stepping units in the upper E reservoir that are also vertically stacked but have increased lateral communication that is likely responsible for higher recovery efficiencies. Frio D reservoir sandstones have more complex facies patterns and a greater degree of stratigraphic variability, and, as a result, the composite reservoir zone has a significantly lower recovery efficiency than do E series reservoirs. The relatively poor recovery efficiency of the Frio D reservoir zone is caused by the fact that current well spacing is greater than the size of reservoir compartments that collectively make up the total storage space of the mobile oil resource in the Frio D reservoir zone.

At the 95-percent confidence level, more than 4.5 MMbbl of mobile oil remains in the Frio D and E reservoirs within the study area. Many specific reserve-growth opportunities in these reservoirs have been identified by comparing the reservoir architecture of individual flow units with the location of past completions within a flow unit and from adjacent flow units which might be in vertical communication. Cumulative production volumes that have been allocated to individual flow units from commingled completions can be integrated with accurate estimates of original mobile oil in place to determine remaining mobile oil in place. These values can then be used to assign probable reserves to each recompletion or infill opportunity. Mobile oil saturations, drainage radii, and production allocation in this study have been improved in accuracy through facies-based petrophysical analyses supported by special core analysis and abundant routine core analysis data.

The economic viability of potential infill wells can be improved by targeting multiple infill opportunities with a single well bore. This can be accomplished by overlaying mapped opportunities from different flow units to identify a vertical string of opportunities or by joining adjacent opportunities within a single flow unit through use of a horizontal well bore.

The techniques of multidisciplinary advance reservoir characterization that have been used in Rincon field serve as a useful template for additional recovery efforts in other mature fluvial-deltaic reservoirs throughout the Frio Fluvial-Deltaic (Vicksburg Fault Zone) Play. The specific methodologies can also be applied to other mature fluvial-deltaic reservoirs throughout the United States because similar facies in those reservoirs will result in similar architectures. Furthermore, the basic tenets of multidisciplinary advanced reservoir characterization, including geological and engineering interpretations enhanced by high-frequency stratigraphic studies and facies-based petrophysical analysis, will enhance the understanding of any mature reservoir, regardless of its depositional setting.

ACKNOWLEDGMENTS

This research was performed for and funded by the U.S. Department of Energy under contract no. DE-FC22-93BC14959. Conoco Oil Company is gratefully acknowledged for its cooperation in providing well logs, cores, production and engineering data, and other miscellaneous geologic information. Particular appreciation is extended to B. Ackman, S. Kershner, and C. Mullenax of Conoco for their assistance. Research was assisted by Douglas Dawson and Syed Ali. Drafting was assisted by John T. Ames, Michele Bailey, William C. Bergquist, Randy Hitt, Susan Krepps, Joel Lardon,and Tari Weaver of the Bureau of Economic Geology, The University of Texas at Austin, under the direction of Chief Cartographer R. L. Dillon. Editing was by Jeannette Miether, word processing was by Susan Lloyd, and layout was by Jamie H. Coggin and Susan Lloyd.

REFERENCES

Almon, W. R., and Davies, D. K., 1981, Formation damage and the crystal chemistry of clays, *in* Longstaffe, F. J., ed., Short course in clays and the resource geologist, Calgary, May, 1981: Chapter 5, p. 81–103.

Alpay, O. A., 1972, A practical approach to defining reservoir heterogeneity: Journal of Petroleum Technology, p. 841–848.

Archie, G. E., 1942, The electrical resistivity log as an aid in determining some reservoir characteristics: American Institute of Mining and Metallurgical Engineers Transactions, v. 146, p. 54–62.

Ashford, T., 1972, Geoseismic history and development of Rincon field, South Texas: Geophysics, v. 37, p. 979–812.

Bebout, D. G., Loucks, R. G., and Gregory, A. R., 1978, Frio sandstone reservoirs in the deep subsurface along the Texas Gulf Coast: The University of Texas at Austin, Bureau of Economic Geology Report of Investigations No. 91, 92 p.

Bebout, D. G., Weise, B. R., Gregory, A. R., and Edwards, M. B., 1982, Wilcox sandstone reservoirs in the deep subsurface along the Texas Gulf Coast, their potential for production of geopressured geothermal energy: The University of Texas at Austin, Bureau of Economic Geology Report of Investigations No. 117, 125 p.

Chen, H. C., and Fang, J. H., 1986, Sensitivity analysis of the parameters in Archie's water saturation equation: The Log Analyst, Sept.-Oct. p. 39–44.

Coleman, J., and Galloway, W. E., 1990, Petroleum geology of the Vicksburg Formation, Texas: Gulf Coast Association of Geological Societies Transactions, v. 40, p. 119–130.

Coleman, J., and Galloway, W. E., 1991, Sequence stratigraphic analysis of the lower Oligocene Vicksburg Formation of Texas, in Armentrout, J. W., and Perkins, R. F., eds., Sequence stratigraphy as an exploration tool: Gulf Coast Section, Society of Economic Paleontologists and Mineralogists research conference, p. 99–112.

Dewan, J. T., 1988, Log interpretation and Applications, Schlumberger Educational Services Course notes: Houston, Texas, unpaginated.

Dreyer, T., Scheie, A., and Walderhaug, O., 1990, Minipermeameter-based study of permeability trends in channel sand bodies: American Association Petroleum Geologists, v. 74, p. 359–374.

Folk, R. L., 1974, Petrology of sedimentary rocks: Austin, Texas, Hemphill Publishing Co., 182 p.

Galloway, W. E., 1977, Catahoula Formation of the Texas coastal plain—depositional systems, composition, structural development, ground-water flow history, and uranium distribution: The University of Texas at Austin, Bureau of Economic Geology Report of Investigations No. 87, 59 p.

Galloway, W. E., 1982, Depositional architecture of Cenozoic Gulf Coastal Plain fluvial systems, *in* Ethridge, F. G., and Flores, R. M., eds., Recent and ancient nonmarine depositional environments: models for exploration: Society of Economic Paleontologists and Mineralogists, Special Publication 31, p. 127–155.

Galloway, William E., 1986, Depositional and structural framework of the distal Frio Formation, Texas coastal zone and shelf: The University of Texas at Austin, Bureau of Economic Geology Geological Circular 86-8, 16 p.

Galloway, W. E., 1989, Genetic stratigraphic sequences in basin analysis II: application to northwest Gulf of Mexico Cenozoic Basin: American Association of Petroleum Geologists, v. 73, no. 2, p. 143–154.

Galloway, W. E., Ewing, T. E., Garrett, C. M., Tyler, Noel, and Bebout, D. G., 1983, Atlas of major Texas oil reservoirs: The University of Texas at Austin, Bureau of Economic Geology, 139 p.

Galloway, W. E., Hobday, D. K., and Magara, K., 1982, Frio Formation of the Texas Gulf Coast Basin—depositional systems, structural framework, and hydrocarbon origin, migration, distribution, and exploration potential: The University of Texas at Austin, Bureau of Economic Geology Report of Investigations No. 122, 78 p.

Grigsby, J. D., and Kerr, D. R., 1993, Gas reservoir quality variations and implications for resource development, Frio Formation, South Texas: examples from Seeligson and Stratton fields: The University of Texas at Austin, Bureau of Economic Geology Geological Circular 93-2, 27 p.

Haq, B. U., Hardenbol, J., and Vail, P. R., 1988, Mesozoic and Cenozoic chronostratigraphy and eustatic cycles, in Wilgus, C. K., Hastings, B. S., Kendall, C. G. St. C., Posamentier, H. W., Ross, C. A., and Van Wagoner, J. C., eds., Sea-level changes: an integrated approach: Society of Economic Paleontologists and Mineralogists, Special Publication No. 42, p. 71–108.

Holtz, M. H., and McRae, L. E., 1995a, Identification and assessment of remaining oil resources in the Frio fluvial-deltaic sandstone play, South Texas: The University of Texas at Austin, Bureau of Economic Geology Report of Investigations No. 227, 46 p.

Holtz, M. H., and McRae, L. E., 1995b, Modeling reservoir attributes and estimating additional hydrocarbon potential for redevelopment in fluvial-deltaic reservoirs: An example from the Frio fluvial-sandstone play in South Texas (abs.), in AAPG Annual convention official program: Houston, American Association of Petroleum Geologists, p. 42A–43A.

Holtz, M. H., McRae, L. E., and Tyler, Noel, 1994, Identification of remaining oil resource potential in the Frio fluvial-deltaic sandstone play, South Texas: The University of Texas at Austin, Bureau of Economic Geology, topical report prepared for the U.S. Department of Energy, Bartlesville Project Office, under contract no. DE-FC22-93BC14959, report no. DOE/BC/ 14959-8 (DE94000132), 67 p.

Honarpour, M., and Mahmood, S. M., 1988, Relative permeability measurements: an overview: Journal of Petroleum Technology, May, 1988, p. 963–966.

Jackson, M. L. W., and Ambrose, W. A., 1989, Influence of reservoir heterogeneity on gas-resource potential for geologically based infill drilling, Brooks and I-92 reservoirs, Frio Formation, South Texas: Gulf Coast Association of Geological Societies Transactions, v. 39, p. 127–140.

Jirik, L. A., 1990, Reservoir heterogeneity in middle Frio fluvial sandstones: case studies in Seeligson field, Jim Wells County, Texas: Gulf Coast Association of Geological Societies Transactions, v. 40, p. 335–352.

Kerr, D. R., 1990, Reservoir heterogeneity in the middle Frio Formation: case studies in Stratton and Agua Dulce fields, Nueces County, Texas: Gulf Coast Association of Geological Societies Transactions, v. 40, p. 363–372.

Kerr, D. R., Grigsby, J. D., and Scott, A. R., 1992, Fluvial deposits of the Frio Formation along the Vicksburg Fault Zone: examples from Stratton and Seeligson fields, in Levey, R. A., Grigsby, J. D., Langford, R. P., Kerr, D. R., Guevara, E. H., Scott, A. R., and Finley, R. J., Core and log analyses of depositional systems and reservoir properties of Gulf Coast natural gas reservoirs: an integrated approach to infield reserve growth in Frio, Vicksburg, and Wilcox sandstones: The University of Texas at Austin, Bureau of Economic Geology Geological Circular 92-1, p. 7–25.

Kerr, D. R., and Jirik, L. A., 1990, Fluvial architecture and reservoir compartmentalization in the Oligocene middle Frio Formation, South Texas: Gulf Coast Association of Geological Societies Transactions, v. 40, p. 373–380.

Knox, P. R., and McRae, L. E., 1995, High resolution sequence stratigraphy: the key to identifying compartment styles in Frio Formation fluvial-deltaic reservoirs, T-C-B field, South Texas (abs.), *in* AAPG Annual convention official program: Houston, American Association of Petroleum Geologists, p. 51A.

Kosters, E. C., Bebout, D. G., Seni, S. J., Garrett, C. M., Jr., Brown, L. F., Hamlin, H. S., Dutton, S. P., Ruppel, S. C., Finley, R. J., and Tyler, Noel, 1989, Atlas of major Texas gas reservoirs: The University of Texas at Austin, Bureau of Economic Geology Special Publication, 161 p.

Lasseter, T. J., Waggoner, J. R., and Lake, L. W., 1986, Reservoir heterogeneities and their influence on ultimate recovery, *in* Lake, L. W., ed., Reservoir characterization: Orlando, Academic Press, p. 545–560.

Lindquist, S. J., 1976, Sandstone diagenesis and reservoir quality, Frio Formation (Oligocene), South Texas: The University of Texas at Austin, Master's thesis, 147 p.

Lindquist, S. J., 1977, Secondary porosity development and subsequent reduction, overpressured Frio Formation sandstone (Oligocene), South Texas: Gulf Coast Association of Geological Societies Transactions, v. 27, p. 99–107.

Lord, M. E., and Collins, R. E., 1992, Simulation system for compartmentalized gas reservoirs, Secondary natural gas recovery: Targeted technology applications for infield reserve growth: Englewood, Colorado, Research & Engineering Consultants, Inc., prepared for Gas Research Institute (Contract No. 5088-212-1718) and U.S. Department of Energy (Contract No. DE-FG21-88MC25031), 75 p.

Loucks, R. G., Dodge, M. M., and Galloway, W. E., 1986, Controls on porosity and permeability of hydrocarbon reservoirs in lower Tertiary sandstones along the Texas Gulf Coast: The University of Texas at Austin, Bureau of Economic Geology Report of Investigations No. 149, 78 p.

McBride, E. F., Lindemann, W. L., and Freeman, P. S., 1968, Lithology and petrology of the Gueydan (Catahoula) Formation in South Texas: The University of Texas at Austin, Bureau of Economic Geology Report of Investigations No. 63, 122 p.

McRae, L. E., and Holtz, M. H., 1994, Integrated reservoir characterization of mature oil reservoirs: an example from Oligocene Frio fluvial-deltaic sandstones, Rincon field, South Texas, Rincon field, South Texas: Gulf Coast Association of Geological Societies Transactions, v. 44, p. 487–498.

McRae, L. E., and Holtz, M. H., 1995, Reservoir architecture and permeability characteristics of fluvial-deltaic sandstone reservoirs in the Frio Formation, Rincon field, South Texas (abs.), *in* AAPG Annual convention official program: Houston, American Association of Petroleum Geologists, p. 64A.

McRae, L. E., Holtz, M. H., and Knox, P. R., 1994, Revitalizing a mature oil play: strategies for finding and producing unrecovered oil in Frio fluvial-deltaic reservoirs of South Texas: The University of Texas at Austin, Bureau of Economic Geology, topical report prepared for the U.S. Department of Energy, Bartlesville Project Office, under contract no. DE-FC22-93BC14959, report no. DOE/BC/14959-5 (DE94000131), 93 p.

Milliken, K. L., 1989, Petrography and composition of authigenic feldspars, Oligocene Frio Formation, South Texas: Journal of Sedimentary Petrology, v. 59, no. 3, p. 361–374.

Pryor, W. A., 1973, Permeability-porosity patterns and variations in some Holocene sand bodies: American Association of Petroleum Geologists, v. 57, p. 162–189.

Stanley, T. B., 1970, Vicksburg Fault Zone, Texas, in Halbouty, M. T., ed., Geology of giant petroleum fields: American Association of Petroleum Geologists Memoir 14, p. 301–308.

Tyler, Noel, Barton, M. D., Bebout, D. G., Fisher, R. S., Grigsby, J. D., Guevara, E., Holtz, M. H., Kerans, C., Nance, H. S., and Levey, R. A., 1992, Characterization of oil and gas heterogeneity: U.S. Department of Energy final report, October 1992, p. 219.

Tyler, Noel, and Ewing, Thomas, 1986, Major oil plays of South and Central Texas, in Stapp, W. L., ed., Contributions to the geology of South Texas: South Texas Geological Society, p. 24–52.

Tyler, Noel, and Finley, R. J., 1991, Architectural controls on the recovery of hydrocarbons from sandstone reservoirs, *in* Miall, A. D., and Tyler, Noel, eds., The three-dimensional facies architecture of terrigenous clastic sediments and its implications for hydrocarbon discovery and recovery: Society of Economic Paleontologists and Mineralogists, Concepts in Sedimentology and Paleontology, v. 3, p. 1–5.

Tyler, Noel, Galloway, W. E., Garrett, C. M., and Ewing, T. E., 1984, Oil accumulation, production characteristics, and targets for additional recovery in major oil reservoirs of Texas: The University of Texas at Austin, Bureau of Economic Geology Geological Circular 84-2, 31 p.

U.S. Department of Energy (DOE), 1991, Opportunities to improve oil productivity in unstructured deltaic reservoirs: Washington, D.C., Technical Summary and Proceedings of the Technical Symposium, Oil Implementation Task Force, Oil Research Program, 92 p.

BUREAU OF ECONOMIC GEOLOGY
THE UNIVERSITY OF TEXAS AT AUSTIN

University Station, Box X · Austin, Texas 78713-8924 · (512) 471-1534 or 471-7721 · FAX 471-0140
10100 Burnet Road, Bldg. 130 · Austin, Texas 78758-4497

October 4, 1995

Ms. Edith Allison
Bartlesville Project Office
U.S. Department of Energy
220 N. Virginia
Bartlesville, OK 74003

Reference: Cooperative Agreement No. DE-FC22-93BC14959

Dear Ms. Allison:

Enclosed is one camera-ready master of the approved Topical Report for the referenced project. One unbound copy of this report has been forwarded to the Document Control Center at DOE's Pittsburgh Energy Technology Center. After this report has been printed, please send me three copies.

Sincerely,

Lynda A. Miller

Lynda A. Miller
Program Coordinator

LAM
Enclosure

cc: M. Holtz
P. Knox
R. Levey